UNIVERSIDAD AUTÓNOMA DE MADRID

DEPARTMENT OF MOLECULAR BIOLOGY

PhD Thesis

The chromatin remodeller BPTF is a novel and critical c-MYC co-factor

LAIA RICHART GINÉS

Madrid, 2015

UNIVERSIDAD AUTÓNOMA DE MADRID

FACULTY OF SCIENCES

DEPARTMENT OF MOLECULAR BIOLOGY

The chromatin remodeller BPTF is a novel and critical c-MYC co-factor

Doctoral thesis submitted to the Universidad Autónoma de Madrid for the degree of Doctor of Philosophy by MSc in Biotechnology,

Laia Richart Ginés

Thesis Directors

Prof. Dr. Francisco X. Real Arribas

Dr. Victor Javier Sánchez-Arévalo Lobo

EPITHELIAL CARCINOGENESIS GROUP

CELL BIOLOGY PROGRAMME

SPANISH NATIONAL CANCER RESEARCH CENTRE

This thesis, submitted for the degree of Doctor of Philosophy at the Universidad Autónoma de Madrid, has been carried out and completed in the Epithelial Carcinogenesis Group at the Spanish National Cancer Research Centre (CNIO), under the supervision of
Prof. Dr. Francisco X. Real Arribas and
Dr. Victor Javier Sánchez-Arévalo Lobo

The work was supported by grants from Ministerio de Economía y Competitividad, Madrid, Spain (grants Consolíder ONCOBIO, Consolider INESGEN, SAF2010-21517 and SAF2011-15934-E), Instituto de Salud Carlos III (grants G03/174, 00/0745, PI051436, PI061614, G03/174, PI080440, PI120425 and Red Temática de Investigación Cooperativa en Cáncer (RTICC)), Asociación Española Contra el Cáncer, EUFP7-201663 and 201333, and US National Institutes of Health grant RO1 CA089715.

"Quan surts per fer el viatge cap a Ítaca,
has de pregar que el camí sigui llarg,
ple d'aventures, ple de coneixences.
Has de pregar que el camí sigui llarg,
que siguin moltes les matinades
que entraràs en un port que els teus ulls ignoraven,
i vagis a ciutats per aprendre dels que saben.
Tingues sempre al cor la idea d'Ítaca."

I-Kavafis (adaptació de Lluís Llach)

Dedicat a la meva mare i la meva àvia.

Index of Contents

INDEX OF CONTENTS

SUMMARY **6**

PRESENTACIÓN **8**

DIRECTORY OF TABLES **10**

DIRECTORY OF FIGURES **12**

ABBREVIATIONS **14-15**

INTRODUCTION **17-36**

1. THE ROLE OF CHROMATIN DURING TRANSCRIPTION **17**

1.1. Nucleosomes are the basic unit of chromatin 17

1.2. Histone covalent modifications 18

1.3. Chromatin remodelling 19

1.4. Histone variants 20

1.5. Transcription in the chromatin context 21

2. c-MYC **22**

2.1. Protein structure and interaction partners 22

2.2. c-MYC control of gene transcription 23

2.2.1. *Widespread binding to chromatin* *24*

2.2.2. *Transcriptional activation* *25*

2.2.3. *Transcriptional repression* *27*

2.3. c-MYC biological roles 28

2.3.1. *Cell proliferation and differentiation* *28*

2.3.2. *Cell growth and metabolism* *30*

2.3.3. *Apoptosis* *30*

2.3.4. *Tumorigenesis* *30*

2.3.5. *Reprogramming* *31*

3. BPTF **32**

3.1. Protein structure and interactors 33

3.2. Biological function of BPTF 34

3.2.1. *Transcriptional activator and repressor* *34*

3.2.2. *Chromatin structure* *35*

3.2.3. *Developmental regulator* *35*

3.3. BPTF in human cancer 36

AIMS **38**

OBJETIVOS 40

MATERIALS AND METHODS 42-55

1. CELL CULTURE 42

1.1. Cell lines and reagents 42

1.2. Plasmids, viral constructs and virus production 42

1.3. iPS Reprogramming 43

1.4. FACS analysis of proliferation and apoptosis 44

2. MOUSE BIOLOGY 44

2.1. Mouse strains 44

2.2. Histopathology and Immunohistochemistry 45

2.3. Hematological analysis and characterization of B cell Compartment 46

3. MOLECULAR BIOLOGY 46

3.1. Western blotting 46

3.2. Co-immunoprecipitation analyses 47

3.3. Generation of polyclonal anti-BPTF anti-sera 47

3.4. Immunofluorescence staining and Proximity Ligation Assay 47

3.5. Quantitative real-time PCR 48

3.6. Chromatin immunoprecipitation 50

3.7. DNAse I hypersensitivity assay 51

4. GENOME-WIDE STUDIES AND BIOINFORMATICS ANALYSES... 51

4.1. ChIP-Seq library construction and massive parallel sequencing . 51

4.2. ChIP-Seq data processing 51

4.3. Motif enrichment analysis, peak annotation and density plot analysis 52

4.4. Gene set enrichment analysis (GSEA) 52

4.5. RNA-seq 52

4.6. RNA-Seq data processing 53

4.7. RNA-Seq GSEA analysis 53

4.8. Analysis of human tumor genomic data 54

5. STATISTICAL ANALYSIS 54

6. INDIVIDUAL CONTRIBUTIONS 54

RESULTS 56-84

1. BPTF IS REQUIRED FOR *IN VITRO* PROLIFERATION OF TUMOR CELLS 57

2. BPTF IS MODULATED DURING CELL CYCLE PROGRESSION AND IS REQUIRED FOR G_0-G_1/S TRANSITION 58
3. BPTF IS NECESSARY FOR c-MYC TRANSCRIPTIONAL ACTIVITY 60
4. BPTF AND c-MYC INTERACT *IN VITRO* 64
5. GENOME-WIDE ANALYSIS OF c-MYC RECRUITMENT TO DNA UPON BPTF KNOCK-DOWN 65
6. BPTF IS REQUIRED FOR c-MYC-INDUCED REMODELLING OF TARGET CHROMATIN 69
7. BPTF IS REQUIRED FOR A SUBSET OF c-MYC BIOLOGICAL FUNCTIONS 71
8. BPTF IS REQUIRED FOR THE REPROGRAMMING OF MOUSE EMBRYONIC FIBROBLASTS 73
9. BPTF CORRELATES WITH c-MYC SIGNATURES IN HUMAN CANCER 77
10. BPTF IS REQUIRED FOR c-MYC-DRIVEN PANCREATIC TUMORIGENESIS 82

DISCUSSION 85-104

1. BPTF AND CELL PROLIFERATION 86
2. BPTF AND c-MYC AXIS 88
2.1. c-MYC recruitment to DNA and/or stability of the complex 88
2.2. Remodelling of c-MYC target chromatin 89
2.3. Long-range interactions 90
2.4. Transcription elongation 93
2.5. Repression by c-MYC 93
3. BPTF IN DEVELOPMENT AND DIFFERENTIATION 94
3.1. Early embryonic development 94
3.2. Cell differentiation 94
4. BPTF AND TUMORIGENESIS 97

CONCLUSIONS 102

CONCLUSIONES 104

REFERENCES 105-125

Summary

SUMMARY

c-MYC is a major oncogene involved in human cancer. Here, I have identified BPTF as a novel interactor of c-MYC required for its biological functions. This interaction is crucial for c-MYC transcriptional activity: BPTF knock-down leads to a decrease in c-MYC binding to DNA, changes in chromatin accessibility, and impaired activation of the c-MYC transcriptional program. In murine embryonic fibroblasts, BPTF is necessary for c-MYC-driven proliferation, G_1-S progression, and replication stress, but not for c-MYC-induced apoptosis. Moreover, BPTF is critical for reprogramming of somatic cells into induced pluripotent stem cells using the four Yamanaka factors. In agreement with these findings, BPTF is required for the proliferation of c-MYC-addicted cancer cells and in human tumors its expression positively correlates with the activation of c-MYC gene signatures.

To determine whether BPTF is required for the oncogenic effects of c-MYC, we used two genetic mouse models: *Ela-Myc* and *Eμ-Myc*. *Ela-Myc* mice develop aggressive acinar and ductal tumors. While BPTF is dispensable for normal pancreatic development and differentiation, its embryonic inactivation in *Ela-Myc* mice is associated with extensive loss of acinar cells. Moreover, deletion of BPTF in young *Ela-Myc* via activation of the *Ptf1a-CreERT2* recombinase results in a significant delay in tumor onset and a corresponding extension in disease-free survival. c-MYC overexpression in the B cell lineage (*Eμ-Myc*) leads to the development of Burkitt-like lymphomas. Inactivation of one *Bptf* allele does not impair B cell maturation but completely blocks lymphoma development. These findings underscore the importance of a more detailed study of BPTF function in mammals and highlight the potential of exploiting the c-MYC:BPTF axis in cancer therapy.

Presentación

PRESENTACIÓN

c-MYC es uno de los principales oncogenes implicados en el cáncer humano. En el presente trabajo he identificado a BPTF como un nuevo interactor de c-MYC que además es requerido para sus funciones biológicas. Esta interacción es crucial para la actividad transcripcional de c-MYC: el knock-down de BPTF se acompaña de una disminución de la unión de c-MYC al DNA, cambios en la accesibilidad de la cromatina y de una inadecuada activación del programa transcripcional de c-MYC. En fibroblastos embrionarios de ratón, BPTF es necesario para la proliferación, progresión G_1-S y estrés replicativo dirigidos por c-MYC, pero no para la apoptosis instruida por el mismo. Además, BPTF es crítico para la reprogramación de células somáticas a células madre pluripotentes por medio de los cuatro factores descritos por Yamanaka. De acuerdo con estas observaciones, BPTF es necesario para la proliferación de líneas cancerosas adictas a c-MYC, y en tumores humanos su expresión correlaciona positivamente con la activación de los programas de expresión génica dirigidos por c-MYC.

Con el objetivo de determinar si BPTF es necesario para los efectos oncogénicos de c-MYC, hemos usado dos modelos genéticos de ratón: *Ela-Myc* y *Eμ-Myc*. Los ratones *Ela-Myc* desarrollan tumores acinares y ductales muy agresivos. Aunque BPTF es dispensable para la diferenciación y desarrollo pancreáticos normales, su inactivación embrionaria en ratones *Ela-Myc* se asocia con una extensa pérdida de células acinares. Además, la depleción de BPTF en ratones Ela-Myc jóvenes por medio de la recombinasa *Ptf1a-CreERT2* resulta en un retraso significativo en la aparición de los tumores y en una consiguiente extensión de la supervivencia libre de enfermedad. La sobre-expresión de c-MYC en el compartimento de células B conduce al desarrollo de linfomas que reproducen la enfermedad del Linfoma de Burkitt. La inactivación de una sola copia de *Bptf* no afecta a la maduración de las células B pero bloquea por completo la formación de tumores. Estas observaciones destacan la importancia de un estudio más detallado de la función de BPTF en mamíferos y subrayan el potencial de explotar el eje c-MYC:BPTF como blanco terapéutico en cáncer.

Directory of Figures

DIRECTORY OF FIGURES

Figure 1. Schematic view of the 30-nm fibre.
Figure 2. Structural organization of c-MYC and interaction partners.
Figure 3. Model of c-MYC transactivation.
Figure 4. Schematic representation of the cellular functions mediated by c-MYC.
Figure 5. BPTF is required for cell proliferation of PDAC cell lines.
Figure 6. BPTF is modulated during cell cycle.
Figure 7. BPTF is required for proliferation of HFF.
Figure 8. BPTF is required for c-MYC transcriptional activity.
Figure 9. Genome-wide analysis of BPTF-dependent c-MYC transcriptional activity.
Figure 10. Analysis of c-MYC:BPTF interaction.
Figure 11. Analysis of MYC-ER recruitment to chromatin in control cells.
Figure 12. BPTF silencing interferes with c-MYC recruitment to its target genes.
Figure 13. BPTF silencing limits DNA accessibility at c-MYC target promoters.
Figure 14. BPTF is required for MYC-induced hyperacetylation of target promoters.
Figure 15. BPTF is required for c-MYC-induced proliferation of MEFs.
Figure 16. BPTF is required for c-MYC-induced replicative stress but not for apoptosis.
Figure 17. BPTF is induced during reprogramming of fibroblasts into iPS cells.
Figure 18. Impact of BPTF loss on OSKM reprogramming efficiency.
Figure 19. Impact of BPTF loss on OSK reprogramming efficiency.
Figure 20. BPTF is required for the reprogramming of mouse fibroblasts.
Figure 21. BPTF and c-MYC expression in a panel of human cancer cell lines.
Figure 22. BPTF is required for the proliferation of c-MYC-dependent cells.
Figure 23. Co-expression of BPTF and MYC genes in human tumors.
Figure 24. BPTF expression correlates with c-MYC signatures in human tumors.
Figure 25. *Bptf* deletion has no impact on normal pancreas homeostasis
Figure 26. c-MYC overexpression in *Bptf*-null mouse pancreata results in extensive loss of the acinar compartment.
Figure 27. BPTF loss delays the onset of c-MYC-driven pancreatic tumors.
Figure 28. Spatial organization of the eukaryotic genome.
Figure 29. B lymphocyte differentiation.
Figure 30. BPTF is required for B cell differentiation from early stages.
Figure 31. BPTF loss delays tumor onset in a murine model of Burkitt lymphoma.

Directory of Tables

TABLES

Table 1. Histone modifications, writers, readers and their function.
Table 2. Representative mouse models used to study c-MYC function.
Table 3. Summary of published NURF interactions with transcription factors.
Table 4. List of RT-qPCR primers used in this study
Table 5. List of ChIP-qPCR primers used in this study
Table 6. Top-ranking gene sets enriched in 4-OHT-treated control cells.
Table 7. Summary of human tumor datasets.

Abbreviations

ABBREVIATIONS

AP: Anterior-Posterior
bHLH-LZ: Basic Helix-Loop-Helix Leucine Zipper
BL: Burkitt Lymphoma
BM: Bone Marrow
BPTF: Bromodomain PHD Transcription Factor
BRCT: BRCA1 C-Terminus domain
BRD: Bromodomain
CDK: Cyclin-Dependent Kinase
CHD: Chromodomain Helicase DNA-binding
ChIP: Chromatin Immunoprecipitation
CLP: Common Lymphoid Progenitors
DDT: DNA binding homeobox and Different Transcription factors
DNA: Deoxyribonucleic Acid
DRD2: Dopamine Receptor D2
DSB: Double Strand Break
ESc: Embryonic Stem cells
FALZ: Fetal Alzheimer Antigen (also known as FAC1)
FDR: False Discovery Rate
GSEA: Gene Set Enrichment Analysis
GSK3: Glycogen Synthase Kinase-3
GTFs: General Transcription Factors
HAT: Histone Acetyl Transferases
HDAC: Histone De-acetylase
HFF: Human Foreskin Fibroblasts
HLH: Helix-Loop-Helix
HSC: Hematopoietic Stem Cells
INO80: INositol requiring 80
isPLA: *In situ* Proximity Ligation Assay
ISWI: Imitation SWItch
IUIM: Inverted Ubiquitin Interaction Motif
LDHA: Lactate DeHydrogenase A
LZ: Leucine-Zipper
MAPK: Mitogen-Activated Protein Kinase
MBD: Methyl-CpG-binding Domain
MBI-IV: MYC boxes
MBT: Malignant Brain Tumor domain
MEF: Murine Embryonic Fibroblast
mRNA: messenger RNA

MSigDB: Molecular Signature DataBase
NES: Normalized Enrichment Score
NLS: Nuclear Localization Sequence
NuRD: Nucleosome Remodelling and Deacetylation
NURF: Nucleosome Remodelling Factor
ORC: Origin Recognition Complex
OSK: Oct4, Sox2 and Klf4
PBZ: Poly ADP-ribose Binding Zinc finger
PHD: Plant Homeodomain
PIC: Pre-Initiation Complex
Pol II: RNA Polymerase II
PSEN1: Presenilin 1
P-TEFb: Positive Transcription Elongation Factor b
PWWP: Proline-tryptophan-tryptophan-Proline domain
rRNA: ribosomal RNA
SEM: Standard Error of Mean
SIM: Sumo Interaction Motif
SWI/SNF: SWItching defective/Sucrose Non-Fermenting
TAD: Transactivation domain (when referred to c-MYC) / Topologically Associated Domain (when referred to chromatin organization)
TBP: TATA-Binding Protein
tRNA: transfer RNA
TSS: Transcription Start Site
UIM: Ubiquitin Interaction Motif
WT: Wild Type

Introduction

INTRODUCTION

1. THE ROLE OF CHROMATIN DURING TRANSCRIPTION

1.1. Nucleosomes are the basic unit of chromatin

Chromatin is the complex of DNA, histones, and non-histone proteins from which eukaryotic chromosomes are formed. The nucleosome is the primary unit of chromatin and is composed of 147 bp of DNA wrapped 1.65 times around an octamer of the four core histones (H2A, H2B, H3, and H4). Structurally, core histones are relatively small proteins with a globular domain (the histone fold) and two N-terminal "tails". Consecutive nucleosome core particles are separated by unwrapped linker DNA of variable length (20-90 bp). In addition, one molecule of histone H1 associates at the position where the DNA enters and exits the nucleosome core, thus sealing the two turns of DNA (Laybourn and Kadonaga 1991). The multiple contact points between histones and DNA make the nucleosome a very stable complex and, for this reason, it is well suited for its packaging function. Nonetheless, its role extends beyond DNA compaction and occlusion. Nucleosomes are also dynamic participants in chromatin-directed processes such as transcription, replication, DNA repair, kinetochore and centromere construction, and telomere maintenance (Saha *et al*. 2006). Cells modulate the way chromatin is packed in order to regulate such processes. This involves the dynamic competition between nucleosomes and DNA-binding factors for regulatory sequences in the DNA (Li *et al*. 2007). This competition is mainly influenced by three different types of protein complexes. One family includes ATP-dependent remodelling complexes that weaken DNA-histone interactions, thereby facilitating nucleosome repositioning, reconfiguration or ejection (Kingston and Narlikar 1999). Another family includes chromatin-modifying enzymes that add or remove covalent modifications at particular residues within histones. The third family is constituted by the DNA methyltransferases (DNMTs) that methylate cytosines within CpG dinucleotides and thus regulate transcription, high-order chromatin structures and genome syability (Espada and Esteller 2010). Of note, histone modifying complexes and DNMTs work in concert with chromatin-remodelling complexes. Thus, the chromatin fibre is a dynamic and flexible structure that continuously changes in response to a wide range of biological inputs (Zhang and Reinberg 2001).

The linear string of nucleosomes ("beads on a string") is further packed into a 30-nm fibre where nucleosomes are arranged in a spiral or solenoid (Hayes and

Hansen 2001). The histone tails, although dispensable for the formation of the nucleosome, are required for inter-nucleosomal interactions and, together with histone H1, help condensing the DNA (Luger *et al.* 1997). Additional levels of compaction enable these fibres to be packaged into the small volume of the nucleus (Fig. 1).

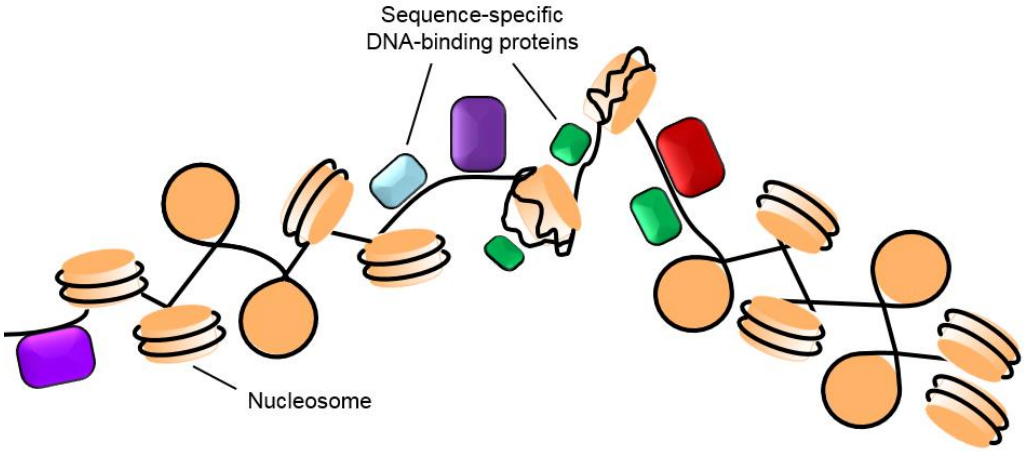

Figure 1. Schematic view of the 30-nm fibre. Sequence-specific DNA-binding factors bind to accessible regions in the linker DNA, the edge of the nucleosome or in remodelled nucleosomes. Regions of chromatin that are nucleosome-free or contain remodelled nucleosomes can often be detected experimentally by the unusually high susceptibility of their DNA to digestion by nucleases - as compared with the DNA in nucleosomes. *Adapted from* Alberts *et al* 2002.

1.2. Histone covalent modifications

Core histones are susceptible to a wide variety of post-translational modifications (up to 130), including methylation, acetylation, ubiquitination, ADP-ribosylation, sumoylation or phosphorylation (Kouzarides 2007; Tan *et al.* 2011) (Table 1). The majority of modifications take place at the N-terminal tails of histones, with a few exceptions occurring within the globular regions (e.g. phosphorylation of H3Y41) (Dawson *et al*. 2009). The distribution of these modifications is tightly regulated and is crucial for their functional outcome.

Histone modifications serve two main functions. First (with the exception of methylation), they alter the net charge of histones and thus enhance or loosen the non-covalent interactions within and between nucleosomes. Second, they serve as docking sites for the recruitment of epigenetic readers with unique domains that specifically recognize these modifications. These chromatin readers recruit in turn additional chromatin modifiers and remodelling enzymes, which perform diverse chromatin functions (Dawson and Kouzarides 2012).

It has been suggested that histone modifications act sequentially or in combination to form a 'histone code' that determines the downstream events (Strahl and Allis 2000).

Histone modification	Residues	Writers	Reader Motif	Role
Acetylation	K-ac	CBP/p300; HAT1; PCAF; TIP60; HB01	Bromodomain Tandem, PHD	Transcription, repair, replication and condensation
Methylation (K)	K-me1, K-me2, K-me3	MLL1,2,3,4,5; CLL8; G9a SET1A,B; NSD1; EZH2; ASH1, SUV39H1,2; RIZ-1; DOT1; SUV420H1,2	Chromodomain, Tudor, MBT, PWWP, PHD, WD40/β propeller	Transcription, repair
Methylation (R)	R-me1, R-me2s, R-me2a	PRMT1,4,5,6	Tudor	Transcription
Phosphorylation (S and T)	S-ph, T-ph	Haspin; MSK1; MSK2; CKII; Mst1	14-3-3, BRCT	Transcription, repair and condensation
Phosphorylation (Y)	Y-ph	JAK2	SH2	Transcription, repair
Ubiquitylation	K-ub	Bmi/Ring1A; RNF20/RNF40	UIM, IUIM	Transcription, repair
Sumoylation	K-su	Unknown	SIM	Transcription, repair
ADP ribosylation	E-ar	PARP	Macro, PBZ	Transcription, repair
Deimination	R → Cit	PADI4	Unknown	Transcription, decondensation
Proline isomerisation	P-cis ↔ P-trans	ScFPR4	Unknown	Transcription
Crotonylation	K-cr	Unknown	Unknown	Transcription
Propionylation	K-pr	Unknown	Unknown	Unknown
Butyrylation	K-bu	Unknown	Unknown	Unknown
Formylation	K-fo	Unknown	Unknown	Unknown
Hydroxylation	Y-oh	Unknown	Unknown	Unknown
O-GLcNAcylation (S and T)	S-GlcNAc; T-GlcNAc	O-GlcNAc transferase	Unknown	Transcription

Table 1. Histone modifications, writers, readers and their function. Modifications: me1, mono-methylation; me2, di-methylation; me3, tri-methylation; me2s, symmetrical di-methylation; me2a, asymmetrical di-methylation; Cit, citrulline. Reader domains: MBD, methyl-CpG-binding domain; PHD, plant homeodomain; MBT, malignant brain tumor domain; PWWP, proline-tryptophan-tryptophan-proline domain; BRCT, BRCA1 C-terminus domain; UIM, ubiquitin interaction motif; IUIM, inverted ubiquitin interaction motif; SIM, sumo interaction motif; PBZ, poly ADP-ribose binding zinc finger. *Adapted from* Dawson and Kouzarides 2012; Kouzarides 2007; and Bannister and Kouzarides 2011.

1.3. Chromatin remodelling

ATP-dependent chromatin remodelling enzymes disrupt DNA-histone contacts and, as a result, mobilize, evict or exchange histones. They operate in the context of multisubunit complexes, which have been divided into four major families according to their biochemical activity and subunit composition. Each of these families has a different mechanism of action and is composed of members with multiple chromatin reader motifs (e.g. bromodomains) that confer some specificity to their remodelling activities (Wang *et al*. 2007).

1. **ISWI** (Imitation Switch): With the exception of NURF and Iswi1, ISWI remodelling complexes slide nucleosomes in an orderly manner to repress gene transcription (Badenhorst *et al*. 2002; Morillon *et al*. 2003). In addition, they play key roles in chromatin assembly after DNA replication and maintenance of higher-order chromatin structures (Erdel and Rippe 2011).

2. **SWI/SNF** (SWItching defective/Sucrose Non-Fermenting): SWI complexes catalyse the sliding or ejection of nucleosomes (in part or as a whole) with the help of histone chaperones. Their function correlates with nucleosome disorganization, increased accessibility for transcription factor binding, and gene activation (Saha *et al*. 2006). Members of this family have also been implicated in DNA repair following DNA damage (Chai *et al.* 2005; Shim *et al*. 2007).

3. **INO80/SWR1** (INositol requiring 80): INO80 complexes have both activating and repressive effects on gene transcription. SWR1 complexes promote the incorporation of the histone variant H2A.Z into nucleosomes in a replication-independent manner (Mizuguchi *et al*. 2004). H2A.Z differs from canonical H2A in its amino acid sequence and stability, which depends on the histone H3 subtype present in the histone octamer. Hybrid nucleosomes containing both H2A.Z and the histone variant H3.3 are more unstable and prone to movement or ejection by chromatin remodellers (Jin and Felsenfeld 2007). In human cells, H2A.Z is preferentially enriched at poised promoters. Upon transcriptional activation, H2A.Z is rapidly evicted and its loss is required for full transcription (Zhang *et al.* 2005).

4. **NuRD/Mi-2/CHD** (Nucleosome Remodelling and Deacetylation/Mi-2/ Chromodomain Helicase DNA-binding): Members of this family primarily mediate transcriptional repression.

1.4. Histone variants

Nucleosomes are constructed from the four canonical histones (H2A, H2B, H3, and H4) or, alternatively, from histone variants with specific expression, localization, and species-distribution patterns (e.g. H3.3, macroH2A, H2A.Z, H2ABbd or H2A.X) (Kamakaka and Biggins 2005).

The genes encoding the four canonical histones cluster together in the genome and are transcribed during S phase. Conversely, genes encoding non-canonical histones are found singly in the genome and are constitutively expressed. Histone variants differ in their primary amino acid sequence from their canonical paralogues. These differences impact on their structure, intrinsic stability, the

length of DNA they wrap and even the direction of wrapping (Talbert and Henikoff 2010).

Whereas canonical histones function primarily in genome packaging and gene regulation; histone variants participate in a wide range of biological processes such as DNA repair, recombination, chromosome segregation, transcription, sex chromosome condensation, and sperm chromatin packaging.

1.5. Transcription in the chromatin context

Chromatin imposes significant obstacles on all aspects of transcription mediated by RNA Pol II, from initiation to elongation. In order for transcription to occur, chromatin structure is modulated through multiple mechanisms, including histone modification, eviction or reconfiguration, and chromatin remodelling.

The prototypical RNA Pol II transcription cycle begins with the binding of sequence-specific activating transcription factors upstream of the core promoter. The binding sites for these activators are primarily found in accessible regions (near the edge of the nucleosome or within the linker DNA) (e.g. c-MYC). However, there is a subset of pioneer transcription factors that can engage their cognate sites on the nucleosome surface as they only bind one face of the DNA and can accommodate nucleosomal DNA curvature (e.g. Oct4, Sox2 or Klf4) (Guccione *et al.* 2006; Soufi *et al*. 2012; Hebbar and Archer 2003).

The binding of activators to their target sequences triggers the recruitment of a variety of co-activators, including chromatin-remodelling complexes, histone-modifying enzymes, and Mediator[1]. The chromatin remodelling directed by co-activators at promoters enhances the binding of activators and makes nucleosomal DNA elements more accessible to both general transcription factors (GTFs: TBP and TFIIA, B, D, E, F and H) and Pol II. The binding of the GTFs and Pol II to DNA occurs in a tightly regulated sequence of events to eventually form the preinitiation complex (PIC). At this point, Pol II remains at the promoter, synthesizing short lengths of RNA until it is released and starts elongating the nascent mRNA.

In order for elongation to occur, the GTF TFIIH phosphorylates RNA Pol II 'tail' (CTD or C-terminal domain) in Ser5 (Phatnani and Greenleaf 2006). The polymerase then disengages from the cluster of GTFs and, as it starts travelling into the coding region, it undergoes a second phosphorylation in Ser2 catalysed

[1] MEDIATOR: Protein complex which allows the activator proteins to communicate properly with RNA polymerase II and the general transcription factors.

by the TAK/P-TEFb/CDK9 complex (Marshall *et al*. 1996). These events signal the recruitment of the elongation machinery (factors involved in polymerization, mRNA processing, and export) and couple them with alterations in chromatin function. One example is PAF, an elongation factor associated with Ser5-phosphorylated CTD that controls the binding of chromatin regulators, such as the H3K4 methyltransferase Set1, the histone ubiquitin ligase Rad6 or the chromatin-remodelling factor CHD1 (Li *et al*. 2007).

2. c-MYC

MYC genes are key modulators of cell proliferation and their deregulation contributes to almost every aspect of tumor cell biology (Adhikary and Eilers 2005). In mammals, the main MYC family constituents are c-MYC, N-MYC, and L-MYC, and they all share significant similarity in their genomic, RNA, and protein sequences. c-MYC was the first to be discovered as the cellular homolog of the transforming gene of the avian myelocytomatosis virus (Vennstrom *et al.* 1982). Despite the enormous progress done during these past 30 years of research, many aspects of c-MYC biology remain elusive (Wolf *et al.* 2014).

2.1. Protein structure and interaction partners

The gene coding for c-MYC is located on the human chromosome 8q24 and is comprised of three exons. The predominant product is c-MYC (also known as p64); however, alternative translational initiation gives rise to two additional naturally-occurring translation products: p67 and S-MYC (Hann *et al.* 1984; Sugiyama *et al.* 1989). A distinct function for p67 is not known, but the shorter S-MYC appears to play a role in stress response and might act as a dominant-negative MYC (Spotts *et al.* 1997).

The N-terminus of c-MYC contains an unstructured transactivation domain (TAD) which spans two highly conserved sequences known as MYC boxes (MBI and MBII). The TAD domain is followed by MYC boxes III and IV and a nuclear localization signal (Sarid *et al*. 1987; Fladvad *et al*. 2005; Cowling *et al*. 2006). MYC boxes participate in protein-protein interactions with E3 ubiquitin ligases that regulate c-MYC protein stability (FBW7 and SKP2) (Yada *et al*. 2004, Kim *et al*. 2003), together with co-factors that modulate its transcriptional activity. The latter include histone acetyltransferases or HATs (GCN5/PCAF, TIP60, and CBP/p300), the histone exchange factor p400, and components of the basal transcriptional machinery such as Mediator and P-TEFb (McMahon *et al.* 2000;

Frank *et al*. 2003; Kanazawa *et al*. 2003; Faiola *et al.* 2005; Martinato *et al*. 2008; Liu *et al*. 2008a). Two residues within the N-terminal domain of c-MYC control its stability: Ser62 (S62) and Thr58 (T58). Phosphorylation of S62 by mitogen-activated kinases stabilizes the protein, whereas phosphorylation of T58 by GSK3 (Glycogen Synthase Kinase-3) marks it for proteosomal degradation (Sears *et al*. 2000; Gregory *et al.* 2003). The C-terminus contains a basic DNA-binding domain tethered to a HLH-LZ motif involved in the dimerization with MAX (Blackwood and Eisenman 1991). In addition to its classical chromatin-recruitment role, the C-terminal domain of c-MYC is also involved in transactivation through the recruitment of the H3K27 acetyltransferase CBP/p300 and the nucleosome remodeler SWI/SNF (Cheng *et al.* 1999; Park *et al*. 2002; Vervoorts *et al.* 2003) (Fig. 2).

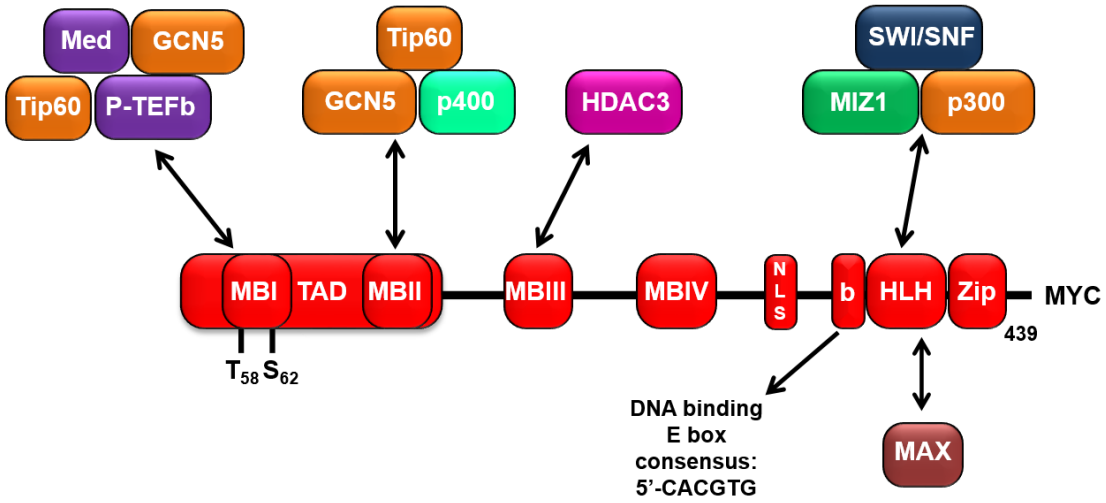

Figure 2. Structural organization of c-MYC and interaction partners. Two key phosphorylation sites are indicated at Thr58 and Ser62. MB, conserved MYC boxes; TAD, transactivation domain; NLS, nuclear localization sequence; b, basic region; HLH, helix-loop-helix; Zip, leucine zipper region; Med, Mediator. *Adapted from* Lüscher and Vervoorts 2012 *and* Adhikary and Eilers 2005.

2.2. c-MYC control of gene transcription

c-MYC mainly operates as a transcription factor that either activates or represses gene expression, although some non-transcriptional roles have been attributed to it as well (Dominguez-Sola *et al*. 2007; Cowling and Cole 2007). Transcriptional activation occurs through dimerization with MAX and binding to the consensus DNA sequence CACGTG (E-box). Of note, c-MYC binding to non-canonical E-boxes and non-E-box targets has also been reported (Blackwell *et al.* 1993; Zeller *et al*. 2006; Guccione *et al.* 2006).

The interaction with MAX is required for many of c-MYC biological functions, although c-MYC appears to function in the absence of a functional MAX protein in PC12 cells and in *Drosophila* (Hopewell *et al.* 1995; Steiger *et al.* 2008).

MAX also binds bHLH-LZ-containing proteins of the MAD family and the resulting dimers recognize the same consensus E-boxes as c-MYC:MAX. MAD proteins antagonize c-MYC function by competing with c-MYC proteins for free MAX, competing with c-MYC:MAX dimers for available binding sites, and recruiting repressor complexes such as SIN3 and its associated factors N-COR and HDAC1 at bound sites (Alland *et al*. 1997). In contrast to MAX, which is ubiquitously expressed, MAD proteins levels are tightly regulated and restrict c-MYC's functional access to DNA.

2.2.1. *Widespread binding to chromatin*

Numerous studies based on chromatin immunoprecipitation (ChIP) have shown that c-MYC associates with a large fraction of cellular genes in a variety of cell types (Schuhmacher *et al.* 2001; O'Connell *et al*. 2003; Fernandez *et al.* 2003; Li *et al.* 2005). These c-MYC target signatures show little overlap (Chandriani *et al.* 2009). The small set of genes common to all c-MYC signatures is involved in processes directed towards biomass accumulation or cell growth (ribosome biogenesis, protein synthesis, and mitochondrial function) (Ji *et al*. 2011). Not only c-MYC modulates hundreds of genes, but it also controls genes transcribed by all three RNA polymerases. Thus, besides protein-coding genes and non-coding RNAs controlled by Pol II, c-MYC regulates rRNAs and tRNAs transcribed by Pol I and Pol III, respectively (Arabi *et al.* 2005; Gomez-Roman *et al.* 2003).

When expressed at low physiological levels, c-MYC tends to occupy canonical E-boxes within CpG-rich promoters (CpG islands). These chromatin domains are H3K4-methylated and constitute high-affinity binding sites common to different cell lines (Fernandez *et al*. 2003; Guccione *et al*. 2006). c-MYC overexpression results in binding to low-affinity non-canonical E-boxes situated at active regulatory elements in a process termed 'invasion' (Fernandez *et al*. 2003; Lin *et al*. 2012; Sabò *et al*. 2014).

Genome-wide mapping of c-MYC-binding sites and associated gene expression studies established that c-MYC is required but not sufficient to drive gene transcription. c-MYC cooperates with other sequence-specific regulators to activate the transcription of its targets, such as E2F (Zeller *et al*. 2006), estrogen receptor α (ERα) (Cheng *et al*. 2006) and the stem cell factors Sox2, Oct4, and Klf4 (Kim *et al*. 2010).

2.2.2. *Transcriptional activation*

c-MYC sequence-specific DNA binding is restricted by epigenetic mechanisms. In particular, c-MYC target sites are preferentially found within *euchromatic islands* of transcriptionally active genes: chromatin domains enriched in CpG islands and activating histone marks (H3K4me3, H3K79me2, and H2A.Z) (Guccione *et al*. 2006; Lin *et al*. 2012). The observation that c-MYC binding does not alter H3K4me3 levels, together with the fact that half c-MYC binding loci do not contain any E-box, suggests that an active chromatin configuration acts upstream and is a better determinant of c-MYC binding than DNA sequence (Martinato *et al*. 2008; Fernandez *et al*. 2003; Guccione *et al.* 2006).

Once bound to its target promoters, c-MYC recruits multiple cofactors that introduce additional changes in the chromatin, resulting in higher DNA accessibility and transcriptional activation (Fig. 3). Among these cofactors are complexes with histone acetyltransferase activity, such as PCAF, TIP60, p300/CBP, and the GCN5-containing complexes TFTC and STAGA (Frank *et al.* 2003; Bedford *et al.* 2010; McMahon *et al*. 2000; Nagy and Tora 2007). Histone hyper-acetylation reduces the ionic interactions of the positively charged histone tails with the negatively charged DNA backbone, thus increasing DNA accessibility. Additionally, histone acetylation promotes the assembly of higher-order transcriptional complexes by recruiting proteins with acetyl-lysine-binding modules or bromodomains. One example is BRD4, a member of the BET subfamily of human bromodomain proteins that associates with acetylated chromatin and facilitates transcription via direct interaction with P-TEFb and Mediator (Dey *et al.* 2009; Dawson *et al*. 2011). c-MYC further modulates DNA accessibility through the recruitment of the chromatin-remodelling complex SWI/SNF. This complex catalyzes ATP-dependent nucleosome eviction and plays an essential role in transcription (Cheng *et al.* 1999). Interestingly, several lines of evidence suggest that the SWI/SNF complex and HATs act synergistically to establish a local chromatin structure that is permissive for subsequent events (Fry and Peterson 2001). c-MYC also promotes the incorporation of H2A.Z at target promoters, a histone variant associated with transcriptionally active genes (Martinato *et al.* 2008).

In addition to increasing promoter accessibility, c-MYC regulates transcription by controlling RNA Pol II activity and mRNA processing. c-MYC recruits P-TEFb and TFIIH to target genes, which phosphorylate RNA Pol II C-terminal domain (CTD) and favour the release of promoter-paused Pol II (Rahl *et al.* 2010; Cowling and Cole 2006). Two mechanisms are involved in P-TEFb recruitment. Firstly, c-MYC

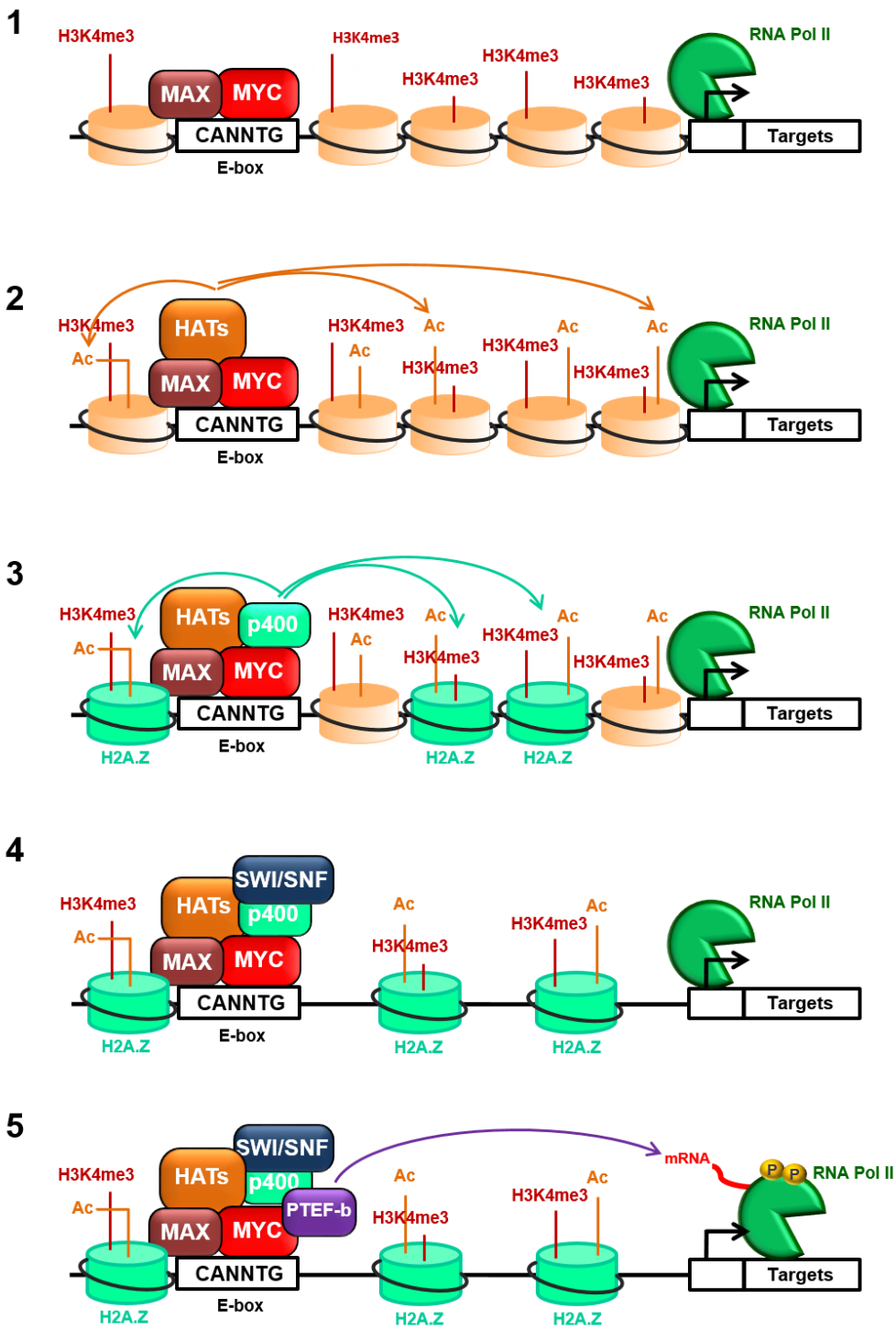

Figure 3. Model of c-MYC transactivation. A series of steps are summarized that provide a model how c-MYC regulates target genes in conjunction with acetyltransferases, chromatin remodelers and Pol II pause release factors. *Adapted from* Lüscher and Vervoorts 2012.

interacts directly with two subunits of P-TEFb: CDK9 and cyclin T1 (Eberhardy and Farnham 2001). Secondly, c-MYC induces histone hyper-acetylation at target chromatin, thus promoting BRD4:P-TEFb recruitment. Phosphorylation of Pol II

also triggers the recruitment of mRNA capping and splicing factors, which are essential for the processing of the emerging transcript (Cowling and Cole 2010). In summary, c-MYC drives transcription by recruiting multiple co-factors to promoters in a pre-existing transcriptionally active or poised state and further modulating their activity.

It has been suggested that c-MYC does not have a unique transcriptional program but, instead, it targets all active promoters and enhancers in the genome and acts as a non-specific general amplifier of transcription (Lin *et al*. 2012; Nie *et al.* 2012). Conversely, two recent reports offered an alternative to the amplifier model, showing that c-MYC can actually activate and repress discrete gene sets. The authors hypothesized that RNA amplification and promoter/enhancer occupancy by c-MYC are in fact separable events. The increase in global RNA production would be an indirect effect, explained by the nature of the targets regulated by c-MYC (e.g. proteins involved in nucleotide synthesis) (Sabò *et al*. 2014; Walz *et al*. 2014; Dang 2014).

2.2.3. *Transcriptional repression*

Ectopic expression of c-MYC leads to down-regulation of specific genes encoding negative regulators of cell proliferation (e.g. *Cdkn2b*, *Cdkn2c* or *Cdkn1a*) and proteins involved in cell adhesion (*Itgb1*) and cell-cell communication. c-MYC represses transcription by binding to the core promoter of target genes. Some original studies suggested that this process occurred independently of c-MYC binding to DNA. However, c-MYC recruitment to *Cdkn2b* requires dimerization with MAX, and E-box elements have been found in the core promoter of genes repressed by c-MYC (Herkert and Eilers 2010).

Mechanistically, c-MYC represses transcription by binding to two transcription factors: MIZ1 and SP1 (Peukert *et al.* 1997; Gartel *et al*. 2001). The interaction with c-MYC results in the displacement of the co-factors CBP/p300 and nucleophosmin (NPM), and recruitment of repressors such as the histone deacetylase HDAC3 and the DNA methyltransferase DNMT3A (Staller *et al.* 2001; Brenner *et al*. 2005; Kurland and Tansey 2008; Wanzel *et al*. 2008). c-MYC also modulates MIZ1 through the induction of RPL23, a ribosomal protein that sequesters NPM to the nucleolus and thus hampers MIZ1 activity (Wanzel *et al*. 2008). The case of TGFβ-mediated cell cycle arrest illustrates the MYC-MIZ1 interaction. In the absence of TGFβ signalling, c-MYC represses *Cdkn2b* ($p15^{INK4B}$) in a complex with MIZ1. Increased levels of TGFβ lead to phosphorylation and nuclear translocation of SMAD proteins, which cooperate with MIZ1 in inducing

Cdkn2b expression. In parallel, activated SMADs inhibit *c-Myc* transcription (Seoane *et al*. 2001).

2.3. c-MYC biological roles

c-MYC is almost universally present in proliferating normal somatic cells, where it operates as an integrator of extracellular stimuli transduced by multiple signaling cascades (e.g. Wnt, Ras/Raf/MAPK, JAK/STAT or TGFb). As a result, it modulates a wide range of cellular processes such as proliferation, growth, apoptosis, metabolism, and differentiation. In normal cells, c-MYC is under tight transcriptional and post-transcriptional control, and its expression is continuously dependent upon mitogenic signalling.

By contrast, cancer cells typically show a deregulated and elevated c-MYC expression, which is responsible for changes in chromatin structure, ribosome biogenesis, metabolic pathways, cell, and angiogenesis among others (Lin *et al*. 2012) (Fig. 4).

2.3.1. *Cell proliferation and differentiation*

c-MYC has a crucial role in cell division by controlling the transition from G_0/G_1 to S phase. It regulates proliferation by transcriptionally activating genes involved in cell cycle progression (e.g. cyclin D1, cyclin D2 or CDK4) and repressing checkpoint genes and cyclin-dependent kinase inhibitors (e.g. GADD45, $p15^{INK4B}$ or $p21^{CIP1}$). Moreover, c-MYC enhances DNA replication by binding to pre-replicative complexes and promoting origin firing (Dominguez-Sola *et al.* 2007). c-MYC overexpression and/or deregulation is associated with unscheduled firing of DNA replication origins, DNA damage response, and checkpoint activation (Murga *et al.* 2011).

Several experiments document the ability of c-MYC to inhibit differentiation of various cell types *in vitro* (e.g. murine ES cells) and *in vivo* (e.g. B cell lymphomas) (Cartwright *et al*. 2005; Langdon *et al*. 1986). However, c-MYC role is far more complex. In tissues where commitment to a specific lineage is linked to an increase in proliferation, c-MYC promotes cell differentiation by controlling the exit from the stem cell niche. One example is the skin, where ectopic expression of c-MYC is associated with the depletion of the stem cell compartment and an accumulation of differentiated layers (Waikel *et al*. 2001). Part of c-MYC role in driving differentiation of keratinocytes involves its ability to reduce adhesive interactions of stem cells with their niche (Gebhardt *et al.* 2006).

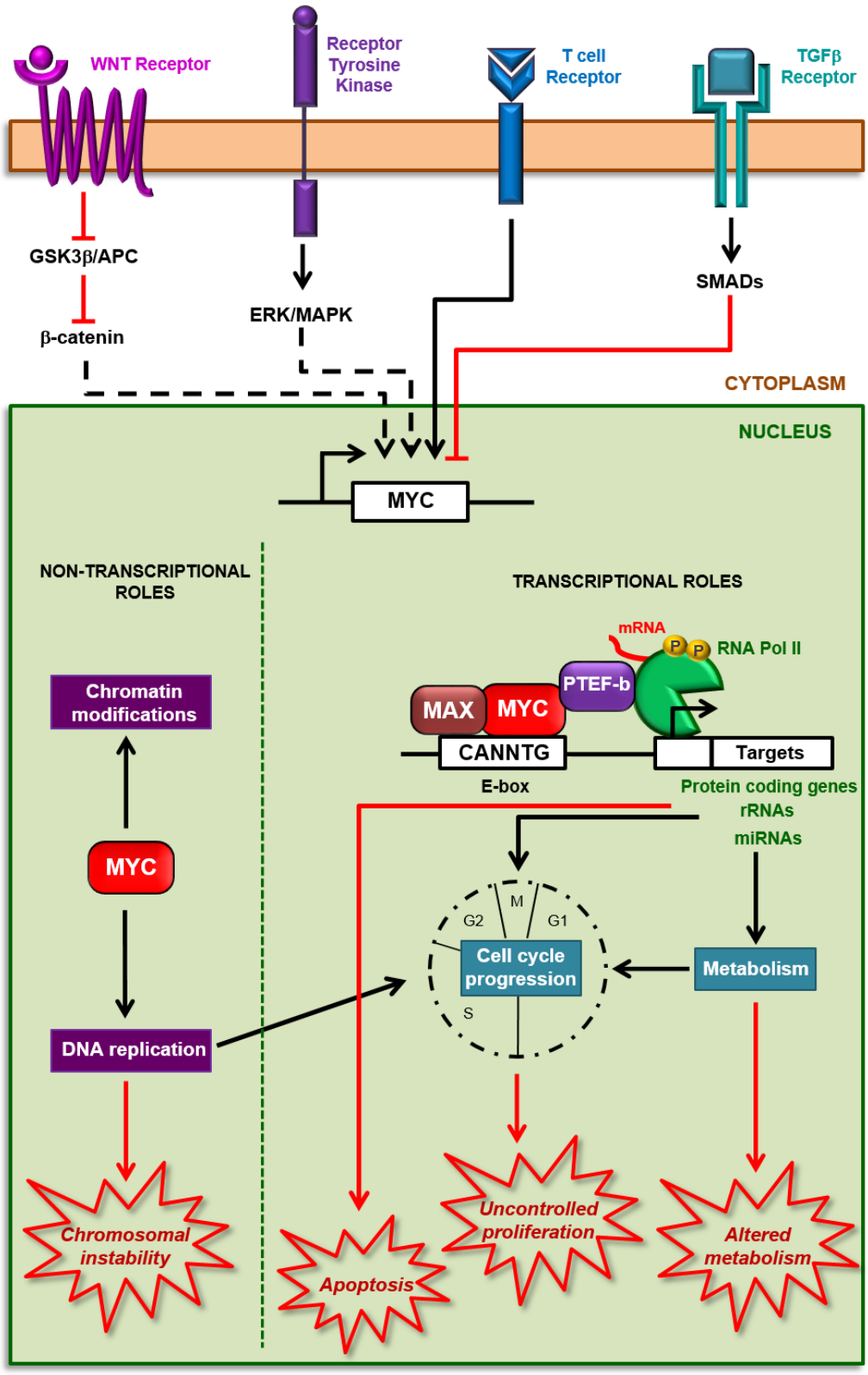

Figure 4. Schematic representation of the cellular functions mediated by c-MYC under physiological and oncogenic (red shapes) situations. c-MYC can influence transcription of protein-coding genes, as well as noncoding rRNAs and miRNAs. c-MYC can also stimulate DNA replication and chromatin remodelling by non-transcriptional functions. Deregulation of c-MYC activity at any of these levels can contribute to oncogenic transformation (red arrows). *Adapted from* Laurenti *et al*. 2009.

2.3.2. *Cell growth and metabolism*

c-MYC promotes cell growth by providing the cell with an abundant supply of basic building blocks as well as increasing cell metabolism and protein synthesis. Several c-MYC target genes participate in this activity, including those associated with metabolism, ribosomal and mitochondrial biogenesis, and protein and nucleic acid synthesis.

2.3.3. *Apoptosis*

Ectopic expression of c-MYC in the presence of limiting survival signals or cell stress sensitizes cells to undergo apoptosis. This phenomenon has been reported in both cells and transgenic mice in which c-MYC is expressed under the control of a foreign promoter (Evan *et al.* 1992; Jacobsen *et al*. 1994). c-MYC-induced apoptosis is an example of intrinsic tumor suppression, a defence mechanism against the tumorigenic potential of oncogenes. In fact, suppression of c-MYC pro-apoptotic activity is essential to tumorigenesis. Noticeably, it is overexpression, rather than deregulation, what is required in order for c-MYC to trigger apoptosis (Murphy *et al.* 2008).

Several mechanisms are involved in c-MYC-mediated apoptosis. High c-MYC levels upregulate $p19^{ARF}$, an inhibitor of the MDM2 E3 ligase, which leads to the stabilization of p53 (Zindy *et al*. 1998). p53 regulates a cohort of target genes involved in apoptosis and growth arrest. FoxO transcription factors have been shown to mediate c-MYC-induced $p19^{ARF}$ expression through direct binding to the *Ink4a/Arf* locus (Bouchard *et al.* 2007).

c-MYC can also trigger apoptosis by altering the balance between pro- and anti-apoptotic factors, in parallel with or independent of p53. c-MYC indirectly suppresses the anti-apoptotic proteins BCL2 and $BCL\text{-}X_L$ and induces the pro-apoptotic Bax and BIM (Strasser *et al.* 1990; Eischen *et al*. 2001; Mitchel *et al*. 2000; Egle *et al*. 2004). These events lead to the release of cytochrome c from the mitochondria and the subsequent activation of downstream effector caspases.

Moreover, c-MYC overexpression activates apoptosis through the induction of DNA instability and breaks. This appears to be the consequence of several mechanisms: inhibition of double-stranded DNA repair and/or increase in reactive oxygen species (Vafa *et al.* 2002; Karlsson *et al.* 2003).

2.3.4. *Tumorigenesis*

c-MYC is over-expressed and/or deregulated in more than half of human cancers (Gabay *et al.* 2014); high levels being associated with aggressive, poorly

differentiated tumors. This occurs through multiple mechanisms, including amplification, chromosomal translocation, single nucleotide polymorphisms in regulatory regions, constitutive activation of upstream signalling pathways and mutations that enhance c-MYC protein stability (Eilers and Eisenman 2008; Meyer and Penn 2008).

Even though c-MYC is one of the most potent oncogenes, its sole activation in normal cells is not able to induce neoplastic transformation. Moreover, tumors that arise from c-MYC transgenic mice are clonal, suggesting that additional mutations are required for tumor formation. c-MYC-induced cell transformation is restrained by two mechanisms. First, c-MYC half-life and function are modulated by Ras-dependent signalling pathways. Second, several mechanisms exist that protect cells from unchecked cell growth: proliferative arrest, senescence, and/or apoptosis. Therefore, Ras activating mutations and genetic events that abrogate these checkpoints (e.g. p53 loss) often synergize with c-MYC to induce tumors (Adhikary and Eilers 2005).

When pathologically activated in a permissive context, c-MYC enforces many of the "hallmark" features of cancer, including relentless DNA replication, cellular proliferation and growth, protein synthesis, and altered metabolism. c-MYC mandates tumor cell fate by inducing stemness and blocking cellular senescence and differentiation. Additionally, c-MYC orchestrates changes in the tumor microenvironment, including the activation of angiogenesis and suppression of the host immune response (Gabay *et al*. 2014).

c-MYC plays a role both in tumor initiation and maintenance. In transgenic mouse models with inducible c-MYC, established tumors regress upon withdrawal of c-MYC ectopic expression (e.g. hematopoietic, epithelial, and mesenchymal tumors) (Arvanitis and Felsher 2006). Interestingly, brief suppression of c-MYC using the inducible dominant negative 'Omomyc' can result in restoration of checkpoint mechanisms, resulting in tumor regression, remodelling of the tumor microenvironment, and shutdown of angiogenesis. Therefore, tumors appear to be "addicted" to c-MYC (Soucek *et al*. 2002; Soucek *et al*. 2008).

Cellular transformation by c-MYC depends on specific cell cycle and metabolic pathways. For example, c-MYC enhances glucose uptake and glycolysis through transcriptional activation of different target genes, including lactate dehydrogenase A (LDHA). Induction of LDHA might explain the "Warburg effect"; namely, the observation that tumor cells show enhanced rates of glycolysis even under aerobic conditions (Shim *et al.* 1997).

Several transgenic mouse models have been developed to elucidate the mechanism whereby deregulated c-MYC contributes to tumorigenesis (Table 2).

Model	Strategy	Tumor	Reference
MMTV–MYC	MYC expression under the control of the hormone-responsive MMTV promoter	Mammary adenocarcinoma developing after first pregnancy	Stewart *et al.* 1984
WAP–MYC	MYC expression under the control of the mammary-specific, hormone-responsive WAP	Mammary adenocarcinoma, expression in tumour material becomes independent of hormone stimulation	Schoenenberger *et al.* 1988
Eμ–MYC	MYC expression under the control of the immunoglobulin enhancer	Clonal B-cell lymphoma	Adams *et al.* 1985
ELA–MYC	MYC expression under the control of the elastase promoter	Acinar cell carcinomas and ductal adenocarcinomas	Sandgren *et al.* 1991
ALB–MYC	MYC expression under the control of the albumin enhancer/promoter	Hepatocellular adenomas	Murakami *et al.* 1993

Table 2. Representative mouse models used to study c-MYC function. *Adapted from* Meyer and Penn 2008.

2.3.5. *Reprogramming*

While not absolutely required, ectopic expression of c-MYC augments the efficiency and kinetics of formation of pluripotent cells from mouse and human fibroblasts and mature B cells (Nakagawa *et al.* 2008; Takahashi *et al.* 2007; Hanna *et al.* 2008). c-MYC facilitates the initial steps of the reprogramming process, both repressing fibroblast-specific genes and enhancing the binding of OSK (Oct4, Sox2 and Klf4) to chromatin (Soufi *et al*. 2012; Sridharan *et al*. 2009). In addition, c-MYC fulfils other functions such as regulating DNA replication and global histone acetylation, which may facilitate the reprogramming process more indirectly.

3. BPTF

Chromatin constitutes a barrier for the interaction of trans-acting factors with DNA and thus regulates processes such as transcription, DNA replication, DNA repair, and recombination. Epigenetic mechanisms that regulate DNA accessibility include post-translational modifications of histones, DNA methylation, incorporation of histone variants, and nucleosome remodelling activities. The latter two are mainly orchestrated by ATP-dependent chromatin remodelling complexes. These complexes are in turn grouped in 4 sub-families based on the sequence homology of the associated ATPase: SWI/SNF, ISWI, CHD, and INO80.

BPTF (Bromodomain PHD Transcription Factor) is the mammalian orthologue of *Drosophila* Nurf301 and constitutes the largest and essential subunit of the ISWI complex NURF (Nucleosome Remodelling Factor). NURF is an ATP-dependent chromatin remodeller that catalyses nucleosome sliding without eviction or exchange of histones from the nucleosome. Mammalian NURF consists of BPTF, SNF2L (an ISWI ATPase), and RbAp46/48, a histone-binding protein found in several chromatin-related complexes (Jones *et al.* 2000; Hamiche *et al.* 1999; Barak *et al*. 2003). BPTF provides sequence specificity to NURF through interactions with transcription factors and histone modifications (Xiao *et al.* 2001; Alkhatib *et al*. 2011).

3.1. Protein structure and interactors

The *BPTF* gene maps to the 17q24.3 locus and codes for two protein products: BPTF (2871 aa) and its C-terminal truncated version FALZ (Fetal Alzheimer Antigen or FAC1). While BPTF is ubiquitously expressed in adult tissues, FALZ is restricted to the brain neocortex. It was proposed that FAC1 acts as a transcriptional regulator through binding to a consensus DNA sequence present in genes implicated in neurodegenerative disorders (e.g. *PSEN1* or *DRD2*) (Jordan-Sciutto *et al*. 1999a).

The functional domains within BPTF are consistent with a role for this protein in chromatin-mediated regulation of transcription. The N-terminus of BPTF contains a HMGA domain or acidic patch, a DDT DNA-binding domain, and a PHD domain. The C-terminal domain of BPTF includes a glutamine-rich region which is intrinsically disordered, a second PHD domain, and a bromodomain. The latter two constitute a histone recognition module that binds H3K4me2/3 and H4K16ac, respectively (Doerks *et al*. 2001; Wysocka *et al.* 2006; Ruthenburg *et al*. 2011). Additional features include nuclear localization signals, proline-rich regions, and LXXLL motifs that could be important for the interaction with nuclear receptors (Savkur and Burris 2004).

Human BPTF preferentially associates with H2A.Z, a histone variant incorporated at promoter and regulatory regions whose deposition correlates with gene expression (Marques *et al*. 2010). Moreover, the ATPase SNF2L preferentially remodels H2A.Z-containing chromatin (Goldman *et al*. 2010).

3.2. Biological function of BPTF

3.2.1. *Transcriptional activator and repressor*

Chromatin remodelling machines have been traditionally thought to be required exclusively during gene activation to expose or "open-up" chromatin. In agreement with this view, NURF has been shown to facilitate transcription of chromatin *in vitro* and *in vivo*. This effect is not observed with naked DNA templates, suggesting that it functions to relieve the inhibitory effects of chromatin on transcription (Mizuguchi *et al.* 1997; Badenhorst *et al*. 2002). However, several lines of evidence indicate that NURF can also repress gene transcription (Goldmark *et al*. 2000; Badenhorst *et al*. 2002; Landry *et al*. 2008).

Many studies have shown interactions between BPTF/Nurf301 and both ubiquitous (AP-1, SRF or Usf1) and cell-type-restricted (PR and Smad) transcription factors (Table 3). As a result, BPTF regulates the expression of a largely non-overlapping set of genes between cell types (Qiu *et al*. 2015). This stands in contrast to members of the SWI/SNF family, which have more global roles in regulating gene expression through interactions with RNA polymerase (Armstrong *et al.* 2002).

Organism	Interaction partner	Biological function	Molecular function
D. melanogaster	GAGA	Heat shock, embryo patterning	Chromatin structure
D. melanogaster	HSF	Stress response	Heat shock
D. melanogaster	EcR	Larval metamorphosis	Ecdysteroid signaling
D. melanogaster	Ken	Innate immune system	Cytokine signaling
D. melanogaster	Armadillo	Wing development	Wingless signaling
D. melanogaster	HP2	Heterochromatin	Gene silencing
D. melanogaster	TRF2 and TAF4b	Cell proliferation	Regulation of genes involved in DNA replication
D. melanogaster	Pzg	Wing development	Notch, ecdysone, JAK/STAT signaling
M. musculus	AP-1	Thymocyte development	T cell receptor signaling
M. musculus/H. sapiens	SRF	Thymocyte development	T cell receptor signaling
M. musculus/H. sapiens	Smad2	Gastrulation	Nodal signaling
D. melanogaster/H. sapiens	PR	MMTV transcription/Female reproduction	Expression of MMTV viral genome Regulator of hCGH response
G. gallus/H. sapiens	Usf1	Globin gene regulation	Insulator function
H. sapiens	MAZ	Tissue development	Cell type specific regulation of GC containing promoters
H. sapiens	hKeap1	Stress response	Redox signaling
H. sapiens	CTCF	Gene expression	Nucleosome occupancy at regions enriched in Ctcf and cohesin

Table 3. Summary of published NURF interactions with transcription factors. Adapted from Alkhatib *et al*. 2011.

3.2.2. *Chromatin structure*

In addition to having key roles in transcription, NURF is a general regulator of chromatin structure.

Inactivation of *Drosophila* Nurf301 leads to dramatic decondensation of the male X chromosome (Badenhorst *et al*. 2002). NURF effects on X chromosome chromatin architecture could be direct, through nucleosome remodelling, or indirect, through the transcriptional regulation of genes involved in this process. One possible mechanism would be through NURF-dependent localization of the ATAC acetyltransferase (Carré *et al*. 2008).

NURF has also been characterized as a regulator of insulator elements in a number of contexts. *Drosophila* NURF has been proposed to be recruited to insulators by the GAGA factor, where it repositions nucleosomes to facilitate insulator function (Xiao *et al*. 2001; Li *et al*. 2010). Similarly, human NURF is critical for the barrier function of the USF-bound insulator 5'HS4, which prevents erythroid genes from encroachment by heterochromatin (Li *et al*. 2011).

Interestingly, a recent report identified BPTF as a facilitator of the interchromosomal interactions that take place between the enhancers of olfactory receptor genes. These long-range interactions account for the robustness of olfactory gene expression (Markenscoff-Papadimitriou *et al*. 2014).

Overall, these data suggest that BPTF:NURF modulates gene expression directly, through the interaction with transcription factors, and indirectly, through the regulation of high-order chromatin structures.

3.2.3. *Developmental regulator*

NURF has been shown to be essential for specific stages of metazoan development, functioning in pathways signalling to the nucleus, including heat shock, TGFβ/Smad, JAK/STAT, WNT/β-catenin, and nuclear hormone receptors.

D. melanogaster: Nurf301 is required to maintain homeotic gene expression during development, represses JAK/STAT signalling in the immune system, and promotes ecdysone signalling during metamorphosis (Xiao *et al.* 2001; Badenhorst *et al*. 2002; Badenhorst *et al.* 2005; Kwon *et al*. 2008). It also plays a role in the development of larval blood cells and in the maintenance of the germ stem cells compartment in *Drosophila* testis (Badenhorst *et al*. 2002; Cherry and Matunis 2010).

M. musculus: *Bptf* knockout mice do not gastrulate due to defects in the differentiation of extra-embryonic tissue lineages: the distal visceral endoderm

and the ectoplacental cone (Goller *et al*. 2008; Landry *et al.* 2008). For this reason, the characterization of NURF function in the adult mammal has been limited. Cre-LoxP conditional knockout technology revealed that BPTF is essential for adult thymocyte development (Landry *et al*. 2011).

H. sapiens: In a competitive epidermal reconstitution assay, BPTF was identified as a negative regulator of epidermal differentiation (Mulder *et al*. 2012).

3.3. BPTF in human cancer

Several lines of evidence suggest that BPTF could play a tumor-promoting role in human cancer. Firstly, primary human cancers and cancer cell lines frequently duplicate the 17q chromosome arm containing the *BPTF* gene. In fact, partial gain of 17q is the most abundant genetic alteration in neuroblastoma (Bown *et al.* 1999; Alkhatib *et al*. 2011). Secondly, mutations targeting *BPTF* have been reported for several human tumors (e.g. lung, breast, bladder, liver, and uterine cancer) (Xiao *et al.* 2014a; Balbás-Martínez *et al*. 2013; Fujimoto *et al*. 2012; González-Pérez *et al*. 2013). Finally, BPTF was appointed in a recent report as an independent marker for survival prediction in hepatocellular carcinoma patients; high BPTF levels being associated with invasiveness, recurrence, and poor outcome (Xiao *et al*. 2014b).

Aims

AIMS

The specific aims for this thesis were:

1. To investigate the role of BPTF in normal mammalian cells by analyzing the effect of its inactivation in both cell lines and mouse tissues.
2. To assess the function of BPTF in c-MYC transcriptional activity using a combination of biochemical assays and genome-wide approaches.
3. To study the role of BPTF in c-MYC biological activity using cell cultures expressing a tamoxifen-inducible form of c-MYC.
4. To determine the relevance of BPTF in tumorigenesis by analyzing publicly available genomic data on human tumors and also by studying the impact of its inactivation on mouse genetic models of cancer.

Objetivos

OBJETIVOS

Los objetivos específicos de esta tesis fueron:

1. Investigar la función de BPTF en células normales de mamífero por medio del análisis de los efectos de su inactivación en líneas celulares y tejidos de ratón.
2. Evaluar el papel de BPTF en la actividad transcripcional de c-MYC usando una combinación de ensayos bioquímicos y aproximaciones genómicas globales.
3. Estudiar el papel de BPTF en la actividad biológica de c-MYC usando cultivos celulares que expresan una forma de c-MYC inducible por tamoxifeno.
4. Determinar la relevancia de BPTF en cáncer por medio del análisis de datos genómicos públicos de tumores humanos así como del estudio del impacto de su inactivación en modelos genéticos murinos de cáncer.

Materials and Methods

MATERIALS AND METHODS

1. CELL CULTURE

1.1. Cell lines and reagents

Primary neonatal human foreskin fibroblasts (HFF), 293T (transformed human embryonic kidney cells), and human cancer cells - MIA PaCa-2, PK9 (pancreas) and VM-CUB-3 (bladder) - were cultured in Dulbecco's modified Eagle's medium (DMEM; Sigma-Aldrich, St Louis, MO, USA) supplemented with 10% Foetal Bovine Serum (FBS; HyClone, Logan, UT, USA), sodium pyruvate (Life Technologies, Madrid, Spain), and penicillin/streptomycin (Life Technologies). Mouse *Bptf*$^{+/+}$ and *Bptf*$^{lox/lox}$ MEFs (Murine Embryonic Fibroblasts) were cultured in DMEM supplemented with 10% FBS, sodium pyruvate, non-essential amino acids (Life Technologies), β-mercaptoethanol (Sigma-Aldrich), and penicillin/streptomycin. NAMALWA and RAJI Burkitt lymphoma cells were cultured in suspension in RPMI medium (Sigma-Aldrich) supplemented with 10% FBS and penicillin/ streptomycin.

MEFs were generated by mechanical disruption and trypsin-digestion of E13.5 embryos from which the foetal liver and the head had been removed. Recombination efficiency of exon 2 upon Cre recombinase expression was evaluated by PCR on genomic DNA as reported elsewhere (Landry *et al*. 2008). The following primers were used: CTCAGGAATTAAGAGGTAATTGACTATC, TGATTTAGTTCTGATTGTTAGGTCTAC, and AGACCAGCCTGTTCTACATGGCCAGCC. Additionally, recombination efficiency was assessed by RT-qPCR using the following primers:

Amplified region		*Sequence*	*Species*
Exon1-Exon2 Junction	Forward	AAGCAGCTTCAGGAGCCATA	Mouse
	Reverse	AGCAAAAAGGGGACAACCT	Mouse
Exon1-Exon3 Junction	Forward	CAGCAGCACTCCAGAGAAGA	Mouse
	Reverse	CGCTAGGAAGGACTTGTTGC	Mouse
Exon1-Exon4 Junction	Forward	CAGCAGCACTCCAGAGGAAA	Mouse
	Reverse	GCTCTTCTCAGCATCCTTGG	Mouse

1.2. Plasmids, viral constructs and virus production

Mission shRNAs (Sigma-Aldrich) were used to carry out RNA-interference experiments. Out of 3 BPTF-targeting shRNAs, two were selected because they provided optimal knockdown (shBPTF-1, clone TRCN0000016819; shBPTF-2, clone TRCN0000016820) and compared to a control non-targeting shRNA. MYC-

ER was expressed from the cDNA cloned into the FG12 plasmid by V.J. Sánchez-Arévalo (CNIO, Madrid). For lentiviral transduction of Cre recombinase, we used the lentiviral vector pLVXpuro-iCRE-ORF, a gift from C. Bar and M.A. Blasco (CNIO, Madrid). The packaging plasmid pCL-Eco and the retroviral constructs expressing pluripotency factors were generously provided by C.J. Lynch and M. Serrano (CNIO, Madrid).

Lentiviral production: Infectious lentiviruses were produced in 293T cells by calcium phosphate-mediated transfection of the lentiviral construct together with the packaging plasmids psPAX2 and pCMV-VSV-G. Post-transfection (48h), the medium was harvested twice for an additional 48h. Viral supernatants were filtered and either frozen down in aliquots or applied on target cells in the presence of 5 μg/ml polybrene. Cells were used after 48h puromycin selection (2 μg/ml). Human fibroblasts were infected first with lentivirus coding for MYC-ER, expanded, and then infected with either control or BPTF-targeting shRNAs. MEFs were infected concomitantly with lentivirus encoding for MYC-ER and Cre recombinase.

Retroviral production for reprogramming of MEFs into iPSc: Retroviral supernatants were produced in HEK-293T cells (5×10^6 cells per 100-mm-diameter dish) transfected with the packaging plasmid pCL-Eco (4 μg) together with one of the following retroviral constructs (4 μg): pMXs-Klf4, pMXs-Sox2, pMXs-Oct4 or pMXs-cMyc. Transfections were performed using Fugene-6 transfection reagent (Roche, Basel, Switzerland) according to the manufacturer's protocol. Two days post-transfection, retroviral supernatants were collected at 12 h intervals, each time adding fresh medium to the cells.

Infection of BL cell lines: BL cells (3×10^5 cells/well) were seeded on plastic plates coated with retronectin (Fisher Scientific, Pittsburgh, PA, USA) and preloaded with viral supernatants. After 3 additional rounds of infection with viral supernatants supplemented with polybrene (8 μg/ml), cells were allowed to recover for 24h, then selected for 48h in puromycin-containing medium (2 μg/ml). After selection, cells (sh#1, sh#2 and shNT) were plated ($5x10^3$/well in 96-well plates) in replicates. Viable cell count was assessed at the indicated time points by adding WST1 cell proliferation reagent (Roche) to each well and determining OD450 nm after 2 h, according to the manufacturer's instructions.

1.3. <u>iPS Reprogramming</u>

Early passage (2-3) primary MEFs were reprogrammed following a protocol described elsewhere (Li *et al*. 2009). Recipient MEFs were seeded the previous

day (150,000 cells on a 6-well plate) and received 1.5 ml of each of the corresponding retroviral supernatants (3F: 4.5 ml in total; 4F: 6 ml in total). This procedure was repeated 4 times in total. At 48 h after the first round of infection, medium was changed to iPSC medium (DMEM high glucose supplemented with serum replacement (KSR, 15%, Invitrogen), leukemia inhibitory factor (LIF) (1000 U/ml), non-essential amino acids, glutamax and β-mercaptoethanol). Cultures were maintained in the absence of drug selection with daily medium changes. At day 12-14, colonies with ES-like morphology were scored after staining for AP activity (BCIP/NBT Colour Development Substrate, Promega, S3771). Colonies were picked at day 14 and expanded on feeder fibroblasts using standard procedures.

1.4. FACS analysis of proliferation and apoptosis

For proliferation assays of MEFs, cells were pulse-labelled with 10 μM BrdU (Sigma-Aldrich) for 1 h, harvested by trypsinization and then fixed in 100% ethanol. Upon DNA denaturation using 2 N HCl, cells were stained with mouse anti-BrdU primary antibody (Santa Cruz Biotechnology, sc-51514; 1μg/10^6 cells) and anti-mouse Alexa Fluor 488-conjugated secondary antibody (Life Technologies, A21202; 1μg/10^6 cells). DNA was stained by resuspension of cells in 0.1 mg/ml propidium iodide and incubated 30 min at room temperature until FACS analysis.

In order to measure apoptosis, MEFs were seeded at high density and then transferred to 0.5% FBS-containing DMEM in the presence of either vehicle (EtOH) or 2 mM 4-OHT. At the indicated time points, cells and supernatants were harvested, washed, and resuspended in Annexin V binding buffer containing 5 μl per sample of Annexin V-APC (BD Biosciences, 550474, Franklin Lakes, NJ, USA). Prior to analysis, DAPI was added.

2. MOUSE BIOLOGY

2.1. Mouse strains

The following mouse strains were used: *Bptf*$^{lox/lox}$ (Landry *et al*. 2008), *Ptf1a-Cre*$^{+/KI}$ (Kawaguchi *et al.* 2002), *Ptf1a-CreERT2*$^{+/KI}$ (Kopinke *et al*. 2011), *Ela1-Myc* (Sandgren *et al*. 1991), *Mb1-Cre*$^{+/KI}$ (Hobeika *et al.* 2006) and *Eμ-Myc* (Harris *et al*. 1988). *Mb1-Cre* mice were provided by Dr. A.M. Ramiro (CNIC, Madrid), and *Eμ-Myc* mice were supplied by Dr. C. Blanco (CNIO, Madrid). C57BL/6 *Bptf*$^{lox/lox}$ mice were obtained from Jackson Laboratories (stock number 009367). Other strains were available at CNIO.

To determine the role of BPTF in c-MYC-driven pancreatic tumorigenesis, we administered 25 mg of tamoxifen (Sigma-Aldrich, T-5648) by gavage over the course of one week to 5-7 weeks old *Bptf*$^{lox/lox}$; *Ptf1a-CreERT2*$^{+/KI}$; *Ela1-Myc* mice and their corresponding controls. Mice were screened for pancreatic tumors once a week using a small animal ultrasound system.

Mice were housed under specific pathogen-free conditions according to institutional guidelines. Mice were observed on a daily basis and sacrificed when they showed signs of morbidity or tumor burden was greater than 10% body weight in accordance with the *Guidelines for Human Endpoints for Animals Used in Biomedical Research*. All experiments were approved by the ISCIII (Instituto de Salud Carlos III) Ethical Committee and performed in accordance with the guidelines for Ethical Conduct in the Care and Use of Animals as stated in The International Guiding Principles for Biomedical Research involving Animals, developed by the CIOMS.

2.2. Histopathology and Immunohistochemistry

Mouse tissues were fixed in 4% PBS-buffered formaldehyde, embedded in paraffin and serially sectioned. 4 μm sections were deparaffinized and stained with hematoxylin-eosin or specific antibodies.

For immunohistochemistry, mouse tissue sections were prepared as follows. After deparaffinization, sections were rehydrated and boiled in 10 mM sodium citrate buffer (pH 6) for 10 min to retrieve the antigens. Next, sections were washed in distilled water and incubated for 30 min with 3% hydrogen peroxide in methanol, after which they were washed again and blocked for 30 min with 2% BSA in PBS/0.5% Triton X-100. After blocking, the sections were incubated with primary antibodies in 2% BSA in PBS/0.1% Triton X-100 for 1h at room temperature. Antibody dilutions used: P-Histone H3 (Abcam ab14955), 1:2000; c-Myc (Millipore 06-340), 1:300; cleaved caspase 3 (R&D AF835), 1:300. Next, sections were washed in PBS/0.1% Triton X-100 three times and incubated for 30 min with Envision+ HRP-labelled secondary antibodies (Dako, Glostrup, Denmark). Sections were washed again and the staining was developed using DAB Chromogen system (Dako). Sections were rinsed with water, counterstained with Carazzi's Hematoxylin solution DC (Panreac, Castellar del Vallès, Spain), dehydrated with increasing concentrations of alcohol and xylol, and mounted using DePeX mounting medium.

2.3. Hematological analysis and characterization of B cell compartment

For the analysis of cellular components of peripheral blood of *Bptf*$^{lox/lox}$; *Mb1-Cre*$^{+/KI}$ mice, samples were collected from 8-10 week old mice and assessed using an Abacus Junior Hematology Analyzer.

In order to assess the bone marrow (BM) and spleen B cell compartments, single cell suspensions were prepared according to standard procedures (Iritani *et al.* 1997). BM cells were harvested by flushing two tibias and two femurs per mouse with 5 ml of RPMI 10% FBS (HyClone). Splenocytes were prepared by crushing spleens through 70μm filters and into the above media. Next, erythrocytes were depleted by incubation in ammonium chloride buffer (0.15 M NH_4Cl, 10 mM $NaHCO_3$, 1 mM EDTA, pH 7.4) for 2 min at 37 ºC. Cells were collected by centrifugation for 5 min at 1,200 rpm and resuspended in 1 ml of FACS buffer (2 mM EDTA in PBS/0.1% BSA) for further analysis. Prior to staining, cell suspensions were blocked for 20 min in FACS buffer supplemented with 1:200 FC block (BD Pharmingen, purified rat anti-mouse CD16/CD32, 553142). 3-4 colour flow cytometry analyses were performed by staining 4×10^6 cells with 0.25 μg of the following mAbs directed against lineage markers (in various combinations): APC-conjugated anti-CD45R/B220 (ebioscience, 17-0452, San Diego, CA, USA), FITC-conjugated anti-CD43 (ebioscience, 11-0431-81), PE-conjugated anti-IgM (ebioscience, 12-5790-81). Samples were analyzed using a FACS Canto II (BD Biosciences) flow cytometer. Analyses were performed using FlowJo flow cytometry analysis software.

3. MOLECULAR BIOLOGY

3.1. Western blotting

Cells were lysed in RIPA buffer supplemented with protease and phosphatase inhibitors. Following sonication, clearing by centrifugation, and protein determination, equal amounts of protein per sample were subjected to electrophoresis in 8% or 10% polyacrylamide SDS gels, or in NuPAGE® 3-8% Tris-acetate precast polyacrylamide gels (Life Technologies). Samples were run under reducing conditions and then transferred to nitrocellulose membranes, which were blocked with TBST, 5% skim milk. Membranes were subsequently incubated with the following primary antibodies: BPTF (ab72036, Abcam, Cambridge, UK; 1:500) and Vinculin (Sigma-Aldrich, V9131-2ML; 1:2000). This was followed by incubation with horseradish peroxidase-conjugated secondary antibodies (Dako). Reactions were detected using the ECL system.

3.2. Co-immunoprecipitation analyses

For the analysis of c-MYC:BPTF interaction, the following plasmids were used: BPTF-Flag (courtesy of O. Barak, Wistar Institute, Philadelphia, USA) and HA-tagged c-MYC (a gift from V.J. Sánchez-Arévalo, CNIO, Madrid).

293T cells transiently transfected with the corresponding plasmids were washed twice with ice-cold PBS and lysed for 30 min on ice with NP-40 lysis buffer (150 mM NaCl, 50 mM Tris pH 8.0, 1% NP-40) supplemented with a protease inhibitor cocktail. Lysates were then centrifuged at 16,000 x g for 20 min at 4 ºC. Total protein (1 mg) was incubated with primary antibody (2 μg) overnight. Protein A/G agarose beads (Laboratorios Conda, Madrid, Spain) preblocked with BSA were then added to the lysates. Following 4 h incubation at 4 ºC, beads were washed 3 times with NP-40 lysis buffer and immunoprecipitated proteins were eluted with SDS sample buffer by boiling at 90 ºC. SDS-PAGE electrophoresis was then performed on 6% and 10% (w/v) gels and proteins were then transferred onto nitrocellulose membranes.

3.3. Generation of polyclonal anti-BPTF anti-sera

The RLHRMTSIEREEKEKVKKKEKKQEEETC peptide was chemically synthesized, coupled to Keyhole limpet hemocyanin (KLH), and used as immunogen for the generation of polyclonal antibodies against BPTF. Two rabbits were inoculated subcutaneously with 500 μg of peptide-KLH conjugate emulsified in Freund's Complete Adjuvant (FCA). Five rounds of 250 μg peptide-KLH boosters were administered together with Freund's Incomplete Adjuvant (FIA) to each animal in the interval of three weeks. Test bleeds were taken 10 days after the last boost. Antibodies raised against BPTF were purified from serum by affinity chromatography on a HiTrap NHS-activated High Performance column (Sigma-Aldrich, GE17-0716-01) and tested by ELISA, in HEK293T-BPTF-Flag transfected cells and in BPTF-silenced VM-CUB-3 cells.

3.4. Immunofluorescence staining and Proximity Ligation Assay

Cells grown on coverslips were fixed with 4% paraformaldehyde for 10 min, washed, and permeabilized with 0.1% Triton X-100 in PBS for 10 min. Samples were washed in PBS and blocked with 3% BSA in PBS for 1 h at room temperature. Primary antibody incubation was performed in blocking solution for 2 h at room temperature. Mouse anti-MYC (C-33, sc-42, Santa Cruz Biotechnology, Dallas, TX, USA) was used at a 1:50 dilution and home-made affinity-purified rabbit anti-BPTF antibodies (residues 913-942) were used at 10 μg/ml. After three washes with PBS, cells were incubated with an appropriate secondary antibody diluted in

blocking solution. Nuclei were counterstained with DAPI and coverslips were mounted on ProLong® (Life Technologies). Images were taken with a confocal microscope, using a 40X immersion oil lens. For the proximity ligation assay (PLA), the DuolinkII fluorescence system was used (Olink Bioscience, Uppsala, Sweden).

3.5. Quantitative real-time PCR

To isolate RNA from cultured cells, we used the GenElute™ Mammalian Total RNA Miniprep Kit (Sigma-Aldrich) according to manufacturer's instructions. To isolate RNA from mouse tissue samples, we first homogenized the tissues using the T10 basic ultra-turrax homogenizer (IKA, Staufen, Germany) in a guanidine thiocyanate buffer (4 M Guanidine thiocyanate, 0.1 M Tris-HCl, 1% β-mercaptoethanol, pH 7.5 in DEPC-treated water). Total RNA was subsequently extracted by phenol-chloroform and isopropanol precipitation.

All samples were treated with DNAse I before reverse transcription. cDNA was generated from 1 μg RNA using random hexamers and Reverse Transcriptase. Real-time PCR amplification and analysis were conducted using the 7900HT Real-Time PCR System (Applied Biosystems, Life Technologies). RNA levels were normalized to GAPDH expression using the ΔΔCt method (Livak and Schmittgen 2001). For RT-qPCR analysis, primers were designed to achieve product lengths of 200-250 bp. Primer sequences are provided in Table 4.

AMPLICON #	SPECIES	FORWARD	REVERSE
RTKN	Human	5'-GACCATGAGATCCGGATGAG-3'	5'-GAATCCGGAGGTCAGAGATG-3'
EARS2	Human	5'-CGGAGAAGGTGGATGTGATT-3'	5'-TACAGGAGGTCCTTGCTGCT-3'
AMD1	Human	5'-ATGGAATGAAATCGGATGGA-3'	5'-TCTGGCAATCAAGACGCTTA-3'
LONP1	Human	5'-GGTGGCATCAAGGAGAAGAC-3'	5'-GATCTCCCGGTAGTGTTCCA-3'
IARS	Human	5'-CGGTCATCATCCCCTTTAGA-3'	5'-GTCCACATCGCTGAAGATGA-3'
NCL	Human	5'-CGTTCGGGCAAGGATAGTTA-3'	5'-AGCCACCTTCACCCTTAGGT-3'
DDX21	Human	5'-TTCCAAAGTGAAGGGAATGG-3'	5'-CCTTCCAGTTCTGGTTGCTC-3'
MDN1	Human	5'-TACTCAGGACACACTGGCGA-3'	5'-CAGCCAAGAACGAGAAGAGC-3'
POLR1B	Human	5'-GAAACACTGGTCTTCTGAGCC-3'	5'-CGGGTCAGCTCTTCCTTATG-3'
PDLIM4	Human	5'-GAGCTCATGACACACCTGGA-3'	5'-GGATCTCAGGATCGATGTGG-3'
EXOSC5	Human	5'-TCCTGGCCTGTTGTCTGAAT-3'	5'-CTGAGTAGAGCCCCTTGGTG-3'
RNF207	Human	5'-AGCCTATCAGCGAGTGGCTA-3'	5'-GTCGTCGTGCGTGTTCTGTA-3'
CAMKK1	Human	5'-AGACAAGAATCCCGAGACGA-3'	5'-GCTTCCTCAGCATGGACTTC-3'
PAICS	Human	5'-GCAGCAAATTGAGCTGATCC-3'	5'-ACTGGGGAGTTCAGGATGTG-3'
NPR3	Human	5'-AGACGTAGAGGAGGATGGCA-3'	5'-GAAGTTTTCCATGGAGGTGAA-3'
TYSND1	Human	5'-TGAAGTTCAGGTGGGGGTAG-3'	5'-CCCTCTTCTCCAACCACTCA-3'
EIF4EBP1	Human	5'-AGTTCCGACACTCCATCAGG-3'	5'-CGGGGACTACAGCACGAC-3'
MRTO4	Human	5'-GGAACAGCAAGCTGAAGGAC-3'	5'-ACCTCACCCCTCAACCTTTT-3'
MYBBP1A	Human	5'-CCAGGTCCTAGCAAAGGTCA-3'	5'-TGCTGTAGGCTCTGCTGTTG-3'

AMPLICON #	SPECIES	FORWARD	REVERSE
CLN6	Human	5'-CTTCCACCTCGACCTCTGGT-3'	5'-ATGACGTTGTAGGCCATGTG-3'
MRAS	Human	5'-GGAGTAGACGATGAGGAAGCC-3'	5'-ACAATCAATGGGCCATCTTG-3'
SLC25A22	Human	5'-ACCTGGGTGCAATCGAGTTA-3'	5'-ACGGTCTTGATGAGGCAGTC-3'
NOLC1	Human	5'-AAGAAGCGGAAGCAGAATGA-3'	5'-CAACTCGTGAATCCACCTCA-3'
FABP5	Human	5'-CACAGCTGATGGCAGAAAAA-3'	5'-CCTGTCCAAAGTGATGATGG-3'
NPW	Human	5'-CGTGGGTTCAGGAGCTGT-3'	5'-CGTCTCTCCGAAGTCTCTGG-3'
CCND2	Human	5'-GTAAAGACAGCCTTGACTCAAGGAT-3'	5'-CGGTGAAGTCCGCCAGC-3'
HPRT	Human	5'-GGCCAGACTTTGTTGGATTTG-3'	5'-TGCGCTCATCTTAGGCTTTGT-3'
GAPDH	Human	5'-GAAGGTGAAGGTCGGAGTCAAC-3'	5'-TGATTTTGGAGGGATCTCGCTC-3'
BPTF	Human	5'-GTTAAGCAAGGCCAGTCAAA-3'	5'-GTGAATTGCTTGTGGTTCCT-3'
CCND1	Human	5'-CCCAACAACTTCCTGTCCTACT-3'	5'-TGACTCCAGCAGGGCTTC-3'
CCNE	Human	5'-GGAAGAGGAAGGCAAACG-3'	5'-GCAATAATCCGAGGCTTG-3'
FOS	Human	5'-CACTGCCATCTCGACCAGT-3'	5'-TCCCTTCGGATTCTCCTTTT-3'
c-JUN	Human	5'-AGCGAGCTGGTGAGGAGGGC-3'	5'-GGGCTGCGCGCACAAGTTTC-3'
Bptf Exon1-2	Mouse	5'-AAGCAGCTTCAGGAGCCATA-3'	5'-AAGCAAAAAGGGGACAACCT-3'
Bptf Exon1-3	Mouse	5'-CAGCAGCACTCCAGAGAAGA-3'	5'-CGCTAGGAAGGACTTGTTGC-3'
Bptf Exon1-4	Mouse	5'-CAGCAGCACTCCAGAGGAAA-3'	5'-GCTCTTCTCAGCATCCTTGG-3'
Bptf	Mouse	5'-GATGGAAGACGACGACGACGACGCT-3'	5'-GGGAGTTAACCACCAGCACC-3'
Nanog	Mouse	5'-CAGGTGTTTGAGGGTAGCTC-3'	5'-CGGTTCATCATGGTACAGTC-3'
Endogenous Oct4	Mouse	5'-TCTTTCCACCAGGCCCCCGGCTC-3'	5'-TGCGGGCGGACATGGGGAGATCC-3'
Endogenous Sox2	Mouse	5'-TAGAGCTAGACTCCGGGCGATGA-3'	5'-TTGCCTTAAACAAGACCACGAAA-3'
Ezh2	Mouse	5'-TGCCTATAATGTACTCTTGGTCG-3'	5'-GCCATCCTGATCCAGAACTTCA-3'
Suz12	Mouse	5'-AGGCTGCCTCCATTTGAGA-3'	5'-TGGTTTCTCCTGTCCATCG-3'
Eed	Mouse	5'-AGGAGACCCTCTGGTGTTTG-3'	5'-AGGACTGCAATAACCGTATCTCC-3'
Hprt	Mouse	5'-GGCCAGACTTTGTTGGATTTG-3'	5'-TGCGCTCATCTTAGGCTTTGT-3'
Reep6	Mouse	5'-GTGCAATGTCATCGGATTTG-3'	5'-TTGCCCGCGTAGTAGAAAG-3'
Ptf1a	Mouse	5'-ACAAGCCGCTAATGTGCGAGA-3'	5'-TTGGAGAGGCGCTTTTCGT-3'
Rbpjl	Mouse	5'-ATGCCAAGGTGGCTGAGAAAT-3'	5'-CTTGGTCTTGCATTGGCTTCA-3'
Rbpjk	Mouse	5'-GTGTTCCTCAGCAAGCGGATA-3'	5'-TGCCACCTTCGTTCCTGAA-3'
Hnf1b	Mouse	5'-TACGACCGGCAAAAGAATCC-3'	5'-TGCGAACCAGTTGTAGACACG-3'
Amy2	Mouse	5'-TGGCGTCAAATCAGGAACATG-3'	5'-AAAGTGGCTGACAAAGCCCAG-3'
Insulin	Mouse	5'-TAGTGACCAGCTATAATCAGAG-3'	5'-ACGCCAAGGTCTGAAGGTCC-3'
Pdx1	Mouse	5'-AAATCCACCAAAGCTCACGC-3'	5'-CGGTCAAGTTCAACATCACTGC-3'
Cbp1	Mouse	5'-TACACCCACAAAACGAATCGC-3'	5'-GCCACGGTAAGTTTCTGAGCA-3'
Gapdh	Mouse	5'-CCATGCCATCACTGCCAC-3'	5'-GGGTAGGAACACGGAAGG-3'
Ela1	Mouse	5'-CGTGGTTGCAGGCTATGACAT-3'	5'-TTGTTAGCCAGGATGGTTCCC-3'
Krt7	Mouse	5'-CACGAACAAGGTGGAGTTGGA-3'	5'-TGTCTGAGATCTGCGACTGCA-3'
Krt19	Mouse	5'-CCTCCCGAGATTACAACCACT-3'	5'-GGCGAGCATTGTCAATCTGT-3'

Table 4. List of RT-qPCR primers used in this study. The following primer sequences were a gift from B. Amati (IFOM, Milan, Italy): NCL, NOLC1 and CCND2. Primers targeting Nanog, Oct4 and Sox2 were designed by Takahashi *et al*. 2007. Primer sequences for murine pancreatic markers were designed by A. Pinho and former members of the Epithelial Carcinogenesis Group in CNIO.

3.6. Chromatin immunoprecipitation

Cells were fixed with 1% formaldehyde for 15 min at room temperature. Fixation was stopped by adding glycine (to 0.125 M) with an additional incubation of 5 min. Cells were harvested by scraping, pelleted, and then lysed for 10 min in 1 ml of buffer LB1 (140 mM NaCl, 1 mM EDTA, 50 mM Hepes pH 7.5, 0.5% NP-40, 0.25% Triton X-100, 10% glycerol) supplemented with protease inhibitors (Qiagen, Valencia, CA, USA). After centrifugation at 3,000xg, pelleted nuclei were resuspended in 1 ml of buffer LB2 (200 mM NaCl, 0.5 mM EGTA, 1 mM EDTA, 10 mM Tris pH 8.0), and incubated at room temperature for 10 min. Pelleted nuclei were resuspended in 1 ml ChIP SDS buffer (100 mM NaCl, 5 mM EDTA, 50 mM Tris pH 8, 0.2% NaN_3, 0.5% SDS) and sonicated for 20 min in a Covaris sonicator, yielding DNA fragments of 300-500 bp. Beads were blocked overnight in PBS with 0.5% BSA and then added to the samples. After a 3 h incubation at 4 ºC, beads were washed with Triton dilution buffer (100 mM NaCl, 5 mM EDTA, 100 mM Tris pH 8.6, 0.2% NaN_3, 5% Triton X-100), mixed micelle wash buffer (150 mM NaCl, 5 mM EDTA, 5% sucrose, 20 mM Tris pH 8, 0.2% NaN_3, 1% Triton X-100, 0.2% SDS), 500 buffer (0.1% Deoxycholic acid, 1 mM EDTA pH 8, 500 mM NaCl, 50 mM HEPES pH 7.5, 0.2% NaN_3, 1% Triton X-100), LiCl buffer (0.5% Deoxycholic acid, 1 mM EDTA, 250 mM LiCl, 10 mM Tris pH 8, 0.2% NaN_3, 0.5% NP-40) and TE. DNA was eluted in elution buffer and cross-links were reversed by incubation overnight at 65 ºC. RNA and protein were digested using RNAse A and Proteinase K and DNA was purified by phenol-chloroform extraction and isopropanol precipitation. Target DNA abundance in ChIP eluates was assayed by quantitative PCR with

AMPLICON #	SPECIES	FORWARD	REVERSE
Neg. CTRL.	Human	5'-AGCACAGGCAATGGTGTTAG-3'	TTGAATGGAGCACTGTGGAG-3'
AchR	Human	5'-CCTTCATTGGGATCACCACG-3'	AGGAGATGAGTACCAGCAGGTTG-3'
RAF1	Human	5'-CCATTTCGAAGCTGAAGAGG-3'	GTGCCTCTCCTGAAAGCAAG-3'
YAP1	Human	5'-GAGTTTCTCTCTGCGGTTGC-3'	CCGGGAAGAAAGAAAGGAAG-3'
EFN2B	Human	5'-CTTAGAGCTCCCGGCTTCTG-3'	CCTGATTAGAGCTGCAAATTCC-3'
TMEM167B	Human	5'-AGTTACCACGGCCAAGTACG-3'	GCCGAACGCTATCAGGAGT-3'
NOLC1	Human	5'-GCTGAGATGACCACAAGGCT-3'	AGGCTTTCTCTGGTCACTGC-3'
NCL	Human	5'-TTTTGCGACGCGTACGAG-3'	ACTAGGGCCGATACCGCC-3'
MRTO4	Human	5'-GACCACAGAGCTGGGATAGC-3'	CACTGCAGCCTGCCTCTC-3'
MRAS	Human	5'-GGTGAAAAAGAGCCAACAGC-3'	CTAACACAGGCTGCACCAGA-3'
RNF207	Human	5'-CCACGTACTTCTGCAACACG-3'	ACTGCACTTCTGGGGCAC-3'
MYBBP1A	Human	5'-CGTAGCTCTGAGCGGAAGTC-3'	CGAGATGGGCCCTTAGAAAT-3'
DDX21	Human	5'-AAATCCAACCACAGTCACAGG-3'	CTCTCGTCACTTCCCGTAGC-3'

Table 5. List of ChIP-qPCR primers used in this study. Primers for AchR and NOLC1 were designed at Dr. Bruno Amati laboratory (IFOM, Milan, Italy).

primer pairs designed to achieve products of 50-200bp. Primer sequences are provided in Table 5. The following antibodies were used: anti-MYC N262 (Santa Cruz Biotechnology, sc-764), anti-H3K4me3 (Abcam, ab8580), anti-panAc Histone H3 (Merck Millipore, 06-599, Billerica, MA, USA), and anti-total Histone H3 (Abcam, ab1791).

3.7. DNAse I hypersensitivity assay

DNAse I experiments were performed as described previously (Di Stefano *et al*. 2014). Briefly, chromatin samples were obtained as described above and subjected to DNAse I digestion. Chromatin (2 μg) was treated with 0.5, 1, and 2 units of RQ1 RNase-Free DNAse I (Promega, Fitchburg, WI, USA) for 3 min at 37 ºC in 1X DNAse incubation buffer. Reactions were terminated by adding 2 mM EGTA and the crosslinking was reversed by incubating samples at 65 ºC. After 6h, proteinase K (40 mg/ml) was added to each reaction and incubated overnight at 37 ºC. After phenol-chloroform extraction, DNA was quantified and used as template for q-PCR reactions with the same primer pairs used for ChIP-qPCR.

4. GENOME-WIDE STUDIES AND BIOINFORMATICS ANALYSES

4.1. ChIP-Seq library construction and massive parallel sequencing

ChIP was performed as described above. DNA (20 ng) was quantified by fluorometry, resolved by electrophoresis, and fractions of 50-250bp were extracted. Input samples correspond to balanced blends of inputs from selected samples. Fractions were processed through subsequent enzymatic treatments of end-repair, dA-tailing, and ligation to adapters following Illumina's "TruSeq DNA Sample Preparation Guide" (part # 15005180 Rev. C). Adapter-ligated libraries were amplified by limited-cycle PCR with Illumina PE primers (12 cycles). The resulting purified DNA library was applied to an Illumina flow cell for cluster generation (TruSeq cluster generation kit v5) and sequenced on the Genome Analyzer IIx with SBS TruSeq v5 reagents following manufacturer's protocols.

4.2. ChIP-Seq data processing

Image analysis and per-cycle base-calling was performed with Illumina Real Time Analysis software (RTA1.13). Conversion to FASTQ read format with the ELAND algorithm (v2e) was performed with CASAVA-1.8 (Illumina). Quality check was done via fastqc (v0.9.4, Babraham Bioinformatics). ChIP-seq reads were aligned to the human reference genome (GRCh37/hg19, Feb 2009) with Burrows-Wheeler Aligner (bwa,v0.5.9-r16) allowing 0-1 mismatches. Unique aligned reads were converted to BED format. All ChIP and input samples were normalized

randomly to the same number of reads (10,512.988). Furthermore, reads were directionally extended to 300 bp and, for each base pair in the genome, the number of overlapping sequence reads was determined and averaged over a 10 bp window to create a wig file to visualize the data in the University of California Santa Cruz (UCSC) genome browser. The number of significant peaks of MYC binding sites was 1762 for sh#1+OHT and 1397 for shNt+OHT, using MACS (version 2.0.9 20111102, tag:alpha) and parameters: -g 2.7e9; -m 10,30; -q 0.05.

4.3. Motif enrichment analysis, peak annotation and density plot analysis

Motifs for the list of peaks in shNt+OHT were identified with the MEME suite and then TOMTOM was used to compare the identified motifs with known transcription factor binding motifs. Sequence logos were generated using WebLogo 2.8.2. Genomic annotation was carried out with Hypergeometric Optimization of Motif EnRichment (HOMER, software v4.2). The tool annotatePeaks.pl was used with parameters by default and defined in the help. A gtf file from UCSC based on GRCh37/hg19 was used for annotations; the latter included whether a segment is in the TSS, TTS, exon, 5' UTR exon, 3' UTR exon, intron, or is intergenic. Since some annotations overlap, the following priority was assigned: TSS (from -1kb to +100bp), TTS (from -100 bp to +1kb), CDS exon, 5' UTR exon, 3' UTR exon, intron, intergenic. More detailed information is available in http://homer.salk.edu/homer/ngs/annotation.html. The SeqMINER (v1.3.3e) platform (Ye *et al.* 2010) was used to generate the density read plots shown in Fig. 11b.

4.4. Gene set enrichment analysis (GSEA)

MYC-bound genes were rank-ordered according to the fold-change in FPKM values (4-OHT vs. vehicle) in HFF MYC-ER control cells and then submitted to analysis using GSEA software (www.broadinstitute.org/gsea). The list of pre-ranked genes was analysed with the gene set matrix composed file c2.all.v4.0.symbols.gmt and c5.all.v4.0.symbols.gmt. Significant gene sets enriched by 4-OHT-treatment of control cells were identified using an FDR q-value < 0.25 and a nominal *P* value < 0.05, as defined by http://www.broadinstitute.org/gsea/doc/GSEAUserGuideFrame.html?Interpreting_GSEA.

4.5. RNA-seq

Total RNA (1 µg) was spiked with ERCC ExFold RNA spike-In mixes (Life Technologies). RNA quality was assessed on an Agilent 2100 Bioanalyzer and samples with a RNA Integrity Number > 8.5 were used. PolyA+ fractions were

purified, randomly fragmented, converted to double stranded cDNA, and processed through subsequent enzymatic treatments of end-repair, dA-tailing, and ligation to adapters following Illumina's "TruSeq Stranded mRNA Sample Preparation Part # 15031047 Rev. D" (this kit incorporates dUTP during 2nd strand cDNA synthesis, which implies that only the cDNA strand generated during 1st strand synthesis is eventually sequenced). Adapter-ligated libraries were generated by PCR with Illumina PE primers (8 cycles). The resulting purified cDNA libraries were applied to an Illumina flow cell for cluster generation (TruSeq cluster generation kit v5) and sequenced on the Genome Analyzer IIx with SBS TruSeq v5 reagents by following manufacturer's protocols.

4.6. RNA-Seq data processing

Image analysis and per-cycle base-calling was performed with Illumina Real Time Analysis software (RTA1.13). Conversion to FASTQ read format with the ELAND algorithm (v2e) was performed with CASAVA-1.8 (Illumina). These files contain only reads that passed "chastity" filtering (flagged with a 'N', for *NOT filtered* in the sequence identifier line). "Chastity" parameter measures signal contamination in raw data and allows to flag unreliable reads. Quality check was done via fastqc (v0.9.4, Babraham Bioinformatics). Raw reads were aligned to the build version GRCh37/hg19 of the human genome where the sequence of the ERCC synthetic spike-in RNAs (http://tools.invitrogen.com/downloads/ERCC92.fa) had been added. Tophat5 (version 2.0.4) was used for alignment with the following parameters: --bowtie1, --max-multihits 5, --genome-read-mismatches 1 --segment-mismatches 1 --segment-length 19 --splice-mismatches 0 --library-type fr-firststrand. Gene expression levels and synthetic spike-in RNA (Fragments Per Kilobase of exon per Million fragments mapped, FPKM) were quantified with cufflinks (version 2.0.2), with the following parameters: -N, --library-type fr-firststrand, -u. Further, we used a loess regression to renormalize the FPKM values by using only the spike-in values to fit the loess following the strategy described (Lovén *et al.* 2012). The *affy* package in R provides a function, loess.normalize, performing loess regression on a matrix of values and allowing to specify which subset of data to use when fitting the loess (see the *affy* package for further details). The result was a matrix of FPKM values normalized to the control ERCC spike-ins.

4.7. RNA-Seq GSEA analysis

Genes were rank-ordered according to the fold change in FPKM values (4-OHT vs Vehicle) in HFF MYC-ER control cells and then submitted to analysis using GSEA software (www.broadinstitute.org/gsea). The list of pre-ranked genes was

analysed with the gene set matrix composed file c2.all.v4.0.symbols.gmt and c5.all.v4.0.symbols.gmt. Significant gene sets enriched by OHT-treatment of control cells were identified using an FDR q-value < 0.25 and a nominal *P* value < 0.05. All analyses were performed using GSEA v2.1 software with pre-ranked list and 1000 data permutations.

4.8. Analysis of human tumor genomic data

Gene expression data from 20 studies profiling human tumors were downloaded from either Oncomine or GEO (Gene Expression Omnibus). The complete list of datasets, together with their GEO accession numbers, is provided in Table 7. Expression data for each study were converted into the GenePattern GCT format. To obtain one expression value per gene and sample, GCT files were subsequently collapsed using the CollapseDataset module in GenePattern. We next rank-ordered the samples within each dataset according to the mRNA levels of BPTF, c-MYC, N-MYC, or L-MYC and performed a single sample GSEA (ssGSEA) to calculate activation scores for 4 MYC-dependent gene signatures in each sample. ssGSEA enrichment score represents the degree to which the genes in a particular gene set are coordinately up- or down-regulated within a sample. The following gene signatures were downloaded from Molecular Signature Database: BILD_MYC_ONCOGENIC_SIGNATURE (M2069), ALFANO_MYC_TARGETS (M2477), and SCHUHMACHER_MYC_TARGETS_UP. The Seitz signature was built from the data published in Seitz *et al.* 2011.

5. STATISTICAL ANALYSIS

All quantitative data are presented as mean ± S.E.M. (Standard Error of Mean) from ≥2 experiments or samples per data point (n is mentioned in each figure legend). Unpaired student's t-test (two-tailed) was used to compare two groups of independent samples. Paired student's T-test (two-tailed) was used to compare matched pairs samples. To compare the data distribution of two separate populations without assuming normal distribution we performed a Wilcoxon Signed-Ranked test. For in vitro experiments, sample size required was not determined a priori. The experiments were not randomized.

6. INDIVIDUAL CONTRIBUTIONS

Antonio C. Picornell performed the initial bioinformatics analysis leading to the identification of BPTF as a candidate regulator of pancreatic cancer cell lines proliferation. Laia Richart designed and performed the majority of the

experiments. Ana Río Machín (CNIO, Madrid) designed and performed the experiments with Burkitt lymphoma cell lines. Enrique Carrillo-de Santa Pau (CNIO, Madrid) was responsible for the bioinformatics analysis of the genome-wide experiments. V.J. Sánchez-Arévalo (CNIO, Madrid) generated the following constructs: HA-tagged c-MYC and FG12-MycER. Natalia del Pozo (CNIO, Madrid) and Mónica Pérez de Andrés (Universidad Complutense, Madrid) helped with mouse experiments. Francisco X. Real and V.J. Sánchez-Arévalo supervised the overall conduct of the study.

Results

RESULTS

1. BPTF IS REQUIRED FOR *IN VITRO* PROLIFERATION OF TUMOR CELLS

We first identified BPTF as part of a candidate network of transcription factors controlling cell proliferation in two pancreatic ductal adenocarcinoma (PDAC) cell lines (SK-PC-1 and IMIM-PC-2) (Vilá *et al*. 1995). Among the other genes identified with this approach there was also GATA6, which has been proven to be a tumor suppressor in $Kras^{G12V}$-driven pancreatic tumorigenesis in mice (Martinelli *et al*. 2015).

The genetic inhibition of BPTF in two additional PDAC cell lines (PK9 and MIA PaCa-2) using two shRNAs was associated with impaired proliferation, assessed by growth curve and colony-formation assays (Fig. 5). This observation was extended to a panel of cell lines established from bladder tumors, a cancer type where BPTF is mutated (Balbás-Martínez *et al*. 2013; González-Pérez *et al*. 2013). These results are in agreement with other reports using human lung embryonal-derived cells and the T47D-MTVL cell line (Buganim *et al*. 2008; Vicent *et al*. 2011).

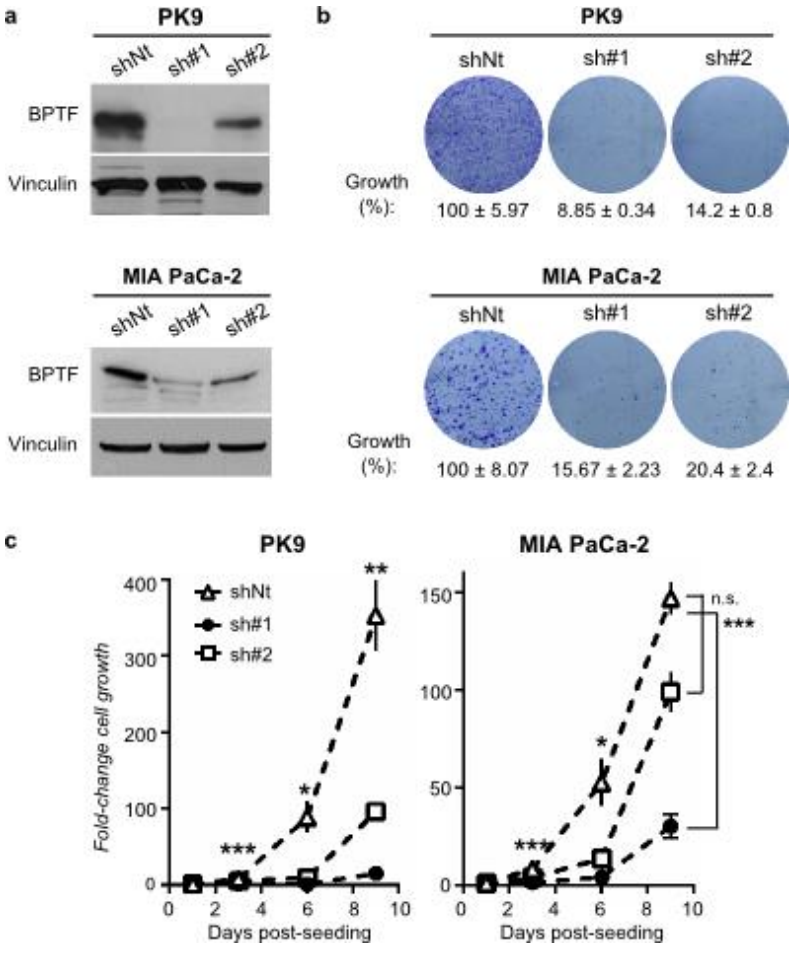

Figure 5. BPTF is required for cell proliferation of PDAC cells. a) Western blotting analysis showing BPTF down-regulation in two PDAC cell lines upon transduction of BPTF-targeting shRNAs (sh#1 and #2). Cells expressing a non-targeting shRNA (shNt) were used as controls. b) Colony-formation assays with the indicated cell lines expressing BPTF-targeting shRNAs or their controls. c) Impact of BPTF down-regulation on cell proliferation of the indicated cell populations. Cells were plated at equal numbers at day 3 post-infection and cell number was quantified during the consecutive days (mean ± SEM; n=3). *, *P* value < 0.05; **, *P* value < 0.01; ***, *P* value < 0.001.

2. BPTF IS MODULATED DURING CELL CYCLE PROGRESSION AND IS REQUIRED FOR G_0-G_1/S TRANSITION

In order to better understand the role of BPTF in cell proliferation, we took advantage of non-transformed non-immortalized human foreskin fibroblasts (HFF). Cells were synchronized by starvation and stimulated to re-enter cell cycle by serum addition. BPTF levels were modulated as cells progressed through the cell cycle, being induced as early as 5 minutes after serum addition and becoming maximal in the G1/S transition. Upon entry into S phase, BPTF protein levels decreased and became undetectable (Fig. 6a,c). The analysis of mRNA expression

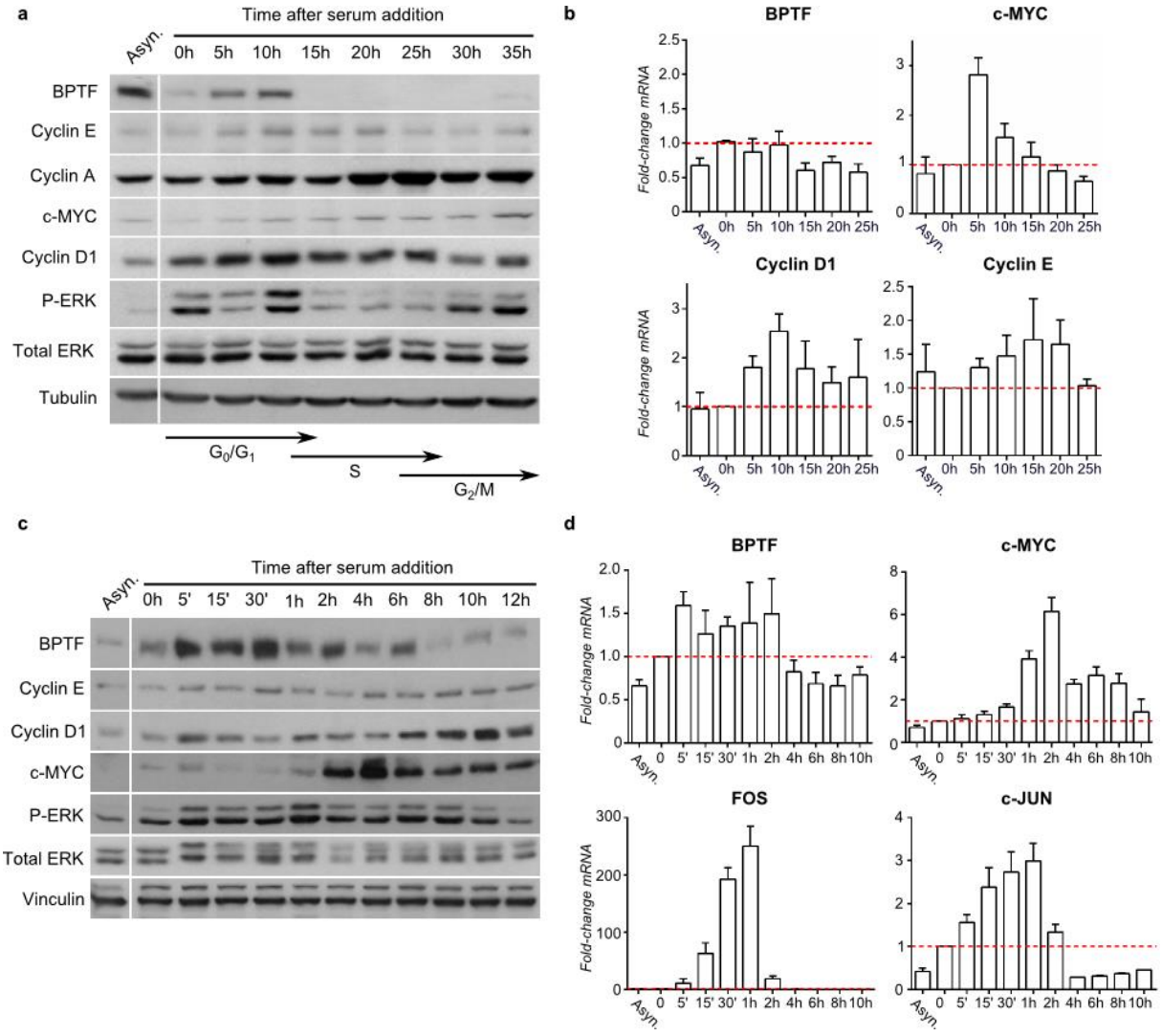

Figure 6. BPTF is modulated during cell cycle progression. Serum-starved HFF were stimulated to cycle by FBS addition and collected at the indicated time points. Western blotting analysis of total cellular fractions is shown in a) and c). Transit through the different cell cycle phases is indicated with arrows. One representative experiment of at least three with similar results is shown. Analysis of mRNA levels is shown in b) and e) (mean ± SEM; n=3). Transcript levels were normalized against HPRT and the 0h time point.

revealed that, unlike cyclins (e.g. D1 and E) or transcription factors classically involved in cell cycle control (e.g. c-MYC and AP-1), BPTF mRNA did not change significantly throughout the experiment. These data suggest that post-translational modifications are involved in the regulation of BPTF protein levels (Fig. 6b,d).

BPTF silencing in HFF using two shRNAs led to a decrease in cell proliferation, assessed by growth curve (Fig. 7a,b). When BPTF-interfered cells were serum-starved and challenged to proliferate by FBS stimulation, they expressed lower levels of c-MYC and Cyclins D1 and A than control cells (Fig. 7c). According to these results, BPTF is necessary for the G_0-G_1/S transition.

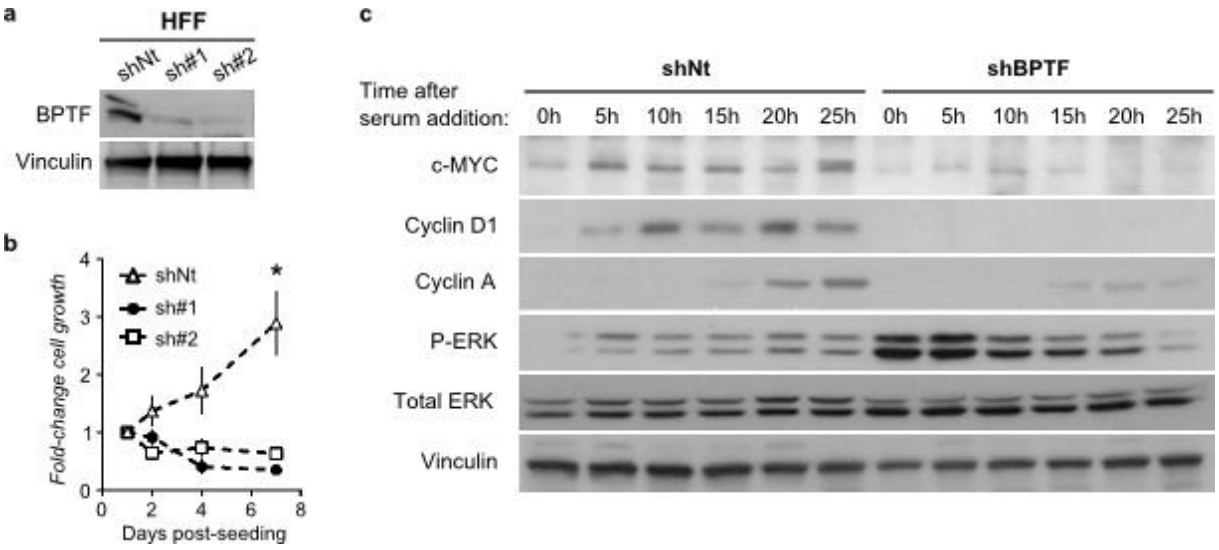

Figure 7. BPTF is required for proliferation of HFF. a) HFF cells expressing control or BPTF-targeting shRNAs (sh#1 and sh#2) were examined by Western blotting. b) Cells in a) were seeded at similar densities at day 3 post-infection and counted at the indicated time points (mean ± SEM; n=3). *, $P < 0.05$. c) HFF cells transduced as in a) were synchronized and collected at different time points. Total cellular fractions were assessed by Western blotting. Only the data regarding shBPTF#1 is shown. One representative experiment of at least three with similar results is shown.

3. BPTF IS NECESSARY FOR c-MYC TRANSCRIPTIONAL ACTIVITY

BPTF modulates gene expression through the interaction with sequence-specific transcription factors. The identity of such regulators has been extensively studied in *Drosophila* but only a few have been discovered in murine and human cells (Alkhatib and Landry 2011; Qiu *et al.* 2015). Since BPTF is necessary for cell proliferation and, more precisely, for G_0-G_1/S transition, we hypothesized that its effects might be mediated, at least in part, by c-MYC.

The hypothesis of BPTF as an interactive partner of c-MYC is attractive for several reasons. First, c-MYC binding sites are highly enriched in H3K4me3, H3K79me2 and H3 acetylation (Guccione *et al*. 2006; Martinato *et al*. 2008). This open chromatin configuration operates upstream of sequence-recognition by c-MYC and, most likely, is 'read' by c-MYC binding proteins and complexes with specialized motifs (bromodomains, PHD fingers or chromodomains). So far, however, the protein(s) involved in the recognition of these marks by c-MYC have not been identified. Human BPTF contains two PHD fingers and one bromodomain that bind to H3K4me2/3 and H4K16ac respectively (Li *et al*. 2006; Ruthenburg *et al*. 2011), thus making it a plausible candidate. Second, c-MYC has long been considered an undruggable oncogene. However, the disruption of chromatin-dependent processes that suppress c-MYC activity - such as the inhibition of the BET bromodomain protein Brd4 by JQ1 - has recently shown promising results in experimental models of multiple myeloma, Burkitt Lymphoma (BL), acute myeloid leukemia and acute lymphoblastic leukemia (Dawson *et al.* 2011; Delmore *et al.* 2011; Mertz *et al.* 2011). BPTF also contains a potentially druggable bromodomain that, if proven relevant for c-MYC function, could be exploited in cancer therapy.

To assess whether BPTF is required for the transcriptional activity of c-MYC, we took advantage of the steroid-activatable construct c-MYC-ER. c-MYC-ER is a fusion protein in which the ligand-binding domain (ER) of a mutant estrogen receptor, G525R (Danielian *et al.* 1993), is fused to the carboxyl terminus of c-MYC. ER lacks intrinsic transactivation activity; it responds to the synthetic steroid 4-hydroxytamoxifen (4-OHT), but not to estrogens (Littlewood *et al.* 1995). The MYC-ER protein is constitutively expressed but it is sequestered in the ctytoplasm unless 4-OHT is supplied. Upon addition of 4-OHT, MYC-ER induces proliferation and apoptosis in the same manner as wild-type MYC (Littlewood *et al.* 1995; Alarcon *et al.* 1996).

HFF were stably transduced with the chimeric MYC-ER cDNA (HFF MYC-ER) and infected with lentiviruses coding for either control (shNt) or BPTF-targeting

shRNAs (sh#1 and sh#2). Before treatment with 4-OHT, cells were serum-starved for 2 days to achieve quiescence, ruling out proliferation-associated effects. Immunofluorescence analysis confirmed that the lentiviral shRNAs inhibited the expression of BPTF and did not interfere with MYC-ER nuclear translocation (Fig. 8a).

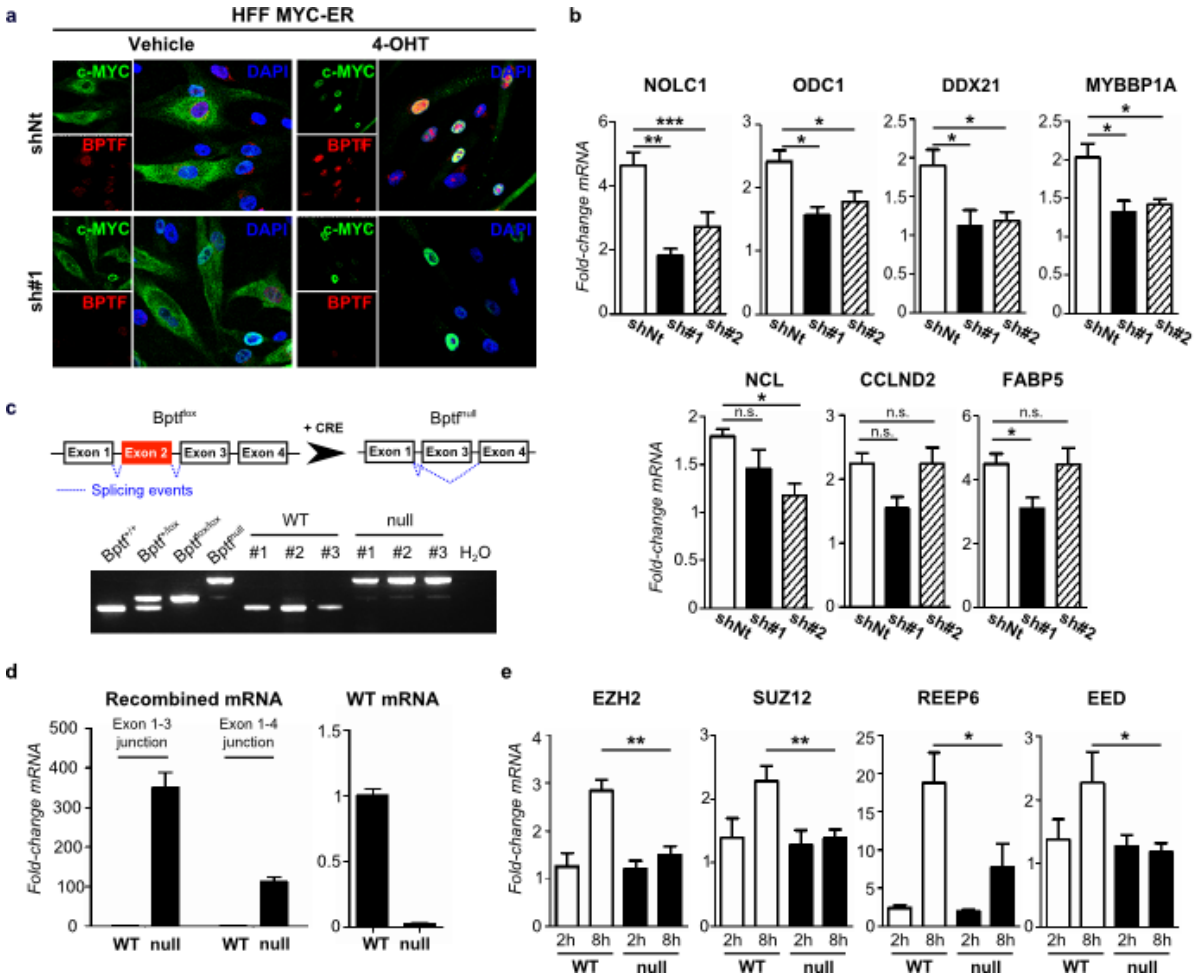

Figure 8. BPTF is required for c-MYC transcriptional activity. a) Immunofluorescence staining of BPTF and c-MYC showing MYC-ER nuclear translocation upon 4-OHT treatment in control and BPTF-silenced HFF. b) Examples of expression of known c-MYC target genes, analysed by RT-qPCR, upon BPTF knockdown. Transcript levels were normalized against GAPDH and the vehicle-treated condition. Data are expressed as the mean ± SEM (n ≤ 5). *P* value was determined using an unpaired T-test. c) Diagram showing the *Bptf* floxed allele and assessment of Cre-mediated recombination at the DNA level. d) Excision of *Bptf* exon 2 does not decrease the expression of BPTF at the mRNA level. Instead, it gives rise to two out-of-frame mutant mRNA species that can be specifically detected by RT-qPCR. e) Expression of a set of c-MYC target genes in WT and *Bptf*-null MEFs (n ≥ 4) expressing MYC-ER. Cells arrested with 0.5% FBS for 24h were treated for the indicated time with 10% FBS with or without 4-OHT 2 µM. Data are represented as the mean ± SEM. *P* value was determined using an unpaired T-test. *, *P* value < 0.05; **, *P* value < 0.01; ***, *P* value < 0.001.

Next, we analysed the expression of a set of well-established c-MYC targets by RT-qPCR. BPTF knockdown resulted in a significantly impaired mRNA induction of 6/7 c-MYC targets tested with at least one of the two shRNAs (Fig. 8b). To extend these findings, we used *Bptf*-null MEFs (Landry *et al*. 2008) transduced with MYC-ER. Successful recombination of the floxed allele was demonstrated by PCR and RT-qPCR analysis (Fig. 8c,d). In these cells, addition of 4-OHT also resulted in an impaired activation of 4 well-documented c-MYC targets (Neri *et al*. 2012) (Fig. 8e).

Next, RNA-Seq was performed to evaluate the requirement of BPTF for the activation of the full c-MYC-driven transcriptional program in HFF MYC-ER cells. BPTF knockdown in HFF MYC-ER cells resulted in a reduced transcriptional response to 4-OHT, both up- and down-regulated genes being significantly affected (Fig. 9a). We interrogated the genes differentially expressed in control cells treated with either vehicle or 4-OHT with publicly available gene signatures using Gene Set Enrichment Analysis (GSEA). Genes up-regulated upon 4-OHT addition showed a statistically significant enrichment in c-MYC-dependent transcriptional signatures (Schuhmacher *et al*. 2001; Schlosser *et al*. 2005; Acosta *et al* 2008) and Gene Ontology (GO) pathways classically associated with c-MYC function (i.e. ribosome biogenesis and translation, mitochondrial function, and RNA/rRNA/tRNA processing). Conversely, genes down-regulated in 4-OHT-treated cells overlapped with gene sets known to be repressed by c-MYC (Kim *et al*. 2006; O'Donnell *et al*. 2006) (Fig. 9b and Table 6).

The mechanisms involved in c-MYC-mediated repression have not been fully elucidated; therefore, we focused on its best established role as a transcriptional activator (Lovén *et al*. 2012). We found an impaired activation of 5 independent c-MYC signatures in BPTF-silenced cells (Fig. 9c). These results were validated by RT-qPCR for an additional 20 genes, 19 of which are c-MYC ChIP-Seq targets in at least one cell line profiled by ENCODE. The extent of induction of these genes was significantly reduced in HFF MYC-ER cells transduced with both BPTF-targeting shRNA lentiviruses [average fold-change (4-OHT vs. vehicle) for shNt, 2.44; sh#1, 1.52; sh#2, 1.97] [*P* (shNt vs. sh#1) < 0.0001; *P* (shNt vs. sh#2) = 0.0485] (Fig. 9d). Representative results are shown in Fig. 9e.

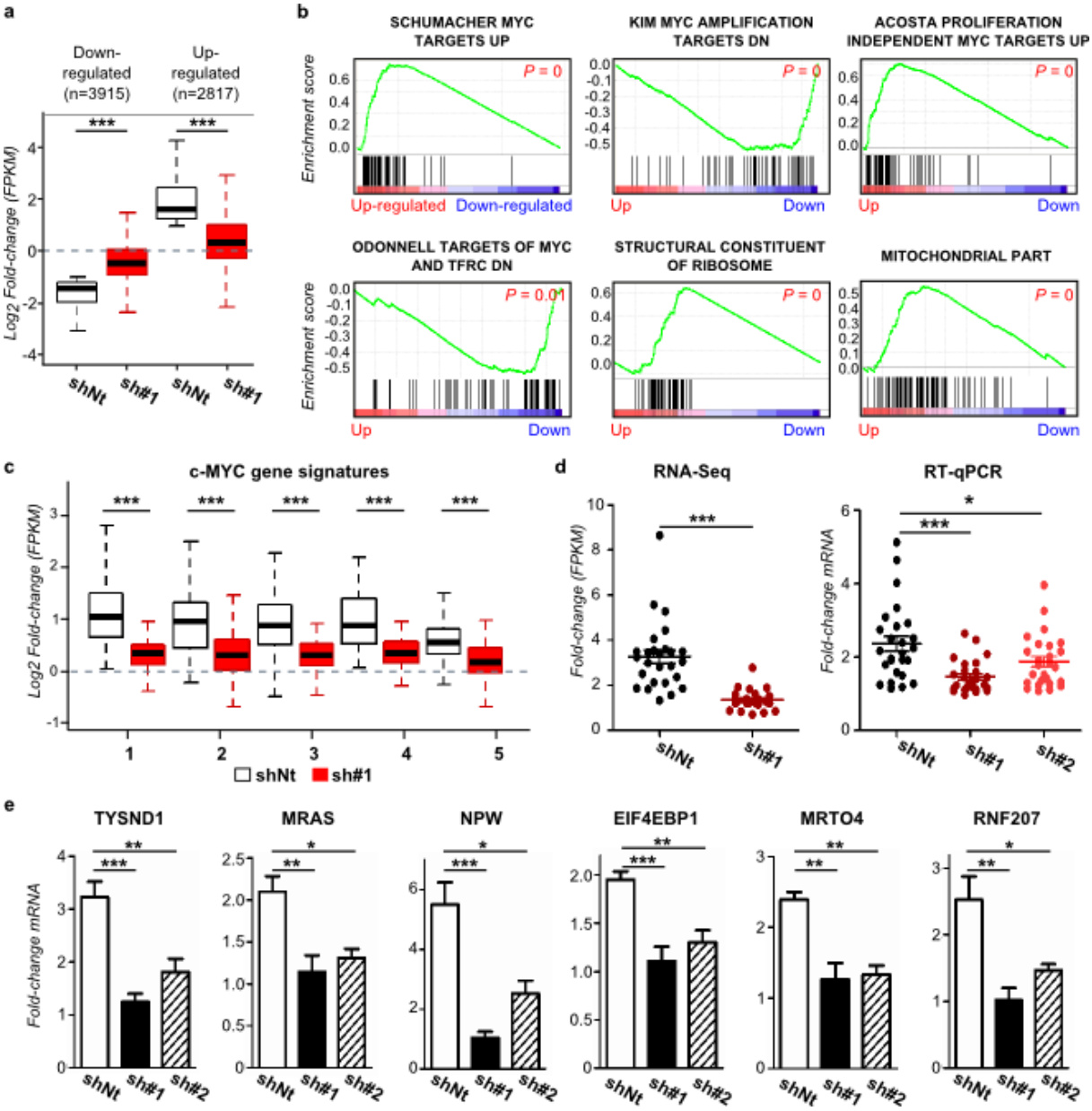

Figure 9. Genome-wide analysis of BPTF-dependent c-MYC transcriptional activity. a) Fold-change in FPKM values (vehicle vs. 4-OHT) of up-regulated [Log_2 F.c. ≥ +1] and down-regulated [Log_2 F.c. ≤ -1] genes in control and BPTF-silenced cells. b) Snapshots of MYC-dependent gene sets displaying a positive or a negative enrichment in 4-OHT-treated control cells. c) Fold-change in FPKM values of c-MYC-dependent gene sets enriched in 4-OHT-treated control cells. Values are displayed for both control and BPTF-silenced HFF MYC-ER cells. Gene sets tested and *P* values: 1, Schuhmacher *et al.* 'MYC Targets Up' ($P = 3.156 \cdot 10^{-15}$); 2, Acosta *et al.* 'Proliferation Independent MYC Targets Up' ($P = 2.034 \cdot 10^{-08}$); 3, Schlosser *et al.* 'MYC Targets Serum Response Up' ($P = 6.62 \cdot 10^{-09}$); 4, Schlosser *et al.* 'MYC Targets Serum Response Dn' ($P = 6.11 \cdot 10^{-09}$); 5, Schlosser *et al.* 'MYC Targets Repressed By Serum' ($P = 2.747 \cdot 10^{-14}$). d) Fold-change in mRNA levels for the set of 20 genes used for validation. Left panel: data calculated from FPKM values. Right panel: data calculated from ≥3 independent experiments assessed by RT-qPCR. e) Examples of genes included in the validation. Transcript levels were normalized against GAPDH and the vehicle-treated condition. Data are expressed as the mean ± SEM. *, *P* value < 0.05; **, *P* value < 0.01; ***, *P* value < 0.001

GENE SETS	SIZE	NES	NOM *P*-val	FDR *Q*-val	
SCHUHMACHER_MYC_TARGETS_UP	78	2.7528589	0	0	
KRIGE_RESPONSE_TO_TOSEDOSTAT_24HR_DN	951	2.7264502	0	0	
PENG_GLUTAMINE_DEPRIVATION_DN	321	2.5907538	0	0	
ACOSTA_PROLIFERATION_INDEPENDENT_MYC_TARGETS_UP	78	2.558087	0	0	
KRIGE_RESPONSE_TO_TOSEDOSTAT_6HR_DN	854	2.5047362	0	0	*Curated Gene Sets (MSigDB c2)*
SCHLOSSER_MYC_TARGETS_REPRESSED_BY_SERUM	151	2.471641	0	0	
PENG_RAPAMYCIN_RESPONSE_DN	235	2.4655156	0	0	
WELCSH_BRCA1_TARGETS_DN	132	2.420463	0	0	
SCHLOSSER_MYC_TARGETS_AND_SERUM_RESPONSE_DN	47	2.3695242	0	0	
SCHLOSSER_MYC_TARGETS_AND_SERUM_RESPONSE_UP	45	2.3654618	0	0	
KIM_MYC_AMPLIFICATION_TARGETS_DN	85	-1.978872	0	0.010278589	
ODONNELL_TARGETS_OF_MYC_AND_TFRC_DN	42	-1.63706	0.01459854	0.18923056	
STRUCTURAL_CONSTITUENT_OF_RIBOSOME	79	2.3599825	0	0	
MITOCHONDRIAL_PART	134	2.1983042	0	5.54E-04	
MITOCHONDRIAL_MEMBRANE_PART	51	2.0519369	0	0.01161756	
RRNA_PROCESSING	15	2.0385666	0	0.00945525	*GO Gene Sets (MSigDB c5)*
RRNA_METABOLIC_PROCESS	16	2.038797	0	0.01181906	
MITOCHONDRIAL_ENVELOPE	91	2.034683	0	0.00861571	
MITOCHONDRIAL_INNER_MEMBRANE	62	2.012977	0	0.00930175	
MITOCHONDRIAL_MEMBRANE	81	1.9780502	0	0.01278298	
MITOCHONDRION	325	1.9676034	0	0.01437254	
RIBOSOME_BIOGENESIS_AND_ASSEMBLY	18	1.9448823	0.00215517	0.0185138	

Table 6. Top-ranking gene sets enriched in 4-OHT-treated control cells. Genes were pre-ranked according to their FPKM fold change (4-OHT/Vehicle) and then submitted to GSEA. The upper group represents curated gene sets (MSigDB collection 2), while the bottom group represents GO gene sets (MSigDB collection 5). MYC-dependent signatures are highlighted in red. NES: Normalized Enrichment Score; FDR: False Discovery Rate.

4. BPTF AND c-MYC INTERACT *IN VITRO*

While this work was being performed, BPTF was also identified as a putative c-MYC interactor in a genome-wide proteomic approach (Agrawal *et al*. 2010). To determine whether the effects observed on transcription could result from the interaction between c-MYC and BPTF, 293T cells were transiently transfected with plasmids encoding HA-MYC and Flag-BPTF. Immunoprecipitation of BPTF followed by Western blotting revealed that both proteins are present in the same complex (Fig. 10a). The interaction between endogenous c-MYC and BPTF was validated in MIA PaCa-2 pancreas cancer cells, expressing high levels of both proteins, using *in situ* proximity ligation assay (isPLA) and home-made affinity-purified rabbit polyclonal antibodies recognizing residues 913-942 of human BPTF (Fig. 10b). Together, these results strongly suggest that c-MYC and BPTF interact directly *in vivo* and that this interaction could contribute to explain the defective c-MYC response in the absence of BPTF.

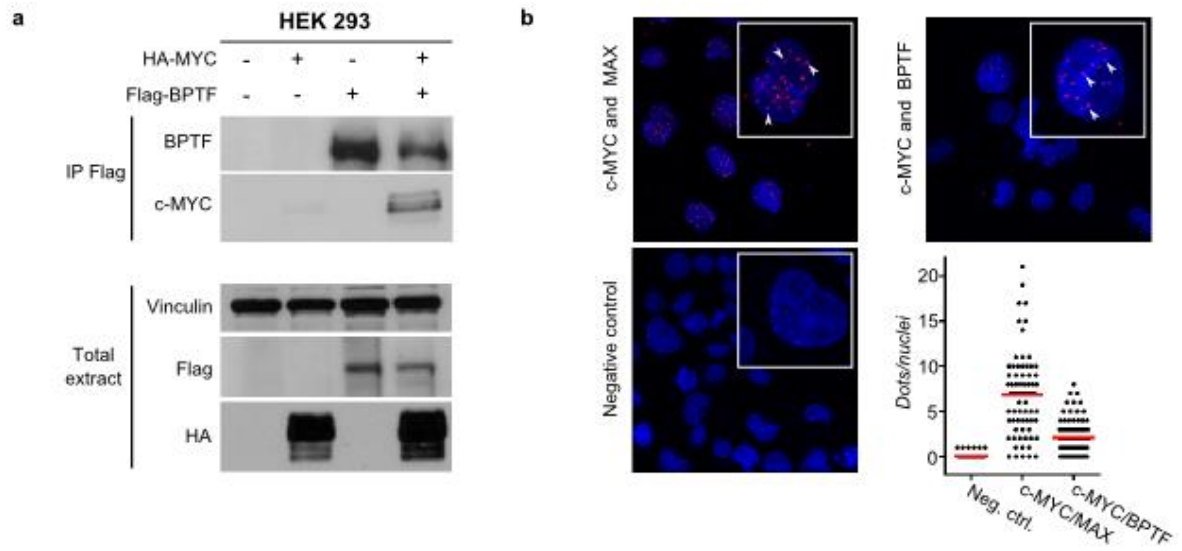

Figure 10. **Analysis of c-MYC:BPTF interaction.** a) Coimmunoprecipitation of Flag-BPTF with HA-tagged c-MYC from lysates of transiently transfected 293T cells; Western blotting with the indicated antibodies. b) Endogenous BPTF and c-MYC interact directly in MIA PaCa-2 cells as shown by *in situ* proximity ligation assay PLA. The interaction events are visible as red dots (nuclear staining in blue) and are marked by arrowheads. The interaction of MYC with MAX is shown as a positive control. Number of dots per nuclei was quantified manually (n=70 nuclei).

5. GENOME-WIDE ANALYSIS OF c-MYC RECRUITMENT TO DNA UPON BPTF KNOCK-DOWN

To identify the mechanisms through which BPTF knockdown attenuates the c-MYC transcriptional response in HFF MYC-ER cells, we conducted chromatin immunoprecipitation with antibodies specific for c-MYC followed by massive parallel sequencing (ChIP-Seq) (Fig. 11a). A total of 1397 peaks were identified in 4-OHT-treated cells. In agreement with previous reports, the analysis of the density profiles of the distance between the summit of peaks and gene transcription start sites (TSS) showed that c-MYC binding sites were concentrated around the TSS (Fernandez *et al.* 2003; Perna *et al.* 2012). Sequence analysis of c-MYC-targeted regions with MEME (Bailey *et al.* 2009) unveiled a significant over-representation of the MYC:MAX binding motif ($P = 2{,}8 \cdot 10^{-69}$) (Fig. 11b). ChIP peaks occurred within promoter regions (TSS±3kb) (35.6%), gene bodies (*intragenic*) (25%), and further upstream or downstream (*intergenic*) (39.4%) (Fig. 11c). Moreover, GSEA analysis of c-MYC-bound promoters showed highly statistically significant overlap with 3 transcriptional signatures of c-MYC-dependent genes and with biological modules associated with c-MYC function (e.g. cell proliferation) (Fig. 11d,e). Induction at the mRNA level of genes directly bound by c-MYC was significantly higher than of those lacking a ChIP-Seq peak (Fig. 11f).

a

Sample	Total high quality reads	Confidently mapped reads	Confidently mapped reads (%)
Input	21929228	15363578	70.06
shNt plus 4-OHT	20609251	11268132	54.67
shBPTF#1 plus 4-OHT	25615737	10512988	41.04

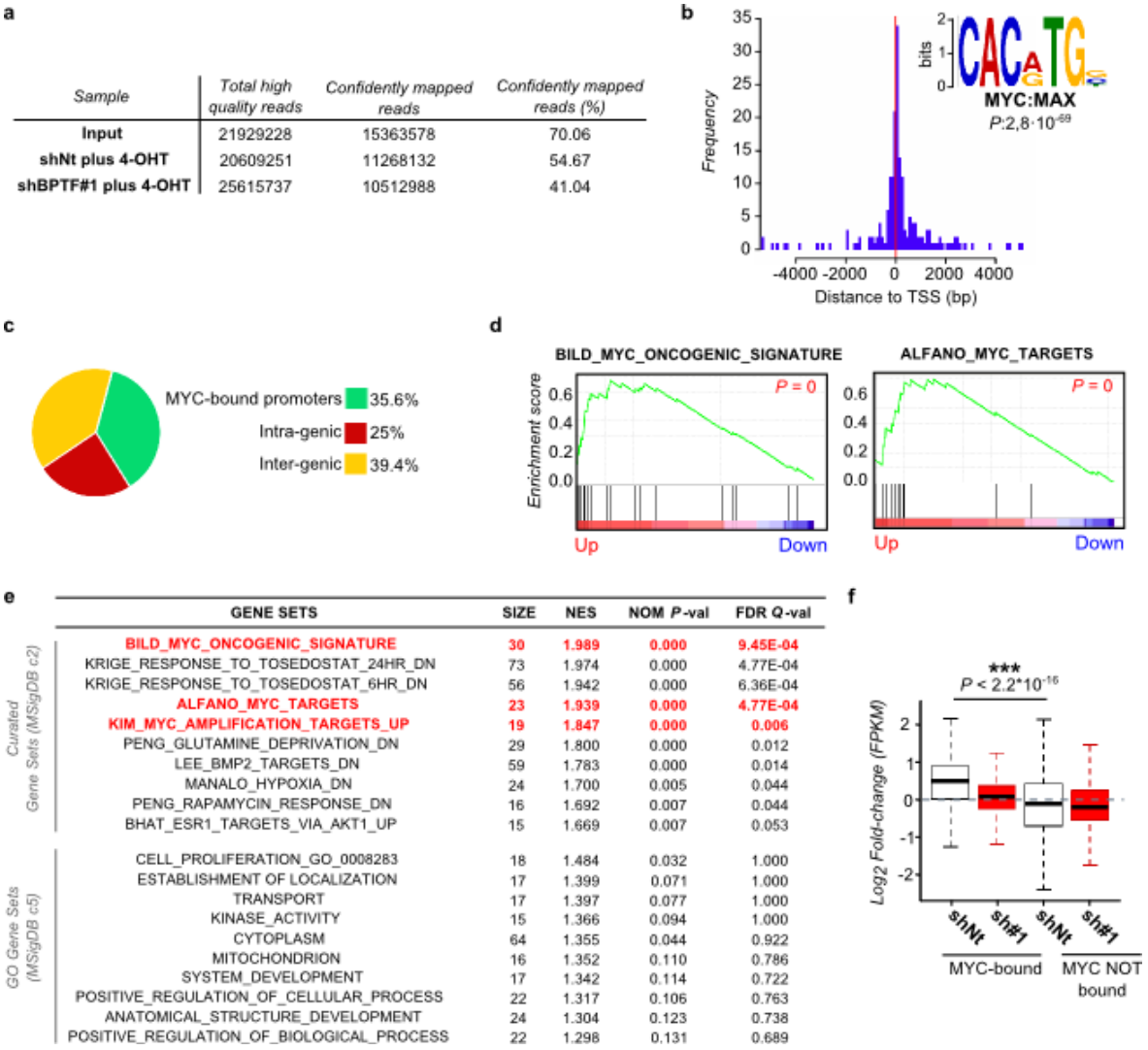

Figure 11. **Analysis of MYC-ER recruitment to chromatin in control cells.** a) Summary of high-quality reads obtained per condition. b) Density profile of c-MYC binding sites relative to TSS. All binding sites within ± 6kb were included in the analysis. TSS distance is measured as the relative base pair distance to peaks' summit. MEME motif prediction of DNA sequences enriched in c-MYC ChIPseq in 4-OHT-treated shNt cells. c) Distribution of c-MYC binding sites relative to the gene bodies of Ref Seq annotated transcripts. d) Snapshots of c-MYC-dependent gene sets enriched among c-MYC-bound promoters in control cells. e) Top-ranking gene sets enriched in MYC-bound promoters pre-ranked according to their FPKM fold change (4-OHT-treated vs. vehicle-treated). The upper group represents curated gene sets (MSigDB collection 2), while the bottom group represents GO gene sets (MSigDB collection 5). MYC-dependent signatures are highlighted in red. NES: Normalized Enrichment Score; FDR: False Discovery Rate. f) Fold-change in FPKM values (4-OHT vs vehicle) for genes bound by c-MYC (with a ChIP-Seq peak within ± 3kb TSS) and genes not bound, both in control and BPTF-silenced cells. *P* value was calculated using a Wilcoxon test.

To determine whether BPTF silencing interfered with c-MYC recruitment to chromatin, we analysed the magnitude and distribution of c-MYC ChIP-Seq peaks upon BPTF knockdown in HFF. Globally, c-MYC binding intensity was significantly lower in shBPTF-expressing cells ($P < 2.2 \cdot 10^{-16}$) (Fig. 12a,b). This reduction was not evenly distributed at the genome wide level, with 50.2% of the peaks showing a read number fold-change ≥ 2. The selective effect of BPTF silencing on a subset of c-MYC ChIP-Seq peaks -regardless of their intensity- suggests that the differences do not result from an inefficient ChIP. We validated these observations by ChIP-qPCR on gene promoters for which a peak was identified in the ChIP-Seq experiment ("target"), as well as on a set of “non-target” control genomic regions, in at least 3 independent experiments. c-MYC was recruited to target regions and did not show significant binding to non-target promoters. c-MYC recruitment to target genes was significantly reduced in cells infected with the BPTF-targeting shRNAs (Fig. 12c,d). High-affinity MYC targets (Fernandez *et al*. 2003; Guccione *et al*. 2006; Perna *et al*. 2012) were significantly enriched among the genes for which BPTF silencing had more effect on c-MYC recruitment (Fig. 12e). The effect of BPTF silencing on the induction of c-MYC target mRNAs was independent from the extent of reduction in c-MYC binding at their promoters (Fig. 12f), suggesting that BPTF operates downstream of c-MYC in the sequence of events resulting in transcriptional activation.

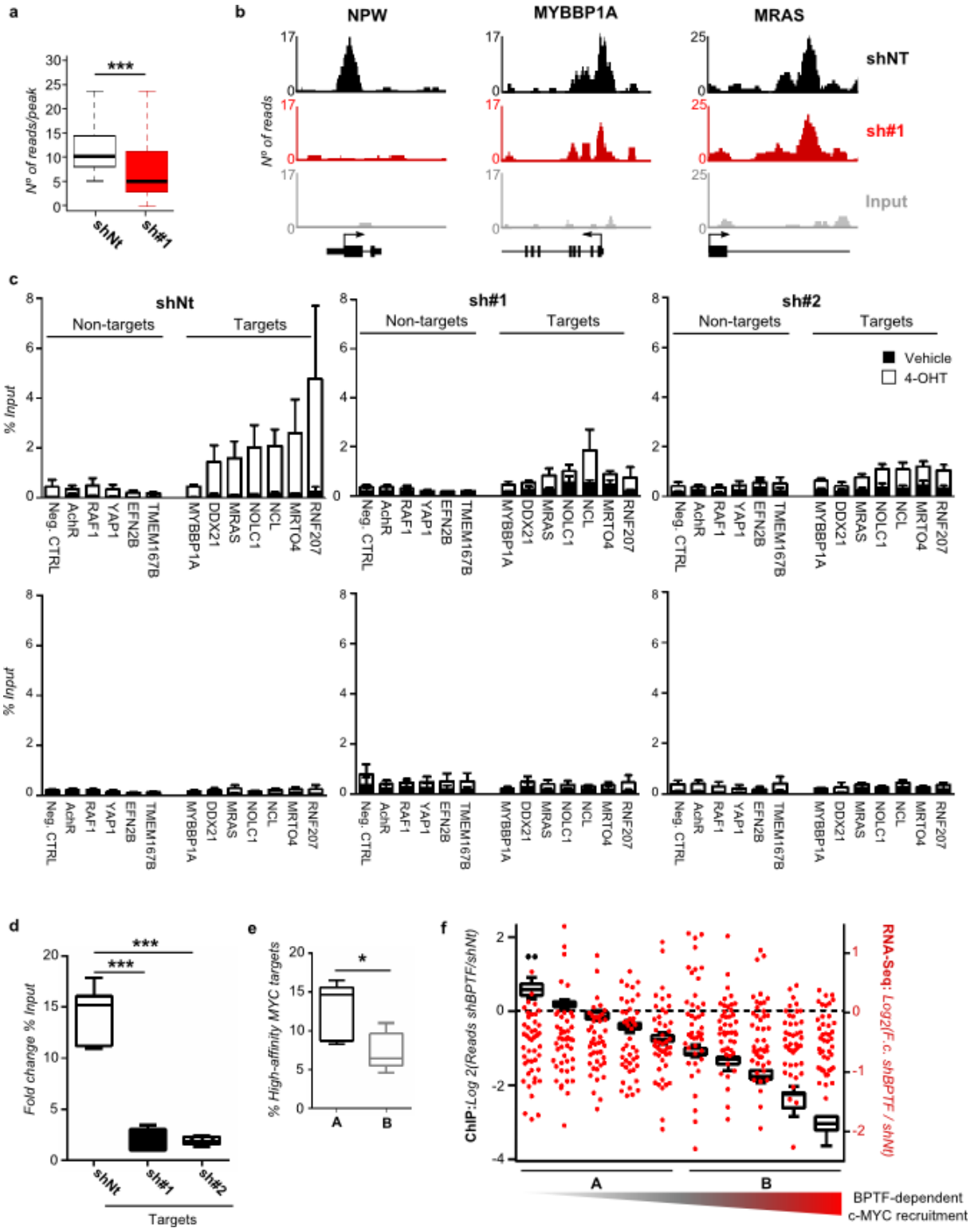

Figure 12. BPTF silencing interferes with c-MYC recruitment to its target genes. a) Box plot showing the intensity of c-MYC ChIP-seq signal (reads/peak) at MYC-enriched regions in control and BPTF-silenced HFF MYC-ER cells. MYC-enriched regions were defined in 4-OHT-treated control cells. c-MYC binding intensity was measured as number of reads per peak. P value was determined using a Wilcoxon test. b) Representative snapshots of c-MYC-bound genomic regions in control and BPTF-silenced HFF MYC-ER cells after stimulation

with 4-OHT. c) ChIP analysis of c-MYC enrichment at the promoters of “Target” and “Non-target” genes in control and BPTF-silenced HFF MYC-ER cells in the presence (white) or absence of 4-OHT (black). ChIP values are expressed as average ± SEM of % input chromatin (n ≥ 3). An isotype-matched IgG antibody was used as control (lower panels). d) Fold-change in % of input following c-MYC induction, averaged for the two different promoter populations in control and BPTF-silenced cells. e) High-affinity MYC-targets are significantly enriched among the genes for which MYC recruitment is less affected by BPTF knockdown. f) c-MYC target genes ranked according to the change in c-MYC binding at their promoters after BPTF silencing. BPTF-dependency of c-MYC recruitment to DNA is calculated as the Log2 (Reads shBPTF/Reads shNt) (left y-axis). For the same collection of ranked genes, the transcriptional response to 4-OHT is shown (scatter plot right y-axis). BPTF-dependency of 4-OHT-dependent mRNA induction is calculated as the Log2 (F.c. shBPTF/F.c. shNt). 4 data points are outside the right y-axis limits. *, P value < 0.05; **, P value < 0.01; ***, P value < 0.001.

6. BPTF IS REQUIRED FOR c-MYC-INDUCED REMODELLING OF TARGET CHROMATIN

c-MYC activates gene expression by recruiting, among others, HATs and chromatin-modifying complexes resulting in histone hyperacetylation, nucleosome displacement, and increased promoter accessibility (Lüscher and Vervoorts 2012). Bromodomain-containing proteins, such as BRD4, recognize acetylated histones and facilitate transcriptional activation through the recruitment of P-TEFb (Yang *et al.* 2005). To assess whether BPTF knockdown led to changes in DNA accessibility, we performed quantitative DNAse I hypersensitivity assays, as described earlier (Di Stefano *et al.* 2014). DNAse I hypersensitive sites mark cis-regulatory elements (i.e. enhancers or promoters) and result from the cooperative binding of transcription factors and chromatin-remodelling complexes (Thurman *et al.* 2012).

We analysed the DNA accessibility of c-MYC “Target” promoters validated in Fig. 12c in the presence or absence of 4-OHT and included “Non-target” regions for comparison. 4-OHT addition to HFF MYC-ER cells led to an increased sensitivity to DNAse I (DDHS) of “Target” regions in control ($P < 0.001$) but not in BPTF-silenced cells (Fig. 13a Top). There was no consistent effect on “Non-target” promoters (Fig. 13a Bottom). Overall, these results indicate that attenuation of the c-MYC transcriptional response is associated with changes in DNA accessibility, suggesting that BPTF is necessary for the c-MYC-induced remodelling of target chromatin.

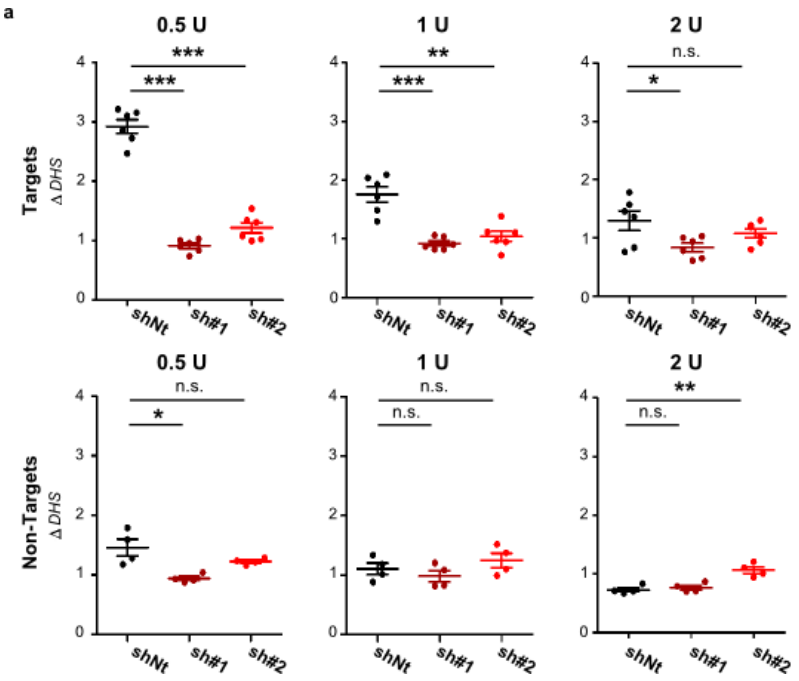

Figure 13. BPTF silencing limits DNA accessibility at c-MYC target promoters. a) DNAse I sensitivity at MYC-bound regions in control and BPTF-silenced HFF MYC-ER cells, determined by enzyme titration. Dots represent the average values of 7 independent experiments. P values were determined using paired t-test. *, *P* value < 0.05; **, *P* value < 0.01; ***, *P* value < 0.001.

We next analysed the levels of acetylated H3 and H3K4me3 in "Target" and "Non-Target" promoters by ChIP-qPCR. As reported previously, c-MYC activation in control cells resulted in the selective hyperacetylation of histone H3 in "Target" promoters (*P* = 0.002). Importantly, this effect was lost upon BPTF knockdown (Fig. 14a Top). By contrast, the levels of H3K4me3 were unaffected by BPTF silencing (Fig. 14b Bottom).

Figure 14. BPTF is required for c-MYC-induced hyperacetylation of target promoters. a) ChIP analysis of Pan AcH3 (Top) and H3K4me3 (Bottom) levels at the promoter of "Target" and "Non-target" genes in control and BPTF-silenced HFF MYC-ER cells. ChIP values are expressed as % of input and normalized for total histone H3. *P* values were determined using paired t-test. *, *P* < 0.05. **, *P* < 0.01. ***, *P* < 0.001.

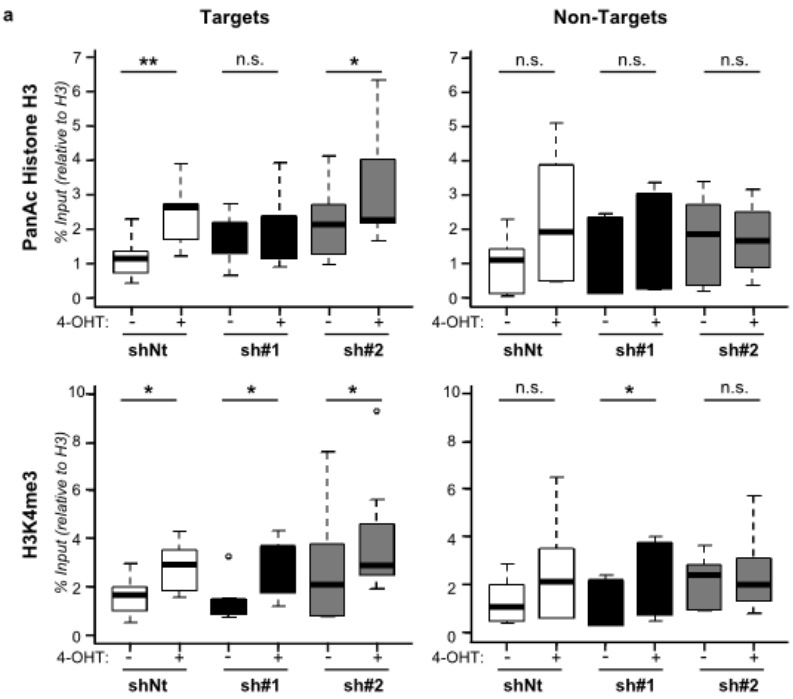

7. BPTF IS REQUIRED FOR A SUBSET OF c-MYC BIOLOGICAL FUNCTIONS

MYC proteins regulate a wide variety of biological processes including cell growth, proliferation, differentiation, and apoptosis. Physiological c-MYC levels induce DNA synthesis through the transcriptional activation of cell cycle-related genes (Liu *et al*. 2008b) and by modulating the activity of DNA replication origins (Dominguez-Sola *et al.* 2007). c-MYC overexpression and/or deregulation is associated with unscheduled firing of DNA replication origins, DNA damage response, and checkpoint activation (Murga *et al*. 2011).

To determine whether BPTF is required for the proliferation-related effects of c-MYC, we used wild type (WT) and *Bptf*-null MEFs. Cells were co-infected with lentiviruses coding for Cre recombinase and the MYC-ER fusion protein. Quiescent MEFs were induced to re-enter the cell cycle by addition of FBS±4-OHT and S phase entry was assessed by BrdU uptake. 4-OHT-treated WT and *Bptf*-null cells showed a significantly higher percentage of cells in S phase than vehicle-

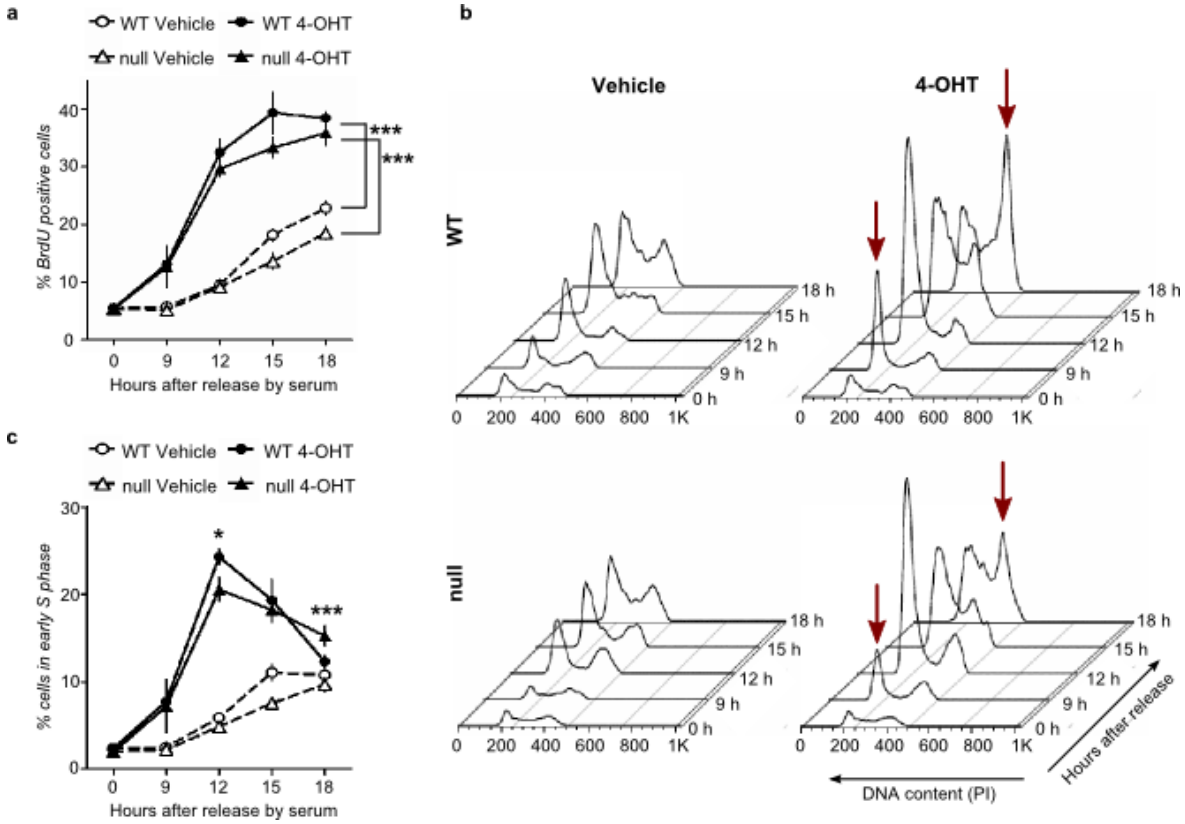

Figure 15. **BPTF is required for MYC-induced proliferation of MEFs.** a) WT and *Bpft*-null MEFs transduced with MYC-ER were seeded at high density, arrested with 0.5% FBS for 48h, and stimulated with serum in the presence/absence of 4-OHT. At indicated time points, cells were pulse-labelled with BrdU for 1h before harvesting. b) Histograms depicting the ploidy of $BrdU^+$ cells throughout the experiment described in panel (a). c) Quantification of early S phase cells. The rate of loss of $BrdU^+$ early S-phase cells represents S-phase progression. *, $P < 0.05$; **, $P < 0.01$; ***, $P < 0.001$.

treated cells as early as 9h after FBS+4-OHT stimulation (P = 0.014), indicative of MYC-induced G1/S progression (Fig. 15a). DNA content analysis of $BrdU^+$ cells followed by quantification of cells in early S phase showed that BPTF deletion resulted in a significantly delayed progression through S phase in MYC-ER-activated cells (at 18h, $P < 0.001$). There were no effects in vehicle-treated cells (Fig. 15b,c).

c-MYC overexpression can induce replication stress (Murga *et al*. 2011). Adding 4-OHT to WT MYC-ER MEFs led to an accumulation of cells with high levels of pan-nuclear γH2AX (P = 0.017), indicative of replication stress, whereas no effect was observed in *Bptf*-null cells (Fig. 16a). c-MYC can also induce apoptosis when expressed from an ectopic promoter in the presence of limiting survival signals or upon cell stress (Evan *et al*. 1992). To assess whether BPTF is required for MYC-induced apoptosis, WT and *Bptf*-null MYC-ER MEFs were seeded at high density and cultured in 0.5% FBS containing either vehicle or 4-OHT. Apoptosis was quantified by Annexin V staining and DAPI exclusion. MYC-ER activation triggered a robust apoptotic response in *Bptf*-null MEFs that was indistinguishable from that observed in wild-type cells (Fig. 16b).

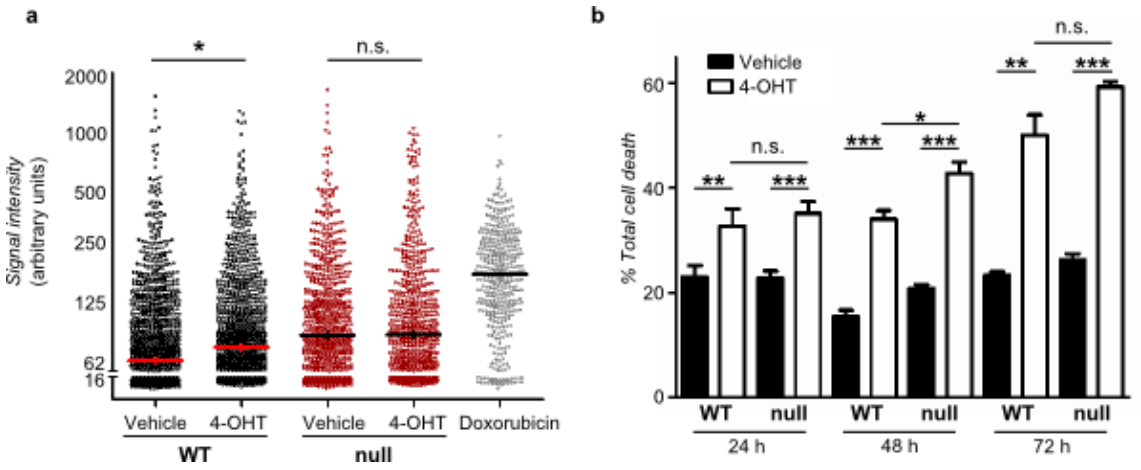

Figure 16. **BPTF is required for c-MYC-induced replicative stress but not for apoptosis.** a) Replication stress - Intensity of γH2AX signal in WT and *Bpft*-null MYC-ER MEFs (n=3/group) in the presence or absence of 4-OHT for 48h. Doxorubicin-treated cells were used as control. b) WT and *Bpft*-null MEFs expressing MYC-ER were seeded at high density and then transferred to 0.5% FBS with or without 4-OHT (2μM). Apoptosis was measured as the proportion of Annexin-postivive cells at the indicated time points by Annexin V staining. *, P value < 0.05; **, P value < 0.01; ***, P value < 0.001.

Therefore, BPTF silencing distinctly affects a subset of c-MYC biological functions. To activate cell proliferation, c-MYC binds directly to genes involved in DNA replication and cell cycle control (i.e. MCM5, MCM6 or DBF4) and enhances

their transcription (Perna *et al*. 2012). By contrast, c-MYC-driven apoptosis is indirect and involves the stabilization of $p19^{ARF}$ and p53 or the down-regulation of anti-apoptotic BCL-2 through inhibition of the transcriptional activator MIZ-1 (Hoffman and Liebermann 2008). We therefore propose that BPTF is only required for those c-MYC functions involving direct binding to chromatin.

8. BPTF IS REQUIRED FOR THE REPROGRAMMING OF MOUSE EMBRYONIC FIBROBLASTS

The combined transduction of fibroblasts with OCT4, SOX2, KLF4, and c-MYC (OSKM) can reprogram fibroblasts to induced pluripotency (Takahashi *et al*. 2007). Ectopic c-MYC expression is dispensable for reprogramming of somatic cells although, in combination with OSK, facilitates the emergence of rare reprogrammed cells. c-MYC has been shown to exert its role during the first days of the reprogramming process, since its depletion after day 5 does not significantly alter the eventual number of iPS colonies (Sridharan *et al*. 2009). Interestingly, two independent studies have shown that BPTF protein and mRNA increase during the first 3 days of reprogramming (Fig. 17a) (Soufi *et al.* 2012; Hansson *et al*. 2012). In addition, a genome-wide study of OSKM occupancy revealed that the *Bptf* promoter is bound by the 4F within the first 48h of reprogramming. In agreement with this, RNA analysis of wild type MEFs infected with each of the 4F individually showed that BPTF mRNA is rapidly induced by each factor in the reprogramming cocktail (Fig. 17b).

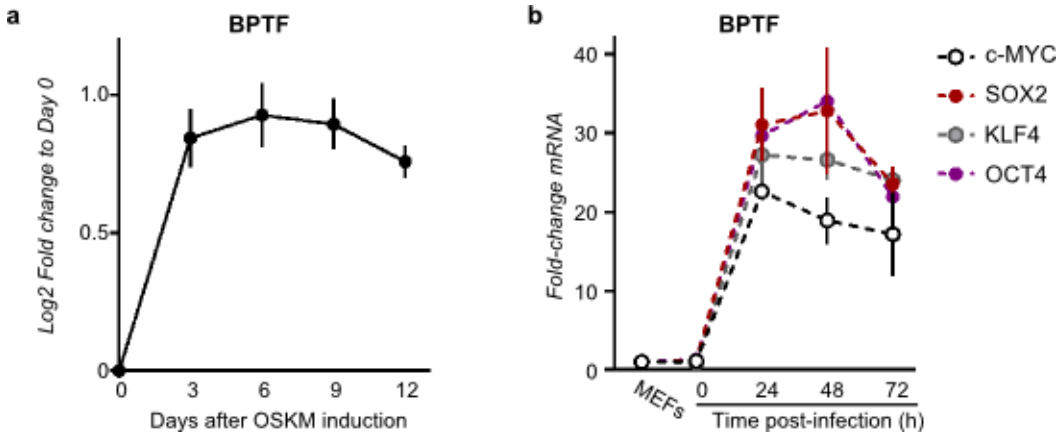

Figure 17. **BPTF mRNA is induced during reprogramming of fibroblasts into iPS cells.** a) Expression profile of BPTF over the course of a reprogramming experiment (data from Hansson *et al.* 2012). b) Analysis of BPTF mRNA levels in wild-type MEFs infected with either c-MYC, SOX2, KLF4 or OCT4. mRNA levels were normalized against HPRT and non-transduced MEFs. Data are represented as mean ± SEM (n=2).

We thus sought to determine whether BPTF depletion had a differential impact on the efficiency of OSKM (4F) and OSK (3F) reprogramming protocols. We used wild type and *Bptf*-null MEFs via 4F and 3F reprogramming. In order to assess both the kinetics and the efficiency of the process, we counted the colonies with ES-like morphology over the course of the experiment and, in addition, scored the yield of alkaline phosphatase (AP) positive colonies between days 12 and 14. The kinetics and efficiency of 4F reprogramming in a series of independent MEF cultures was significantly impaired in the absence of BPTF (Fig. 18a,b). These results were corroborated by reprogramming wild type MEFs with either control

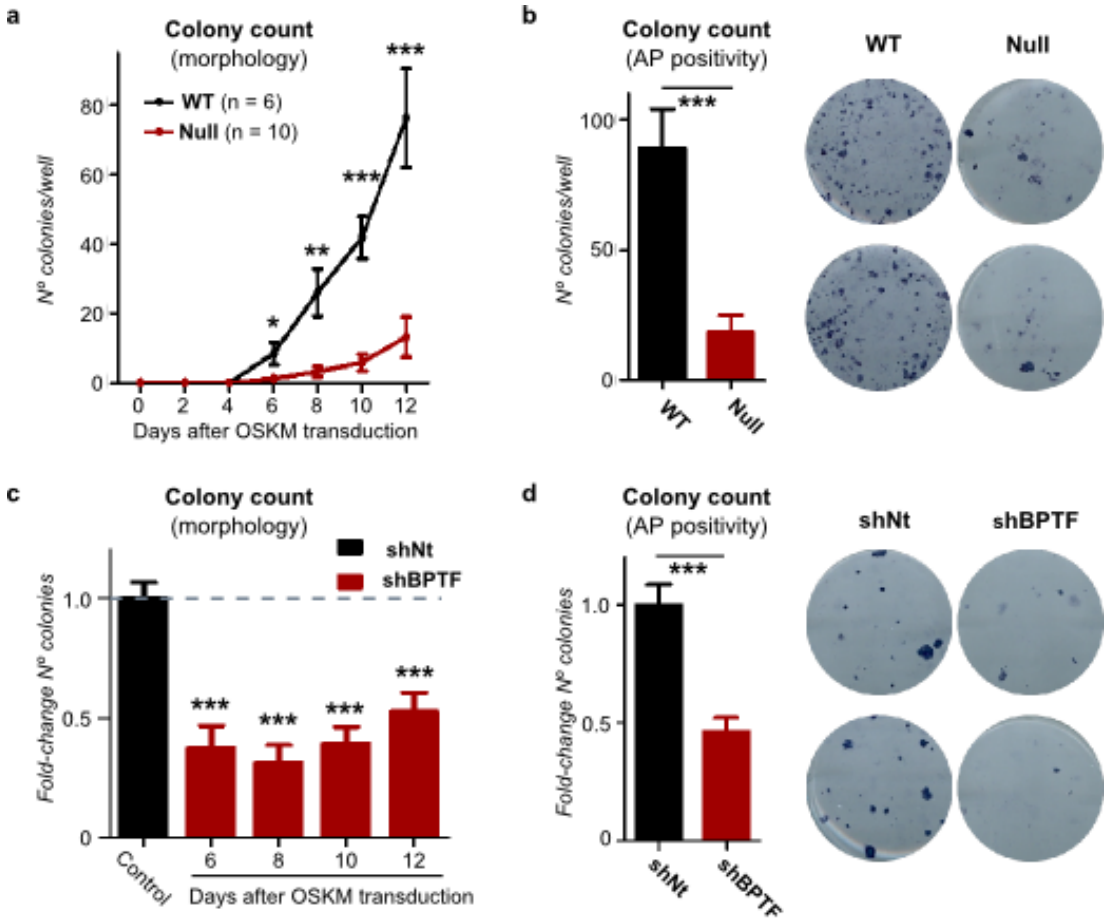

Figure 18. BPTF is required for optimal OSKM reprogramming efficiency. a) Kinetics of appearance of colonies with iPS morphology of WT and *Bptf*-null MEFs infected with 4F. Data correspond to mean ± S.E.M.; n, independent MEF isolates. b) Number of AP-positive colonies obtained at 12 day post-infection; mean ± S.E.M (left). Representative wells of AP-positive colonies, showing reduced reprogramming efficiency in *Bptf*-null MEFs (right). c) Fold-change of reprogramming efficiency of primary WT MEFs retrovirally infected with 4F plus control (shNt) or a BPTF-targeting shRNA. Data correspond to the average ± S.E.M. d) Number of AP-positive colonies obtained at 12 day post-infection; mean ± S.E.M (left). Representative wells of AP-positive colonies, indicating reduced reprogramming efficiency in BPTF-silenced MEFs when compared to control (right).

or a BPTF-targeting shRNA (Fig. 18c,d). Similar observations were made when c-MYC was removed from the reprogramming cocktail (Fig. 19).

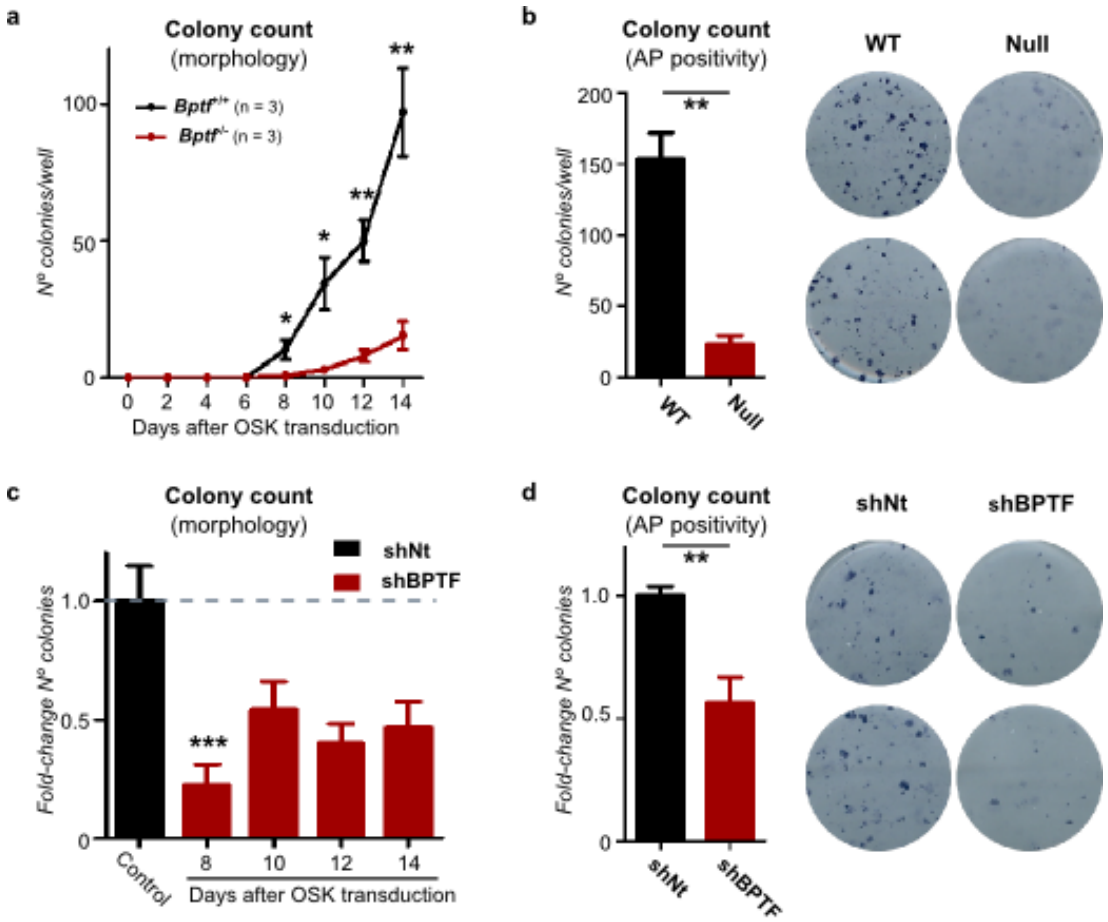

Figure 19. BPTF is required for optimal OSK reprogramming efficiency. a) Kinetics of appearance of colonies with iPS morphology of WT and *Bptf*-null MEFs infected with 3F. Data correspond to mean ± S.E.M.; n, independent MEF isolates. b) Number of AP-positive colonies obtained at 14 day post-infection; mean ± S.E.M (left). Representative wells of AP-positive colonies, indicating reduced reprogramming efficiency in *Bptf*-null MEFs (right). c) Fold change of reprogramming efficiency of primary WT MEFs retrovirally infected with 3F plus control (shNt) or a BPTF-targeting shRNA. Data correspond to the average ± S.E.M. d) Number of AP-positive colonies obtained at 14 day post-infection; mean ± S.E.M (left). Representative wells of AP-positive colonies, indicating reduced reprogramming efficiency in BPTF-silenced MEFs when compared to control (right).

To confirm that the iPS colonies arising from *Bptf*-null MEFs had indeed undergone recombination, we picked colonies with ES-like morphology (n=60) from multiple MEF cultures and assessed the extent of recombination of the *Bptf* allele via PCR on genomic DNA. Strikingly, the majority of colonies were either escapers or heterozygous for the recombined allele; only one colony was a complete knock-out (Fig. 20a,b). Fig. 20c portrays representative pictures of iPS colonies of different genotype after expansion on feeders. Both the heterozygous

and the *Bptf*-null iPS expressed lower levels of Nanog, Sox2 and Oct4 when compared to wild type (Fig. 20d). Overall, these results indicate that loss of BPTF significantly impairs reprogramming. Although we have not reported any differences between the 4F and 3F protocol, we cannot rule out the possibility that the observed effects are due to the loss of c-MYC function, since the endogenous c-MYC protein is likely to play a key role in the reprogramming process.

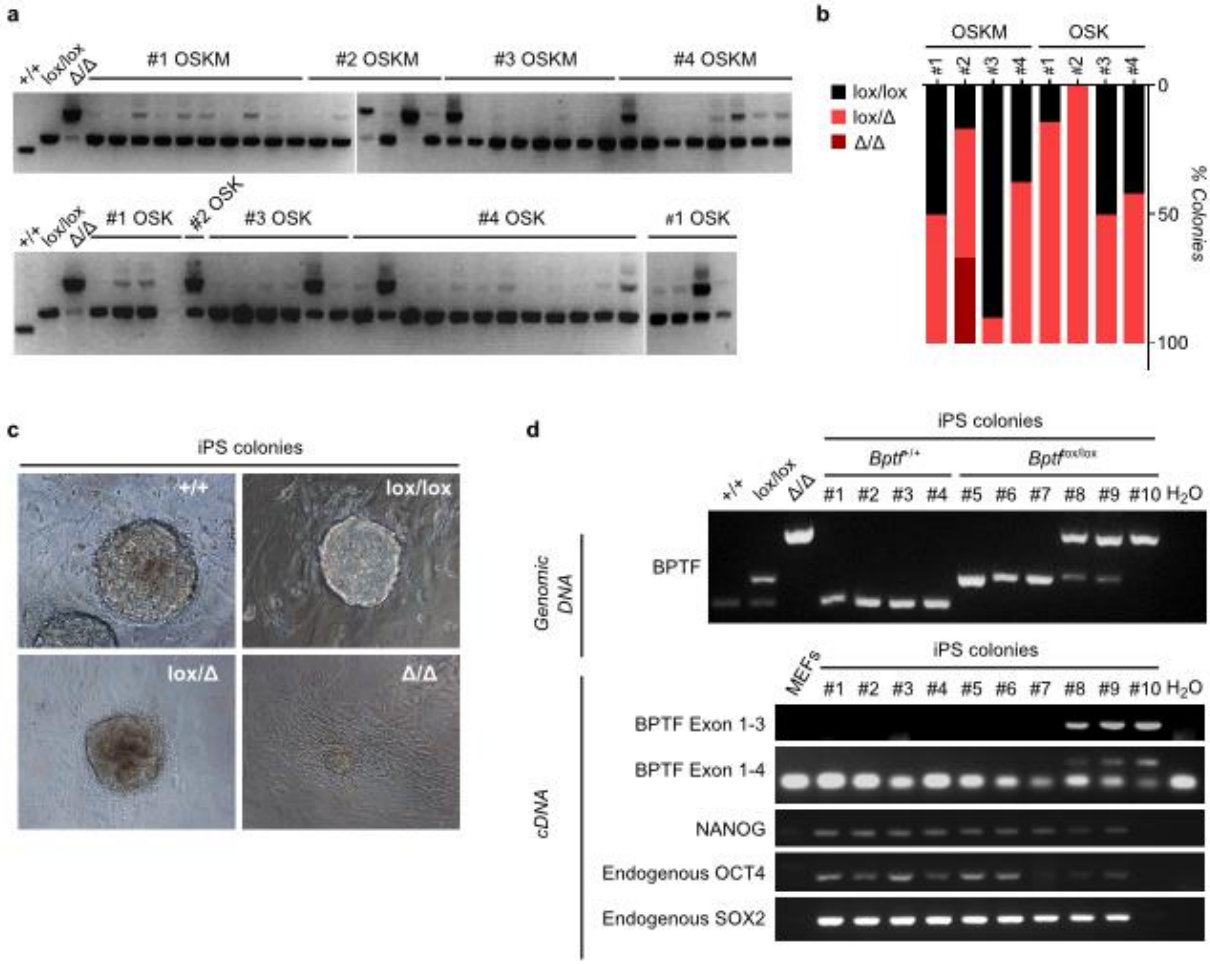

Figure 20. BPTF is required for the reprogramming of mouse fibroblasts. a) Assessment of Cre-mediated recombination of the *Bptf* allele by PCR on genomic DNA from a panel of colonies arising from *Bptf*-null MEFs. Colonies were picked from different MEF preparations and reprogramming protocols. b) Quantitation of the percentage of colonies with the indicated genotypes in the MEF cultures reprogrammed in (a). c) Representative pictures of colonies of the corresponding genotypes after expansion *in vitro*. d) RT-PCR analysis of ES cell marker genes in iPS cells. MEFs were used as control.

9. BPTF CORRELATES WITH c-MYC SIGNATURES IN HUMAN CANCER

c-MYC expression is deregulated in the majority of human tumors through a variety of mechanisms, including amplification, translocations, and aberrant activation of upstream signalling pathways (Dang 2012). A paradigm of c-MYC-addicted tumors is Burkitt lymphoma (BL), characterized by chromosomal translocations leading to c-MYC overexpression under the control of Ig regulatory sequences (Taub *et al*. 1982). Interestingly, BL cell lines express high BPTF mRNA levels compared to other tumor types (Fig. 21). BPTF knockdown in two BL cell lines, NAMALWA and RAJI, significantly impaired cell proliferation and was accompanied by a reduction in the mRNA levels of c-MYC target genes (Fig. 22). These results indicate that BPTF is required for the growth of c-MYC-addicted BL cells.

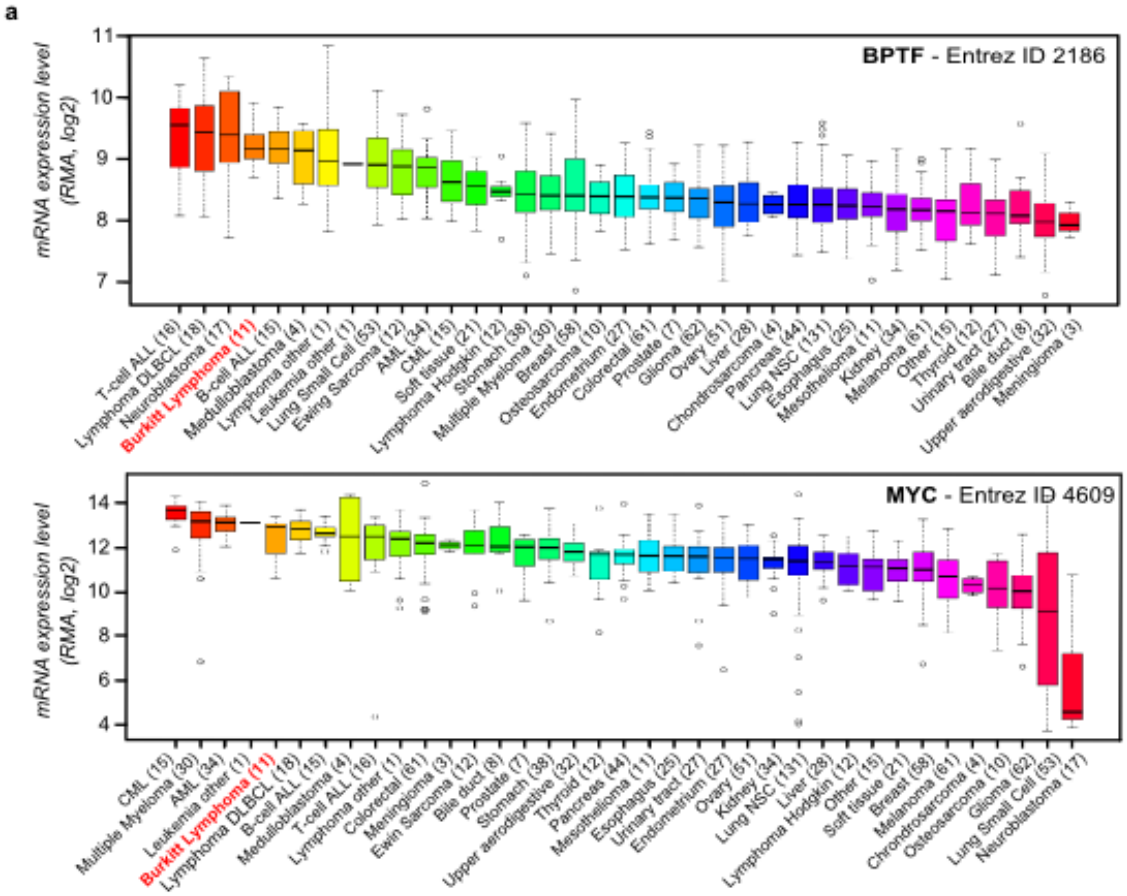

Figure 21. BPTF and c-MYC expression in a panel of human cancer cell lines. a) Top: Box plot showing the relative BPTF mRNA levels across the different tumor types, extracted from CCLE_Expression_Entrez_ID_2186, with gene-centric robust multiarray analysis-normalized mRNA expression data. Bottom: Box plot showing the relative c-MYC mRNA levels across a panel of human cell lines, extracted from CCLE_Expression_Entrez_ID_4609. The number of cell lines of each tumor type analysed is indicated in parentheses.

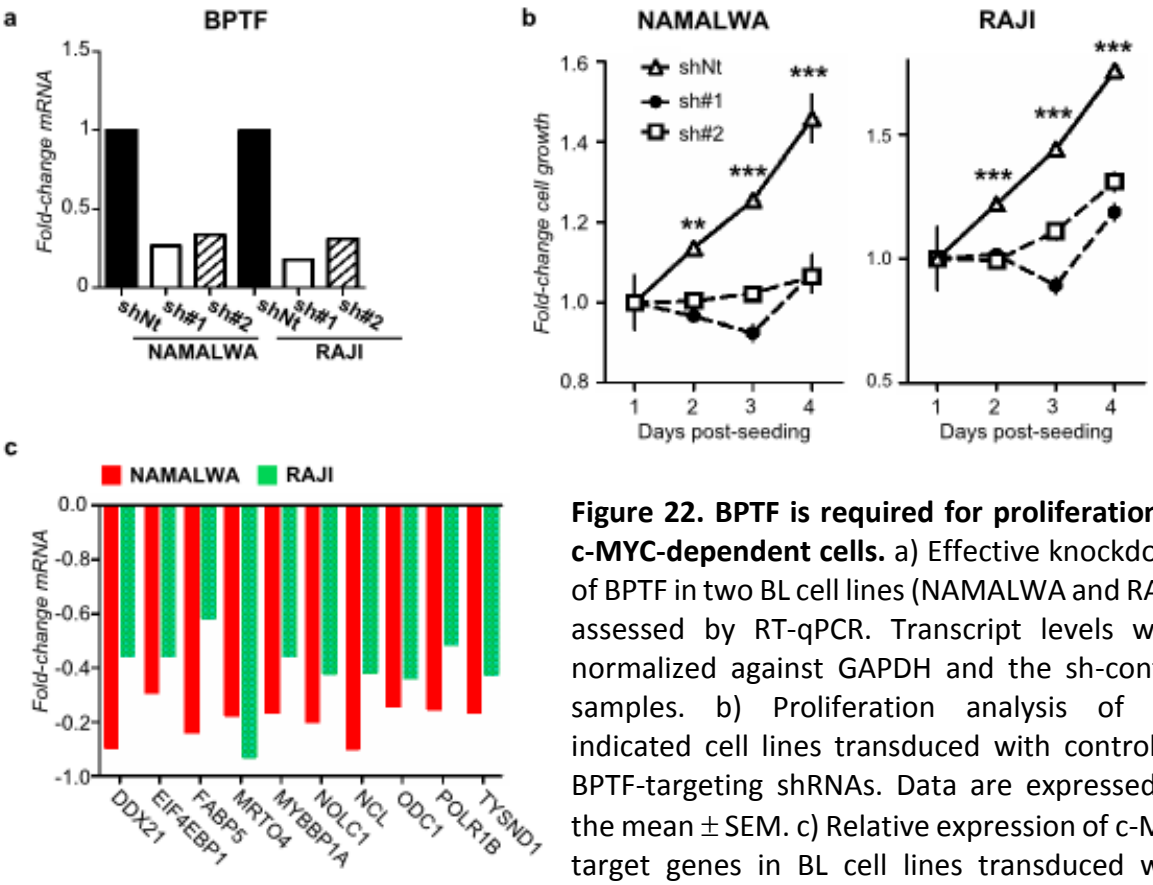

Figure 22. BPTF is required for proliferation of c-MYC-dependent cells. a) Effective knockdown of BPTF in two BL cell lines (NAMALWA and RAJI), assessed by RT-qPCR. Transcript levels were normalized against GAPDH and the sh-control samples. b) Proliferation analysis of the indicated cell lines transduced with control or BPTF-targeting shRNAs. Data are expressed as the mean ± SEM. c) Relative expression of c-MYC target genes in BL cell lines transduced with sh#1. Transcript levels were normalized against GAPDH and the sh-control samples.

To gain further insight into the relevance of the c-MYC:BPTF axis in human cancer, we compared the levels of BPTF and c-MYC with the activation of c-MYC gene signatures in a collection of 20 expression datasets encompassing human tumors of diverse origin (Table 7). Our analyses included tumor types known to be driven by different MYC family members: BL, colorectal, prostate, and pancreatic tumors are mainly driven by c-MYC (Taub *et al*. 1982; Sansom *et al*. 2007; Taylor *et al.* 2010; Saborowski *et al*. 2014) whereas medulloblastoma and ovarian carcinoma commonly show amplification and/or overexpression of N-MYC and L-MYC, respectively (Garson *et al*. 1989; Wu *et al*. 2003). BPTF is over-expressed in tumors together with c-MYC and, in some cases, N-MYC and L-MYC (Fig. 23a).

DATASET ID	GEO ID	N° OF SAMPLES	TUMOR TYPE	REFERENCE
Piccaluga	GSE26673	16	Burkitt Lymphoma	Piccaluga *et al.* (2011). *Blood*, 117, 3596-608.
Jima	GSE48435	21	Burkitt Lymphoma	Love *et al.* (2012). *Nat Genet.*, 44, 1321-5.
Hummel	GSE4475	37	Burkitt Lymphoma	Hummel *et al.* (2006). *N Engl J Med.*, 354, 2419-30.
Northcott	GSE37382	188	Medulloblastoma	Northcott *et al.* (2012). *Nature*, 488, 49-56.
Donson	GSE50161	35	Medulloblastoma	Griesinger *et al.* (2013). *J Immunol.*, 191, 4880-8.
Robinson	GSE37418	76	Medulloblastoma	Robinson *et al.* (2012). *Nature*, 488, 43-8.
Grasso	GSE35988	122	Prostate carcinoma	Grasso *et al.* (2012). *Nature*, 487, 239-43.
Yu	GSE6919	112	Prostate carcinoma	Yu *et al.* (2004). *J Clin Oncol.*, 22, 2790-9.
Varambally	GSE3325	19	Prostate carcinoma	Varambally *et al.* (2005). *Cancer Cell.*, 8, 393-406.
Sun	GSE25136	79	Prostate carcinoma	Sun and Goodison (2009). *Prostate*, 69, 1119-27.
Taylor	GSE21034	185	Prostate carcinoma	Taylor *et al.* (2010). *Cancer Cell.*, 18, 11-22.
Kaiser	GSE5206	105	Colorectal Carcinoma	Kaiser *et al.* (2007). *Genome Biol.*, 8, R131.
Ahmed	GSE32323	44	Colorectal Cancer	Khamas *et al.* (2012). *Cancer Genomics Proteomics*, 9, 67-75.
Skrzypczak	GSE20916	105	Colorectal Carcinoma	Skrzypczak *et al.* (2010). *PLoS One*, 5, pii: e13091.
Badea	GSE15471	78	PDAC	Badea *et al.* (2008). *Hepatogastroenterology*, 55, 2016-27.a.
Grutzmann		25	PDAC	Grutzmann *et al.* (2004). *Neoplasia*, 6, 611-22.
Ishikawa	GSE1542	49	PDAC	Ishikawa *et al.* (2005). *Cancer Sci.*, 96, 387-93.
Meyniel	GSE20565	140	Ovarian Adenocarcinoma	Meyniel *et al.* (2010). *BMC Cancer.*, 10, 222.
Hendrix	GSE6008	103	Ovarian Adenocarcinoma	Hendrix *et al.* (2006). *Cancer Res.*, 66, 1354-62.
Jönson	GSE57477	72	Ovarian Adenocarcinoma	Jönson *et al.* (2014). PLoS One., 9, e107643.

Table 7. Summary of human tumor datasets.

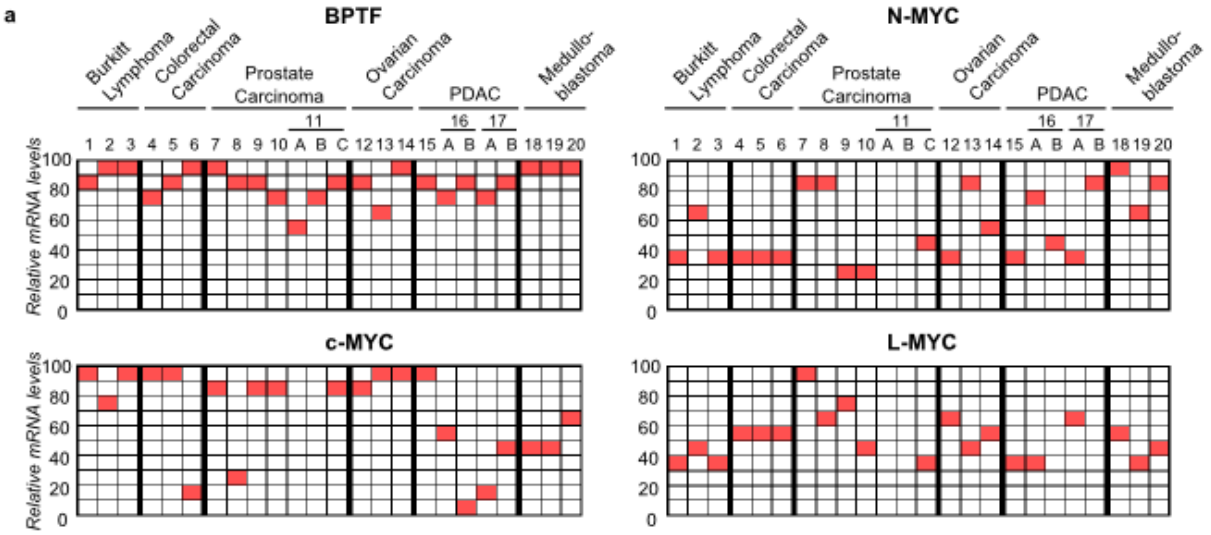

Figure 23. Co-expression of BPTF and MYC genes in human tumors. a) Position of *BPTF*, *c-MYC*, *MYCN* and *MYCL1* mRNAs within the lists of transcribed genes rank-ordered by their expression values in a collection of human tumors.

Samples within each data set were rank-ordered by the mRNA levels of either BPTF, c-MYC, N-MYC or L-MYC and then interrogated by single-sample GSEA (ssGSEA) (Barbie *et al*. 2009) for enrichment of four c-MYC gene sets showing a modest degree of overlap (Fig. 24a). c-MYC signatures correlated with c-MYC expression levels in BL, colorectal, prostate, and pancreatic carcinomas. In these tumors, BPTF expression levels also correlated positively with c-MYC signatures and BPTF knockdown resulted in a marked decrease in proliferation and colony formation by pancreatic cancer cells (Fig. 5 and 24b).

By contrast, c-MYC expression signatures correlated with N-MYC and L-MYC expression levels only in medulloblastoma and ovarian carcinoma, respectively, and in these tumors the signatures correlated negatively with BPTF expression levels (Fig. 24b,c). These data point to a selective role of BPTF in the activation of MYC gene signatures in c-MYC-driven, but not in N-MYC- or L-MYC-driven, tumors.

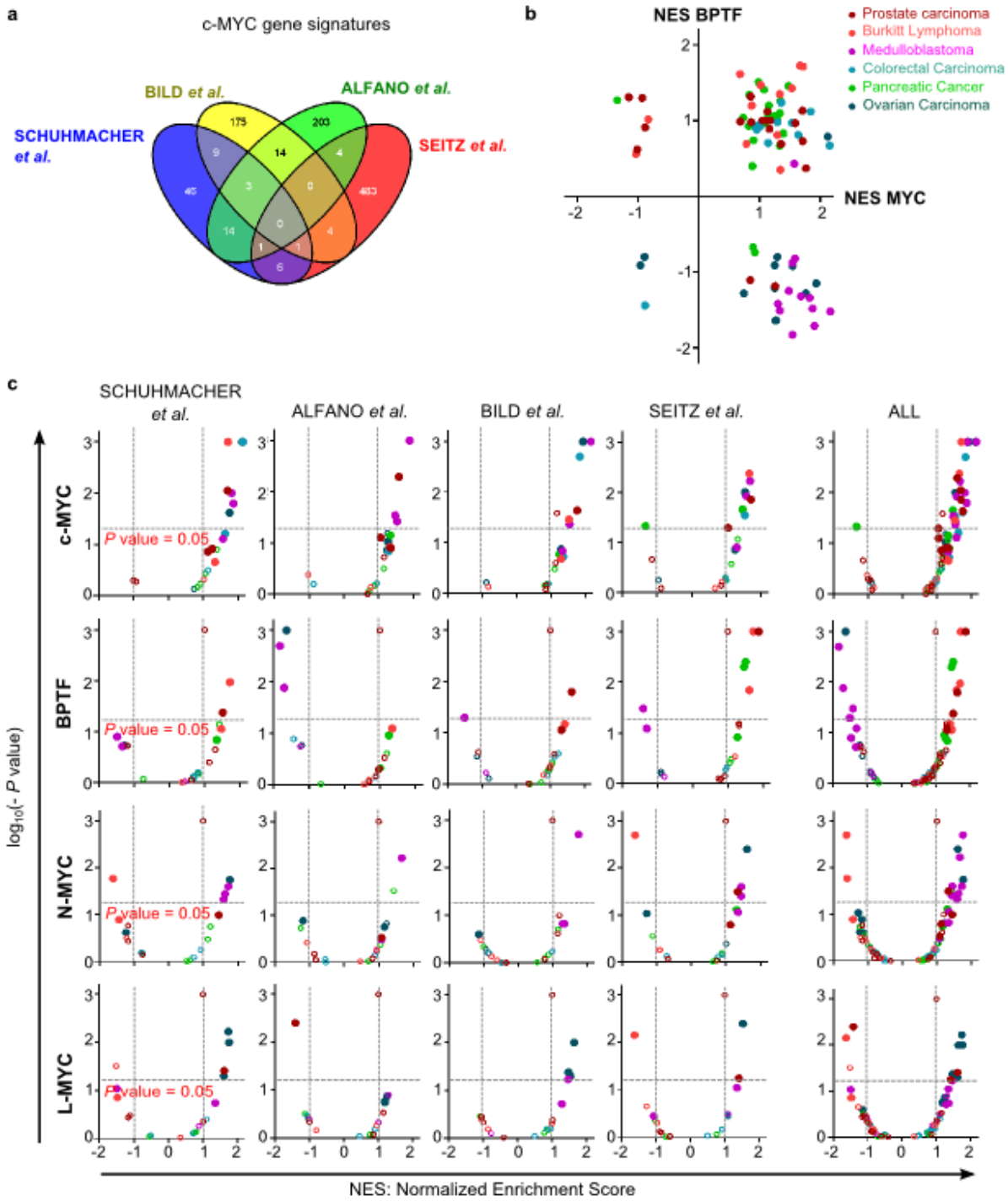

Figure 24. **BPTF expression correlates with c-MYC signatures in human tumors.** a) Venn diagram showing the overlap of the c-MYC signatures used in the following analyses. b) Dot plot of Normalized Enrichment Scores (NES) of the 4 c-MYC signatures based on GSEA. NES values were calculated for each data set previously ranked-ordered by either BPTF or c-MYC levels. c) Volcano plots of NES and enrichment *P* values of c-MYC signatures based on GSEA. NES values were calculated for each data set previously ranked-ordered by either BPTF, c-MYC, N-MYC or L-MYC mRNA levels. Filled circles represent gene sets with a FDR < 0.25.

10. BPTF IS REQUIRED FOR c-MYC-DRIVEN PANCREATIC TUMORIGENESIS

Transgenic mice in which c-MYC is overexpressed under the control of the acinar-specific elastase 1 promoter (*Ela-Myc*) develop mixed acinar/ductal pancreatic adenocarcinomas between 2 and 7 months of age (Sandgren *et al*. 1991). To investigate the role of BPTF in c-MYC-driven pancreatic neoplasia, we generated *Bptf*$^{lox/lox}$*;Ptf1a*$^{+/KI}$*;Ela-Myc*$^{+/T}$ mice (*Bptf*$^{P-/-}$*;Ela-Myc*) where BPTF is deleted in Ptf1a^{+} pancreatic progenitors around day E9.5-10. In agreement with previous reports showing highly efficient recombination mediated by *Ptf1a-Cre* in the pancreas (Martinelli *et al*. 2013), we detected full recombination of the *Bptf* allele in *Bptf*$^{P-/-}$ mice by PCR and RT-qPCR analysis (Fig. 25a). At 9-12 weeks, *Bptf*$^{P-/-}$ pancreata were histologically indistinguishable from controls (Fig. 25b). The analysis of mRNA of a panel of acinar, ductal and endocrine markers did not unveil important differences either, thus suggesting that BPTF is dispensable for pancreatic development after e10.5 (Fig. 25c).

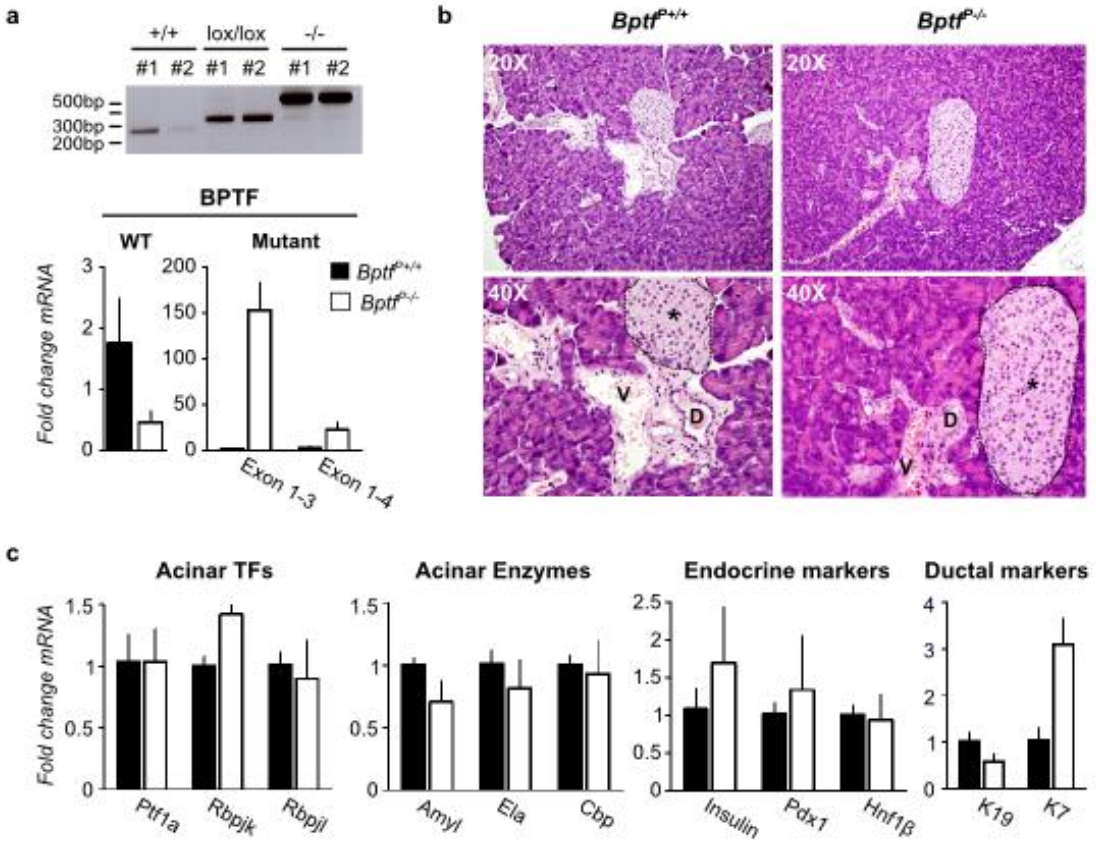

Figure 25. BPTF deletion has no impact on normal pancreas homeostasis. a) PCR on genomic DNA showing efficient recombination at the *Bptf* locus in *Bptf*$^{P-/-}$ pancreas (top). RT-qPCR analysis of BPTF WT and mutant mRNA species in control (n=6) and *Bptf*$^{P-/-}$ (n=7) mice (bottom). b) Hematoxylin-eosin staining of wild type and *Bptf*$^{P-/-}$ mouse pancreatic sections. V: Blood vessel; D: Duct; *: Islet of Langerhans. c) mRNA expression of acinar transcription factors, digestive enzymes and endocrine and ductal markers in pancreata of WT and *Bptf*$^{P-/-}$ mice assessed by RT-qPCR (n=3).

In contrast, *Bptf*$^{p-/-}$ mice where c-MYC was overexpressed in acinar cells were significantly smaller in size (Fig. 26a) and displayed extensive pancreas atrophy. The exocrine compartment was almost completely lost and replaced by fat as soon as 4 weeks of age (Fig. 26b). The response to glucose overload was normal, indicating preservation of endocrine function (Fig. 26c). Transdifferentiation of acinar cells into adipocytes has been reported elsewhere (Martinelli *et al.* 2013; Bonal *et al.* 2009); whether this is the mechanism behind the presence of fat in *Bptf*$^{p-/-}$*;Ela*-Myc mice remains to be determined.

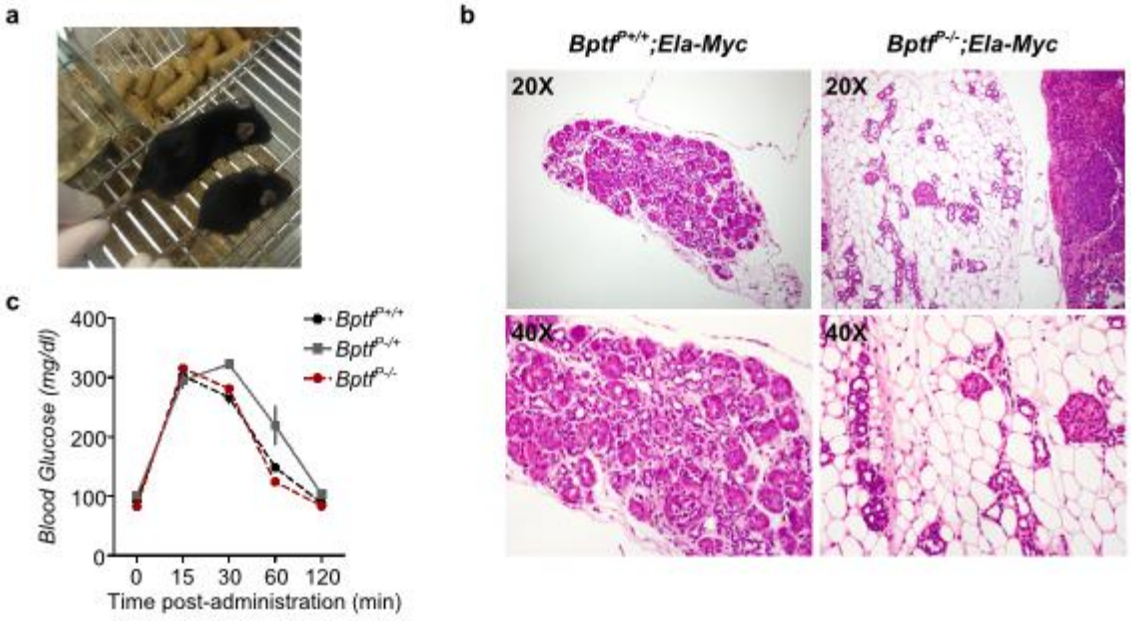

Figure 26. c-MYC overexpression in *Bptf*-null mouse pancreata results in extensive loss of the acinar compartment. a) Picture showing reduced body size of a *Bptf*$^{p-/-}$ mouse (right) when compared to a control mouse (left). e) Hematoxylin-eosin staining of mouse pancreatic sections of the indicated genotype showing extensive acinar loss in *Bptf*$^{p-/-}$ mice. f) Glycaemia after intraperitoneal glucose injection, in *Bptf*$^{p+/+}$ (n=2), *Bptf*$^{p-/+}$ (n=3), and *Bptf*$^{p-/-}$ (n=2) mice. Data are mean ± SEM.

In order to better discriminate the effects of BPTF loss on pancreatic cancer, we generated *Bptf*$^{lox/lox}$; *Ptf1a-CreERT2*$^{+/KI}$; *Ela-Myc* mice where recombination of the *Bptf* allele is induced upon oral delivery of 4-OHT. This mouse model allows to delay *Bptf* inactivation and to more effectively assess its role in the early stages of the disease. Tamoxifen administration to 5-7 weeks-old mice resulted in recombination of 60-70% of the *Bptf* allele as assessed by PCR on genomic DNA (Fig. 27a). A cohort of 10 *Bptf*$^{p+/+}$*;Ela-Myc*, 5 *Bptf*$^{p-/+}$*;Ela-Myc* and 8 *Bptf*$^{p/-}$*;Ela-Myc* mice was monitored once a week by ultrasound for pancreas cancer development. Animals were sacrificed when tumor burden reached ethical end-points or showed overt signs of morbidity. *Bptf*$^{p+/+}$*; Ela-Myc* mice displayed a

typical course of pancreatic cancer development, with a mean disease-free survival of 13 weeks. In contrast, *Bptf*$^{P-/+}$ and *Bptf*$^{P-/-}$ *Ela-Myc* mice showed delayed tumor onset and corresponding extensions in lifespan (P = 0.017) (Fig. 27b). Moreover, analysis of tumor volume revealed that control mice developed pancreatic tumors faster than *Bptf*$^{P-/+}$ and *Bptf*$^{P-/-}$*;Ela-Myc* (Fig. 27c). Finally, we evaluated by PCR the genotype of tumors arising in *Bptf*$^{P-/+}$ and *Bptf*$^{P-/-}$ *Ela-Myc* mice and seen that the majority were escapers or else had a low percentage of recombination (Fig. 27d). In summary, BPTF is necessary for the establishment and/or maintenance of c-MYC-driven pancreatic tumors.

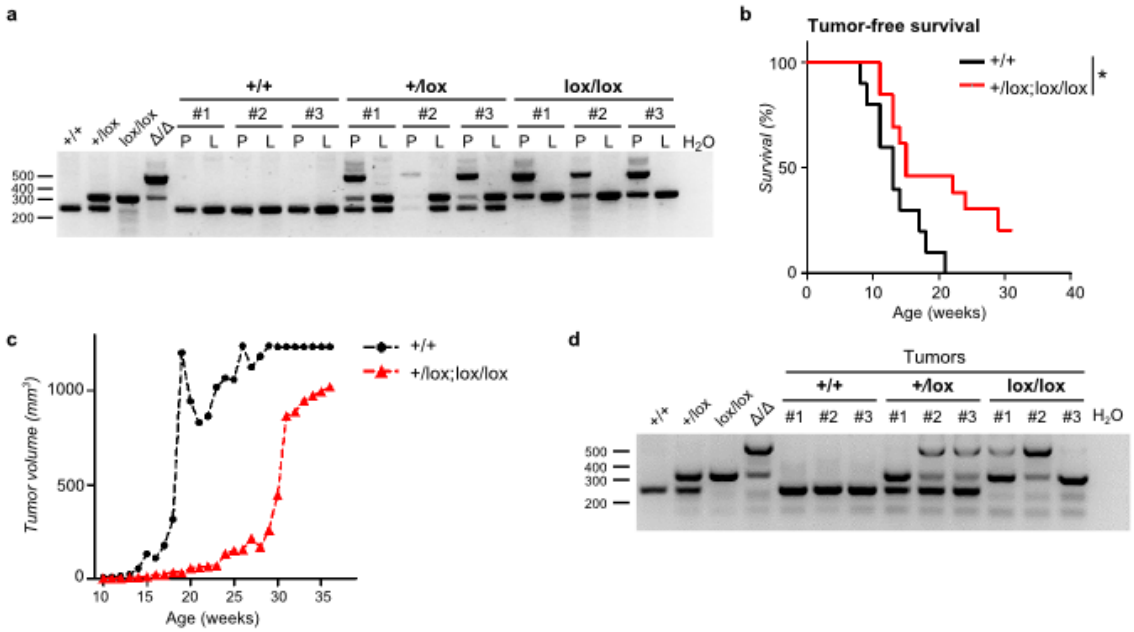

Figure 27. BPTF loss delays the onset of c-MYC driven pancreatic tumors. a) PCR on pancreas (P) genomic DNA assessing the extent of recombination at the *Bptf* locus in 5-7 weeks-old *Ptf1a-CreERT2*$^{+/KI}$*; Ela-Myc* mice of the corresponding genotypes. Liver (L) samples were used as negative controls. b) Kaplan-Meier curves of tumor-free survival are shown for *Ela-Myc* mice of the indicated *Bptf* genotypes. *P* value was determined using a Log-rank test. c) Tumor volume of *Ela-Myc* mice of the indicated *Bptf* genotypes as determined by ultrasound. d) PCR analysis of genomic DNA from tumors arising in *Bptf*$^{P+/+}$, *Bptf*$^{P-/+}$ and *Bptf*$^{P-/-}$ *Ela-Myc* mice.

Discussion

DISCUSSION

We initially identified BPTF as an element of a network of transcription regulators whose expression was modulated during proliferation/cell cycle arrest of two pancreatic cancer cell lines. In agreement with our *in silico* prediction, BPTF down-regulation in these cells was associated with impaired proliferation. We have expanded this observation to other human cancer cell lines (bladder and Burkitt lymphoma) and to non-transformed, non-immortalized human fibroblasts. Based on these findings, we focused on the study of its biological functions.

1. BPTF AND CELL PROLIFERATION

In quiescent human fibroblasts, BPTF depletion impedes cells from progressing into S phase and completing cell cycle. Of note, *Bptf*-null MEFs do not show significant proliferation defects when compared to wild type cells, which could reflect species- and/or cell type-specific BPTF roles. Alternatively, MEFs could have a distinct ability to adapt and bypass the need of BPTF.

DNA replication requires extensive chromatin rearrangements; it is thus conceivable that chromatin remodelling by BPTF:NURF might contribute to this process via multiple mechanisms.

Initiation of DNA synthesis takes place through a series of tightly coordinated events occurring from early G_1 to the G_1/S transition. During early G_1, ORC (Origin Recognition Complex) proteins assemble at replication origins throughout the genome. The mechanisms involved therein are not well understood because replication origins are widely distributed and do not share a common DNA sequence, but epigenetic factors such nucleosome phasing and histone modifications are plausible candidates (McNairn and Gilbert 2003; Cohen *et al*. 2010). Not all origins initiate replication, but many are licensed when the replicative helicases MCM2-7 are recruited in a CDC6- and CDT1-dependent manner (Falbo and Shen 2006). Licensed origins that fire early during S phase tend to have higher histone acetylation levels than those that fire later (Goren *et al*. 2008; Vogelauer *et al*. 2002). The final step in replication initiation is the loading of the replicative polymerases. NURF-dependent chromatin remodelling could be critical to multiple steps of this process, from unmasking replication origins by reconfiguring the nucleosomes around them, to facilitating the loading of MCMs and replicative polymerases. Alternatively, NURF could interact with and facilitate the activity of transcription factors involved in G_0/G_1 or G_1/S transition (e.g. E2F,

AP-1 or c-MYC). A role in the early steps of DNA replication has been already established for other chromatin remodellers such as BRG1, the catalytic subunit of the SWI/SNF complex, which co-localizes with proteins of the replication machinery (Cohen *et al*. 2010).

Once replication has been initiated, the replication forks progress along the genome and the synthesis of new strands of DNA takes place. If DNA polymerases encounter a lesion, or else nucleotide pools are depleted, replication forks stall. Similarly to other ISWI family members (e.g. ACF or WICH), NURF could be in charge of keeping an open chromatin structure around replication forks and thus facilitate their progression (Collins *et al*. 2002; Poot *et al*. 2004). In addition, NURF might participate in rescuing stalled replication forks, either through their stabilization or the activation of checkpoint responses (Falbo and Shen 2006). These mechanisms remain to be experimentally addressed.

Given the essential role of chromatin remodellers during DNA synthesis, both their levels and activity are subjected to tight mechanisms of control. In agreement with this, the experiments with human fibroblasts arrested in G_0 show that BPTF protein levels fluctuate during the cell cycle: it is rapidly induced upon mitogenic stimulation and its levels drop as cells progress into S phase. BPTF re-expression is only detected 35 hours post-release, after G_2/M is completed and cultures become asynchronous. Additional experiments are required in order to confirm that BPTF protein is indeed restricted to G_0-G_1, such as synchronization of U2OS cells at the G_1/S boundary or in metaphase via double-thymidine block or colcemid, respectively (Marqués *et al*. 2008).

The changes in BPTF protein levels during cell cycle are not accompanied by concomitant alterations in its mRNA levels, thus suggesting that post-translational modifications are involved. In fact, independent large scale proteomics studies have identified multiple residues in the BPTF sequence that are susceptible to phosphorylation and acetylation (Olsen *et al*. 2006; Matsuoka *et al*. 2007; Dephoure *et al*. 2008; Mayya *et al*. 2009; Rigbolt *et al*. 2011; Choudhary *et al*. 2011; Olsen *et al*. 2010). One example is the phosphorylation on S216, which has been uncovered by three studies and appears to be mutated in cutaneous squamous cell carcinoma (Durinck *et al*. 2011). In line with these observations, examples of both phosphorylation and acetylation of chromatin remodellers have been reported in the literature. Phosphorylation of the SWI/SNF subunits BRG1 and BAF155 by ERK1 inhibits the remodelling activity of the complex (Sif *et al.* 1998), while phosphorylation of FAC1 enhances its DNA binding activity (Jordan-Sciutto *et al*. 1999b). Also, acetylation of *Drosophila* ISWI

by the histone acetyltransferase Gcn5 controls NURF function during chromosome condensation (Ferreira *et al.* 2007).

The roles of BPTF post-translational modifications are not yet known but they probably impact the half-life or the DNA-binding activity of the NURF complex. The generation of cell lines and, eventually, mice carrying point mutations in these residues using the CRISPR/Cas9 technology would provide key insights into BPTF function (Inui *et al*. 2014). Another important issue that needs to be tackled is the identification of the effectors of such modifications. Taking into account the amino acid sequence, plausible candidates are the MAPK kinases for P-Ser216 (PR**S**P), and the CDK kinases for P-Ser2465 (**S**PVR) (Holmes and Solomon 1996; Songyang *et al*. 1996). Furthermore, and considering the expression pattern of BPTF during cell cycle, we could narrow down the latter to the interphase CDKs (2, 4 and 6) or the transcriptional CDKs (7-11) (Malumbres 2011).

2. BPTF AND c-MYC AXIS

We have shown that BPTF and c-MYC are found within the same complex in 293 cells and that they interact in cultured cells using the isPLA assay. Unfortunately, and due to the lack of immunoprecipitation-grade antibodies for BPTF, we have not been able to conduct the co-IP with the endogenous proteins. Nonetheless, our experiments confirm a functional interaction between BPTF and c-MYC, since BPTF down-regulation in human fibroblasts transduced with MYC-ER impairs the transcriptional response to c-MYC activation. Several mechanisms might account for the attenuation of c-MYC transcriptional activity in the absence of BPTF, as hypothesized below:

2.1. c-MYC recruitment to DNA and/or stability of the complex

c-MYC target promoters cluster into 'high-affinity' or 'low-affinity' sites. High-affinity targets are bound by c-MYC in different cell lines regardless of c-MYC levels. Conversely, low-affinity sites vary among cell types and are only engaged when c-MYC is expressed at high levels (Fernandez *et al*. 2003). The two groups of promoters cannot be differentiated on the basis of sequence motifs but can be discriminated according to their associated epigenetic marks. High-affinity promoters typically display higher levels of H2A.Z, H3K4/K79me, and global H3/H4ac. In contrast, low-affinity promoters show enrichment in macroH2A, H3K27me3, and H4K16ac (Guccione *et al*. 2006; Martinato *et al*. 2008).

We have shown that BPTF depletion impairs c-MYC-mediated transcriptional response. This is accompanied by a reduction in c-MYC recruitment to some, but not all, target promoters. For the sake of clarity we will refer to them as 'sensitive' and 'non-sensitive' to BPTF levels. The distinctive feature between the two collections of genes is the relative abundance of high-affinity targets: it is significantly higher in the set of 'non-sensitive' promoters.

These data suggest that BPTF requirement for target recognition by c-MYC depends on the epigenetic context: while dispensable for c-MYC binding to H3K4me3-rich 'high-affinity' promoters, it might participate in the recognition of low-affinity sequences, presumably through H4K16ac. An alternative explanation is that BPTF-mediated chromatin remodelling stabilizes the association of c-MYC with low-affinity promoters. There are indeed precedents in the literature for chromatin remodellers securing the binding of transcription factors to their cognate sites in the genome. For instance, stable binding of MyoD, a key regulator of muscle differentiation, requires the recruitment of the remodelling complex SWI/SNF (de la Serna *et al*. 2005). Alternative mechanisms may also contribute to explain these observations.

The impact of BPTF silencing on c-MYC recruitment to distal enhancer elements remains to be determined. Active enhancers are characterized by high H3K4me1-2, H3K27ac, recruitment of the HAT p300, and the presence of transcription factor binding motifs and DNAse I hypersensitivity sites (Heintzman *et al.* 2007; Krebs *et al*. 2011; Smallwood and Ren 2013). The C-terminal PHD finger of BPTF shows a predilection for H3K4me3 but can also bind H3K4me2 (Ruthenburg *et al*. 2011). It is thus possible that the NURF complex is recruited to enhancers through the recognition of H3K4me2, along with other chromatin remodellers such as CHD7 and BRG1 (Schnetz *et al.* 2010; Rada-Iglesias *et al.* 2011).

2.2. Remodelling of c-MYC target chromatin

BPTF silencing also dampens the transcriptional response of 'non-sensitive' promoters. The impact of BPTF knock-down on these genes is likely due to a defective chromatin remodelling at their promoters, as suggested by the fact that BPTF silencing blocks the increase in DNA accessibility at c-MYC promoters typically linked to c-MYC activation. The putative mechanisms accounting for such observation are discussed henceforth.

c-MYC recruits the chromatin remodeller SWI/SNF (Cheng *et al*. 1999), whose activity is partially inhibited by the linker histone H1 (Hill and Imbalzano 2000, Ramachandran *et al.* 2003). Moreover, NURF is necessary for H1 displacement at

the promoters of progesterone receptor target genes (Vicent *et al.* 2011). We could hypothesize that NURF-mediated eviction of H1 at c-MYC-bound promoters is a pre-requisite for subsequent remodelling and nucleosome eviction by the SWI/SNF complex.

BPTF binds H3K4me3 through its PHD domains but does not appear to affect the levels of this histone modification at c-MYC target promoters. By contrast, BPTF silencing reduces the hyper-acetylation of H3, commonly associated to c-MYC activation (Martinato *et al*. 2008). These data suggest that BPTF, either on its own or through its interaction with c-MYC, is required to recruit and/or modulate the activity of HATs at relevant promoters. In fact, there is evidence of the latter in *Drosophila*, where Nurf301 is needed for the histone acetyl-transferase ATAC to access chromatin and maintain the condensed architecture of the male X chromosome (Carré *et al*. 2008). A putative role on histone deacetylases cannot be ruled out.

2.3. Long-range interactions

The organization of eukaryotic genomes in the 3D nuclear space is determinant of their function. Chromosome conformation capture techniques have shown that genomes are organized into thousands of topologically associating domains (TADs) (Dixon *et al*. 2012). TADs demarcate active and repressed regions of the genome and typically contain tens of genes and hundreds of enhancers. They show a high degree of conservation between cell types and species, suggesting that physical partitioning of the genome is a fundamental principle of genome organization (Smallwood and Ren 2013). Regulatory elements display extensive long-range interactions within a TAD but interact far less frequently with elements located outside (Sanyal *et al.* 2012; Shen *et al.* 2012).

In vertebrates, this organization is partly established by the architectural proteins CTCF (CCCTC-binding factor) and TFIIIC (Ong and Corces 2014). Transcriptional activity might also play a role since the boundaries of topological domains are enriched in highly transcribed sequences including housekeeping genes, tRNAs and SINE elements (Hou *et al*. 2012; Dixon *et al*. 2012) (Fig. 28). Such boundaries allow the coordinated regulation of gene expression within TADs, contain repressive regions and segregate antagonistic elements.

Inside TADs, long and short-range interactions are established between *cis*-regulatory sequences and promoters in order to modulate transcription. The chromatin loops originating from such interactions place promoters and enhancers in close proximity and thus favour transcription. The way chromatin

looping alters transcriptional output is not yet understood, but it might enhance RNA Pol II recycling, mRNA export and recruitment of remodelling and histone modification complexes (Maksimenko and Georgiev 2014). Moreover, enhancer-promoter pairs may move to a more favourable transcriptional compartment within the nucleus (Krivega and Dean 2012). These chromatin loops are orchestrated by sequence-specific transcription factors, CTCF, Cohesin[1], and Mediator, either alone or in various combinations (Fig. 28).

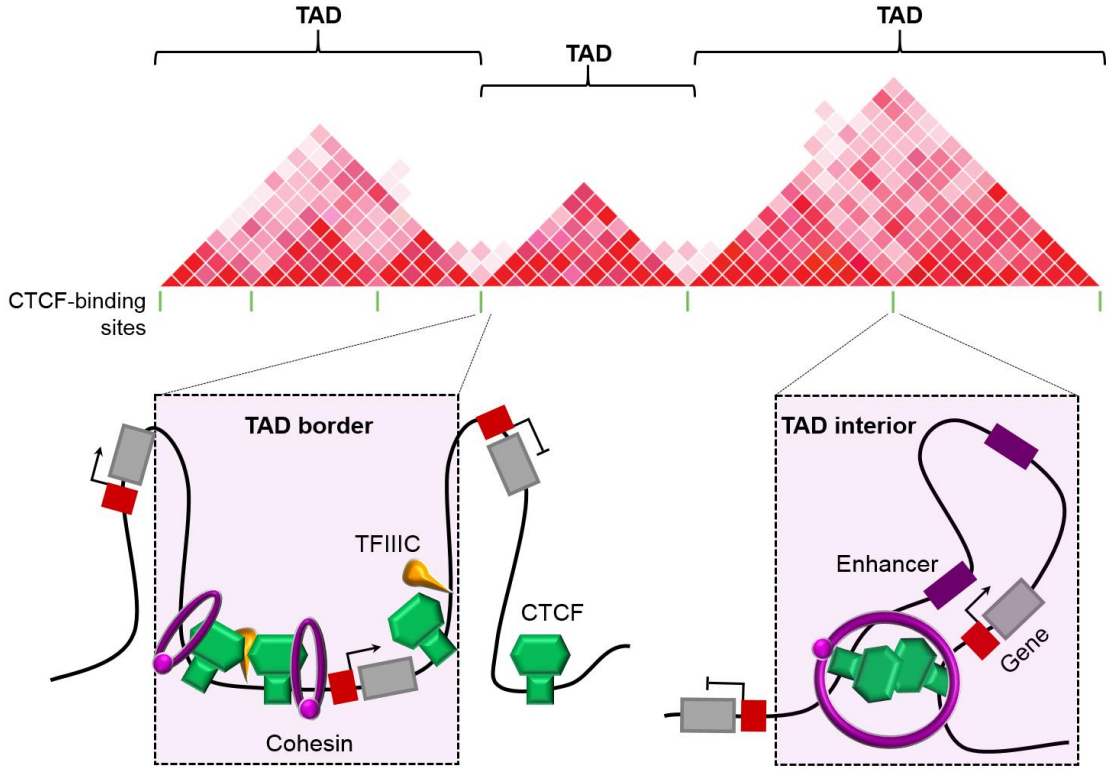

Figure 28. **Spatial organization of the eukaryotic genome**. (Top) Schematic data generated by Hi-C representing an interaction heat map of a chromosome segment. (Bottom) TAD borders are established by the cooperative action of CTCF, TFIIIC and Cohesin. Within TADs, CTCF facilitates enhancer-promoter looping and plays an essential role in controlling gene expression (Erokhin *et al.* 2011). One mechanism is through the interaction with TAF3, a component of the basal TFIID transcriptional machinery. TAF3 localizes at promoters and distal sites containing CTCF, and both sequences form a loop in a TAF3-dependent manner (Liu *et al.* 2011). CTCF recruits Cohesin, which stabilizes the enhancer-promoter DNA loops built by CTCF, transcription factors and mediator (Kagey *et al.* 2010; Schmidt *et al.* 2010; Yan *et al.* 2013; Smallwood and Ren 2013). *Adapted from* Ong and Corces 2014.

[1] COHESIN: Multiprotein complex that forms a ring-like structure which holds together two DNA helices and is critical for sister chromatid cohesion (Nasmyth and Haering 2009). Strong evidence indicates that, besides its role in mitosis and meiosis, cohesin regulates transcriptional activity during interphase (Merkenschlager and Odom 2013).

There is ample evidence suggesting the involvement of BPTF in the organization of long-range chromatin interactions. First, it interacts with *Drosophila* GAGA Factor and USF1, two proteins with insulator properties, and it is critical for the function of the 5'HS4 insulator (Xiao *et al*. 2001; Li *et al*. 2011). Second, it binds to the architectural proteins CTCF and STAG2 and regulates nucleosomal occupancy at genomic sites occupied by both proteins (Qiu *et al*. 2015). Lastly, BPTF has been involved in the establishment/maintenance of the interactions between the enhancers of olfactory receptor genes (Markenscoff-Papadimitriou *et al*. 2014).

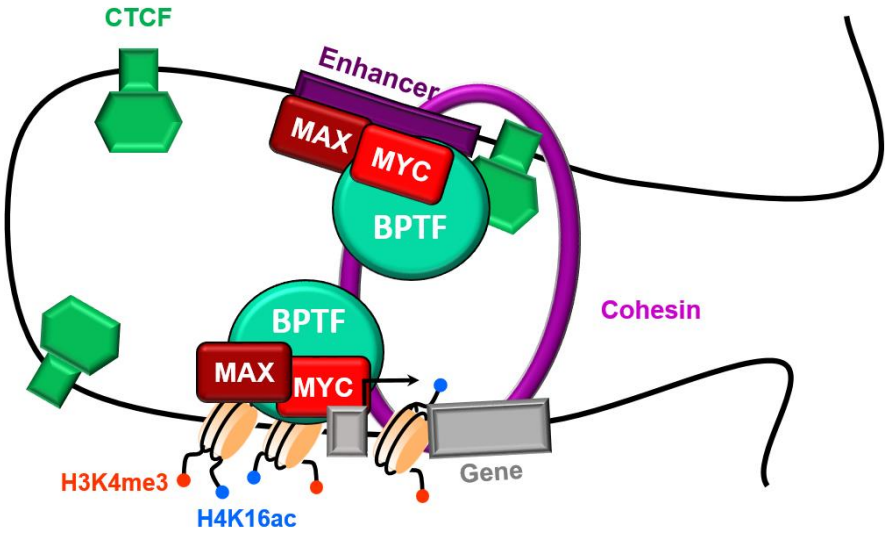

Figure 29. Mechanisms of control of c-MYC transcriptional activity by BPTF. BPTF enhances c-MYC-dependent transcriptional activation through a wide range of mechanisms. First, it participates in the recruitment and/or stabilization of c-MYC onto gene promoters via recognition of the histone marks H3K4me3 and H4K16ac. Second, it contributes to the remodelling of chromatin at c-MYC target promoters; either by altering nucleosome positioning or by recruiting/modulating the activity of HATs. Moreover, BPTF may also be involved in the formation of DNA loops between c-MYC target enhancers and promoters. One possible mechanism could be the recruitment of c-MYC to enhancer sequences through the recognition of H3K4me2. Alternatively, BPTF would stabilize the enhancer-promoter pairs in collaboration with CTCF and STAG2.

Altogether, we can speculate that BPTF participates in the control of gene expression by enhancing the interplay between promoters and other *cis*-regulatory sequences. Multiple mechanisms might account for such function: on one hand, BPTF could facilitate the recruitment of sequence-specific transcription factors to enhancers and regulatory elements in *cis*; alternatively, BPTF could play a more architectural role, assisting the formation of chromatin loops along with CTCF and STAG2. By extension, BPTF could facilitate c-MYC 'invasion' of distal

enhancer elements (Lin *et al*. 2012; Sabò *et al*. 2014) and boost transcription by helping to build the DNA loops between c-MYC target enhancers and promoters (Fig. 29).

2.4. Transcription elongation

Among other mechanisms, c-MYC enhances gene transcription by recruiting P-TEFb and promoting RNA Pol II pause-release (Rahl *et al.* 2010; Cowling and Cole 2006). We could also speculate that BPTF:NURF plays a role in transcription elongation, since the yeast chromatin remodelling complex Iswi has been found in gene bodies, where it coordinates RNA Pol II elongation, termination and pre-mRNA processing (Morillon *et al*. 2003; Zentner *et al*. 2013).

2.5. Repression by c-MYC

The effects of BPTF silencing on the output of c-MYC transcriptional activity involve not only genes whose expression is up-regulated but also those that are down-regulated. The mechanisms involved in "repression" by c-MYC are a highly debated topic (Lovén *et al.* 2012). Chromatin remodelling complexes can repress gene transcription by restricting the access to DNA (Morillon *et al.* 2003) or by removing DNA-binding factors required for transcriptional activation. In this regard, the yeast Isw1 complex displaces TBP from the PHO8 promoter and effectively inhibits basal transcription (Moreau *et al*. 2003). Alternatively, chromatin remodellers associate with chromatin modifiers that help enforce repression. This is the case of *Drosophila* ISWI, which interacts with the HDAC RPD3 to inhibit gene expression (Burgio *et al*. 2008).

Identification of BPTF target sequences will significantly improve our understanding of the mechanisms whereby it modulates c-MYC transcriptional activity. So far, the lack of ChIP-grade antibodies has rendered this task unfeasible. Vicent *et al.* have published the only ChIP-Sequencing experiment against endogenous BPTF to date using a home-made antibody that is no longer available. Interestingly, in their study 40.8% of BPTF peaks were located in introns and only 5% fell into promoter regions, further supporting the hypothesis that BPTF function extends beyond remodelling of nucleosomes at promoters.

3. BPTF IN DEVELOPMENT AND DIFFERENTIATION

Extensive evidence indicates that chromatin remodellers play decisive roles in regulating gene expression during development. They not only regulate the global body plan but they also contribute to tissue specification and maintenance of stem cell compartments in the adult (Clapier and Cairns 2009).

3.1. Early embryonic development

BPTF is essential for the embryonic development of different animal species. Mutation of *Drosophila* Nurf301 results in lethality at the third larval stage and deregulation of homeobox, heat shock, JAK/STAT and ecdysone pathways (Badenhorst *et al*. 2002; Deuring *et al*. 2000). Similarly, Nurf301 knock-down at the 2 cell stage of *Xenopus* is associated with defective axial development, gut formation, blood cell development and expression of homeobox genes (Wysocka *et al.* 2006). In this regard, BPTF-deficient mouse embryos fail to develop the ectoplacental cone and show defective AP patterning of the epiblast (Landry *et al.* 2008; Goller *et al*. 2008). *c-Myc* null mouse embryos also exhibit severe developmental defects and die before midgestation. These abnormalities arise secondary to placental insufficiency, since specific deletion of c-MYC in the epiblast using a Sox2-Cre rescues the majority of developmental anomalies. Epiblast-restricted *c-Myc* knock-out embryos progress normally but die around E12 due to a severe anemia (Dubois *et al*. 2008).

3.2. Cell differentiation

There is little information on NURF function in adult mouse tissues. So far, NURF has been proven to be required for the full maturation of thymocytes after positive selection: BPTF deletion impairs differentiation without interfering with proliferation, apoptosis or co-receptor expression (Landry *et al*. 2011). There are some hints, as well, suggesting that BPTF participates in the homeostasis of epidermis, since its down-regulation in human keratinocytes favours their differentiation (Mulder *et al*. 2012).

As a step towards the understanding the role of BPTF in c-MYC-driven tumorigenesis, we have developed two mouse models to conditionally delete Bptf in the pancreas and in B cells, both tissues showing a dependence on c-MYC for their full development. c-MYC inactivation in pancreatic progenitors is associated with impaired growth, defective acinar cell maturation and accumulation of adipocytes with time (Bonal *et al.* 2009). Similarly, depletion of

c-MYC in early stages of B cell maturation results in impaired activation of lineage-specifying genes and a blockade of differentiation (Habib *et al*. 2007; Vallespinós *et al*. 2011; Calado *et al*. 2012). Importantly, BPTF inactivation had strikingly different results in the two tissues: while having no evident impact on pancreatic development or differentiation, it completely abrogated B cell differentiation.

BPTF and B cell differentiation. B cells constitute an excellent model to study differentiation since the generation of mature B cells proceeds through well-defined stages with critical checkpoints that have been extensively examined. Each stage is characterized by the expression of a unique combination of surface molecules that can be readily assessed by flow cytometry (Fig. 30).

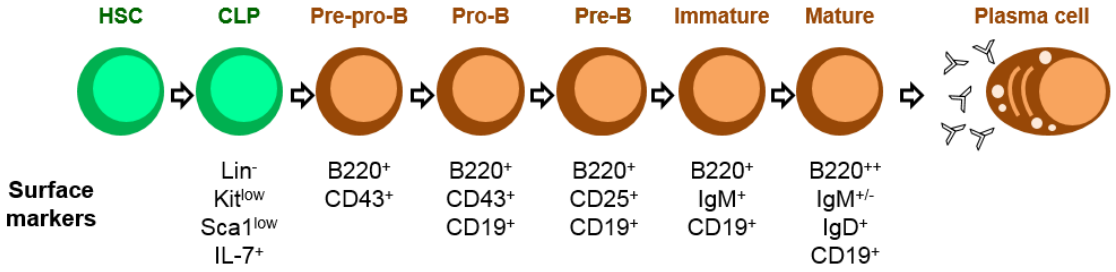

Figure 30. B lymphocyte differentiation. Successive stages of differentiation from the HSC (Hematopoietic Stem Cells) and CLP (Common Lymphoid Progenitors) cells. Key cell-surface markers are shown. *Adapted from* Fernandez et al. 2012.

We have conditionally deleted *Bptf* in the mouse B cell lineage (*Bptf*$^{B\Delta/\Delta}$) using the *Mb1-Cre* allele (Hobeika *et al.* 2006), which becomes active at the earliest steps of B cell development, and shown successful recombination by genomic PCR analysis of bone marrow (BM) B220^{+} cells (Fig. 31a). Spleens of *Bptf*$^{B\Delta/\Delta}$ mice are significantly smaller than their wild-type counterparts, what is suggestive of impaired B cell maturation (Fig. 31b). In agreement with this, flow cytometry analyses of both spleen and BM revealed that, upon loss of BPTF, B cell development is blocked at the pro- to pre-B cell transition. Pre-pro B and Pro-B cells (B220^{low}; IgM^{-}; CD43^{+}) accumulate in the BM of mutant animals, while pre-B cells (B220^{low};IgM^{-};CD43^{-}) are significantly reduced. Immature (B220^{low}; IgM^{+}) and mature B cells (B220^{high}; IgM^{+}) are virtually absent in *Bptf*$^{B\Delta/\Delta}$ mice (Fig. 31c). Annexin V staining has shown similar levels of apoptosis in pre-pro and pro-B cells of WT vs. *Bptf*$^{B\Delta/\Delta}$ mice (25.7 vs. 21.6%); by contrast, the number of apoptotic cells is significantly increased in pre-B cells of *Bptf*$^{B\Delta/\Delta}$ mice (66.2% vs. 29.9%). These data indicate that BPTF is necessary for pre-B cell survival and is therefore required from early stages of B cell differentiation. Whether BPTF is dispensable at later stages of B cell development is an open question. For this purpose, we propose to breed *Bptf*$^{fl/fl}$ conditional mice with *Mx-Cre* transgenic mice, where

Cre recombinase is induced upon injection of IFN or pIpC (Hobeika *et al*. 2006; Vallespinós *et al.* 2011).

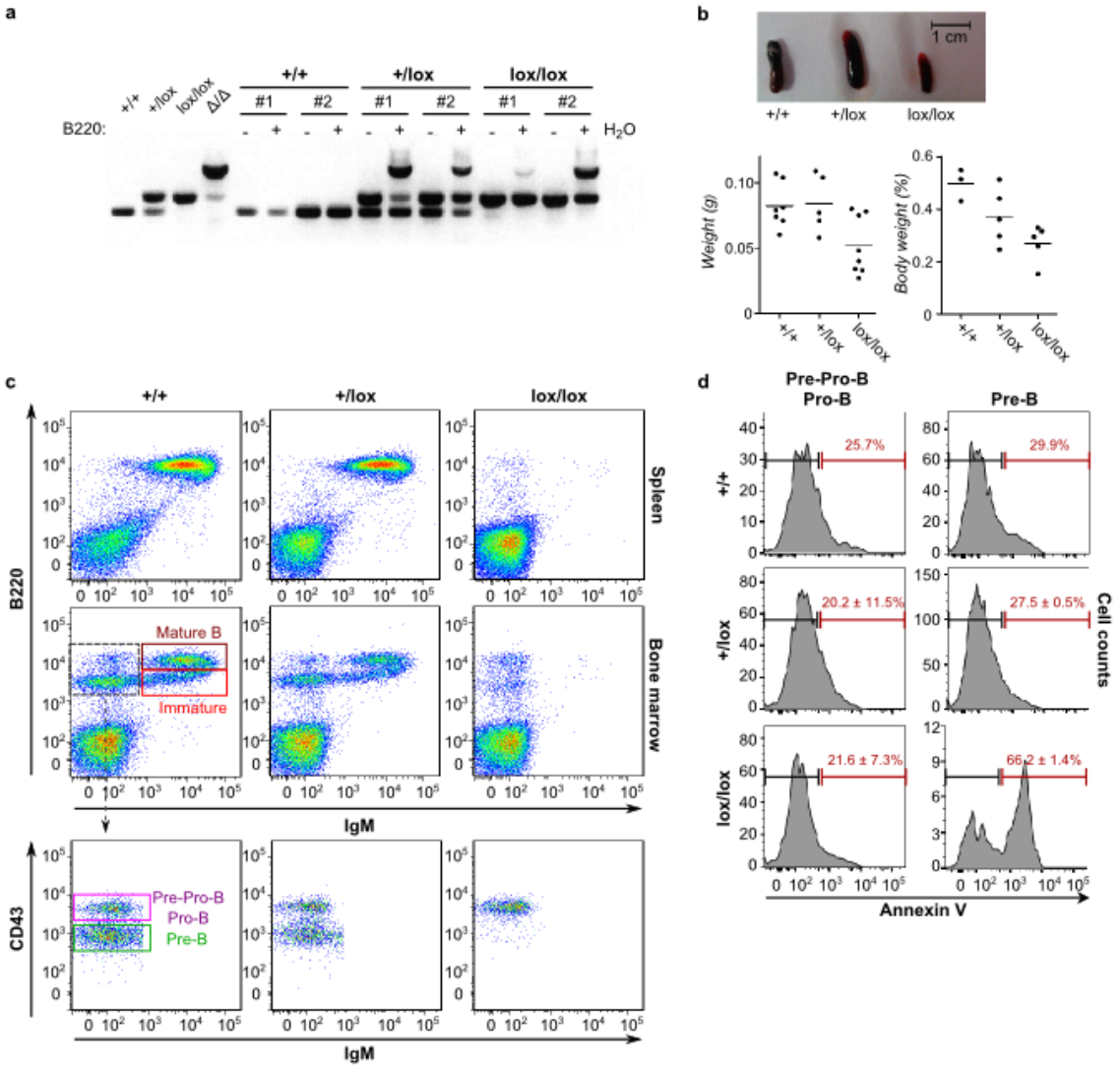

Figure 31. BPTF is required for B cell differentiation from early stages. a) Genomic PCR analysis of wt, floxed and recombined *Bptf* alleles from sorted B220^{+} and B220^{-} BM cells from the indicated mouse genotypes. b) Top: Representative picture of spleens from 8-10 weeks-old *Mb1-Cre*$^{+/KI}$ mice of the indicated genotypes showing a significant reduction in spleen size upon Bptf depletion. Bottom: Spleen weight in grams and in % of body weight of mice in the upper panel. c) FACS analysis of B cell populations in BM and spleen from *Mb1-Cre*$^{+/KI}$ mice of the indicated genotypes. Deletion of BPTF in B cells lineage leads to a reduction in the pre-B, immature B, and mature B cell compartments in both BM and spleen. d) BM single cell suspensions were stained with Annexin V and the same markers as in c. Upon BPTF depletion, we detect increased apoptosis in the compartment of pre-B cells.

Interestingly, the phenotype of *Bptf*$^{B\Delta/\Delta}$ mice is reminiscent of that of *c-Myc*$^{lox/lox}$; *Mb1-Cre*$^{+/KI}$ mice (Vallespinós *et al*. 2011), suggesting that it could partially arise from faulty c-MYC transcriptional activity. EBF-1 is a c-MYC target and a critical transcription factor in early B cell maturation and its overexpression rescues the differentiation defects of *c-Myc*$^{\Delta/\Delta}$ B cells (Vallespinós *et al*. 2011). Therefore, overexpressing c-MYC or EBF-1 in *Bptf*$^{\Delta/\Delta}$ B lymphocytes and subsequently assessing their differentiation status would shed light on the mechanisms involved therein. An alternative explanation to the blockade in B cell differentiation is that BPTF is required for the productive rearrangement of the immunoglobulin genes, a bottleneck in B lymphocytes maturation.

Other chromatin remodellers that cooperate with transcription factors in activating genes necessary for B cell commitment, survival and proliferation are Srg3/mBaf155 (Choi *et al*. 2012), a core subunit of the SWI/SNF-like BAF complex, and Brg1 (Holley *et al*. 2014). The distinct phenotypes observed upon NURF or SWI/SNF inactivation suggest that chromatin remodellers have specific and non-overlapping roles during B cell differentiation.

In summary, the tissue-specific functions of the NURF complex call for a more detailed assessment of its role in different cell types. We are currently breeding the *Bptf*$^{fl/fl}$ conditional mouse with UBC-Cre-ERT2 (Ruzankina *et al.* 2007) and Krt5-Cre mice (Tarutani *et al.* 1997) to begin exploring these questions.

4. BPTF AND TUMORIGENESIS

Cancer research has identified six capabilities acquired by malignant cells that enable tumor growth and metastatic dissemination: continuous proliferative signaling, insensitivity to growth-inhibitory signals, resistance to cell death, replicative immortality, sustained angiogenesis and tissue invasion (Hanahan and Weinberg 2011). Increasing evidence suggests that alterations in epigenetic processes (e.g. chromatin remodelling, histone modifications or DNA methylation) can result in genomic instability, DNA damage and transcriptional changes and hence contribute to the acquisition of such features. Inactivating mutations in genes encoding the catalytic and regulatory subunits of the SWI/SNF complex have been detected in several human cancers: bi-allelic loss of SNF5 occurs in most malignant rhabdoid tumors and some epithelioid sarcomas, while BRG1 gene is lost in cancer cell lines of multiple origins (Versteege *et al*. 1998; Helming *et al*. 2014).

Early work in *Drosophila* showed that deletion of Nurf301 is associated with neoplastic transformation of circulating blood cells, leading to the formation of inflammatory or melanotic tumors (Kwon *et al*. 2008). In *C. elegans*, inhibition of ISWI function suppresses the defects associated with loss of the tumor suppressor lin-35 Rb or the activation of oncogenic let-60 Ras (Andersen *et al*. 2006). More recently, mutations in *BPTF* have been found in several tumor types (Fujimoto *et al*. 2012; Balbás-Martínez *et al*. 2013; González-Pérez *et al*. 2013; Xiao *et al.* 2014a). The impact of such mutations has not been analysed in detail yet due to the size of the protein and little knowledge of its biological roles. Nonetheless, and according to the data integrated in IntOGen, 10% of the mutations reported so far are truncating and cold give rise to BPTF fragments with dominant negative properties (Gundem *et al.* 2010). Moreover, high BPTF levels have been reported to be associated with poor prognosis and invasiveness in hepatocellular carcinoma, melanoma and colorectal carcinoma (Xiao *et al*. 2014b; Xiao *et al*. 2015; Dar *et al.* 2015). These findings suggest that BPTF may play an important role in tumorigenesis and therefore it constitutes an attractive candidate for drug targeting in cancer therapy. There are indeed precedents in the literature for inhibition of chromatin remodellers as successful cancer therapeutic strategies. One example is Brd4, whose inhibition has been proven successful in c-MYC-driven experimental models of hematologic malignancies (Dawson *et al*. 2011; Delmore *et al*. 2011; Mertz *et al*. 2011).

Until now, however, the power of genetic mouse models of cancer has not been exploited to assess the role of BPTF in tumor formation and/or maintenance. As a proof of concept, we set out to explore this notion using two mouse models of highly aggressive c-MYC-driven tumors: the *Ela-Myc* and the *Eμ-Myc*.

We have preliminary data suggesting that inactivation of *Bptf* in the pancreas of adult *Ela-Myc* mice inhibits the formation of pancreatic tumors. Moreover,

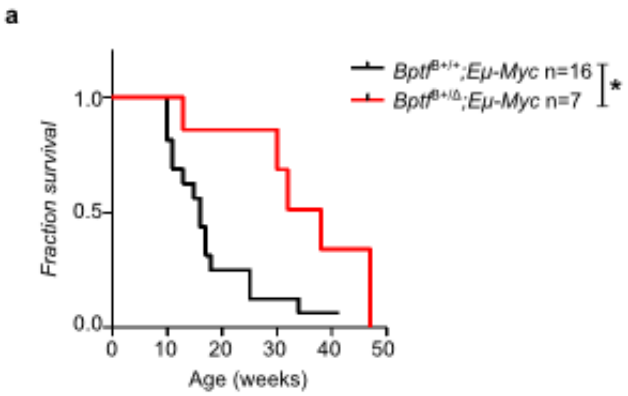

Figure 31. BPTF loss delays tumor onset in a murine model of Burkitt lymphoma. In *Eμ-Myc* mice, c-MYC is overexpressed in the B cell lineage under the control of the IgH enhancer. These mice develop spontaneous pre-B and B cell lymphomas at 15-20 weeks of age. This graph depicts the Kaplan-Meier curves of tumor-free survival for *Eμ-Myc* mice of the indicated *Bptf* genotypes. *P*-value was calculated with the log-rank test.

inactivation of only one *Bptf* allele has no major impact on B cell maturation but is sufficient to block the formation of c-MYC-driven B cell lymphomas (Fig. 31). These promising results highlight the relevance of the c-MYC:BPTF axis as a target for cancer therapy. A more detailed molecular, structural, and functional dissection of BPTF will allow the development of therapeutic strategies exploiting its function in cancer. One strategy could consist of disrupting the interaction between the two proteins. Alternatively, drugs could be designed specifically targeting the BPTF bromodomain.

The biochemical properties of the NURF:BPTF complex have been well characterized, but the importance of its function in mammals has just begun to emerge. Here we have provided some key insights into BPTF function, although many important questions remain to be answered (Box 1). First, we have unveiled the interaction with the oncogene c-MYC. This observation could lead to a new field of research by itself and raises the possibility of developing new anti-cancer strategies. We have also assessed BPTF role in adult tissue homeostasis and shown that, while dispensable for formation of the pancreas, it is crucial for the maturation of B cells. In addition, we have preliminary data suggesting that it plays a critical role in tumorigenesis. In conclusion, we provide strong evidence that BPTF is an important protein involved in chromatin remodelling required for the action of c-MYC that merits additional study. Unravelling the molecular function of BPTF may also provide opportunities to develop novel antitumor drugs.

1. **Is Nurf301/BPTF exclusive to the NURF complex?** It will be essential to determine if BPTF only works as a component of the NURF complex, or rather, it has ATPase-independent functions. We find a precedent for this in Brg1, which has been proven to have gene regulatory functions separate from its ATPase activity (Jani *et al*. 2008).

2. **How is NURF function regulated?** The activity of chromatin remodelling complexes can be modulated by alterations in their subunit composition (Lessard *et al*. 2007) or alternative splicing events. *Drosophila* NURF is an example of the latter. The gene *nurf301* gives rise to three distinct isoforms by alternative splicing, one of them lacking the C-terminal domains involved in the recognition of H3K4me3 and H4K16ac. Interestingly, full-length Nurf301 is not essential for the correct expression of most NURF targets, with the exception of genes related to spermatogenesis (Kwon *et al*. 2009). The existence of an isoform with similar properties in mammalian cells remains unknown.

3. **Which are the direct targets of NURF *in vivo*?** Genome-wide mapping of NURF localization coupled to high-throughput methods assessing changes in chromatin structure upon Bptf/Nurf301 knockout will help to identify these sites.

4. **What are the transcription factors BPTF interacts with in human cells?** The development of high-quality immunoprecipitating antibody would facilitate the identification of BPTF interactome using immunoprecipitation and mass-spectrometry-based analysis.

5. **Does BPTF participate in the DNA damage response?** Bptf is phosphorylated in response to activation of the ATM/ATR pathway (Matsuoka *et al*. 2007), thus suggesting that it could play a role in the DNA damage response. We can find examples in the literature of chromatin remodelling complexes that participate in such pathway. For instance, INO80 is phosphorylated by the Mec1/Tel1 kinases that coordinate the DNA damage response and is recruited to DSBs (Double Strand Breaks) marked by γ-H2AX (Morrison *et al*. 2007).

Box 1. Some pending questions on NURF biology.

Conclusions

CONCLUSIONS

1. BPTF is a component of the NURF complex playing a critical role in the proliferation of normal and cancer cells. Its knock-down in human fibroblasts blocks S phase entry.

2. BPTF levels are modulated during cell cycle progression: in human fibroblasts, it is induced upon entry into G_1 and is down-regulated in S phase.

3. Using a combination of biochemical assays we demonstrate that BPTF and c-MYC are found within the same protein complex and that they interact directly.

4. In human fibroblasts transduced with the MYC-ER fusion protein, BPTF is required for the activation of the full c-MYC transcriptional program through chromatin remodelling of its target promoters.

5. In MEFs transduced with Myc-ER, BPTF is necessary for c-MYC-driven proliferation but not for apoptosis, suggesting that BPTF is only required for those c-MYC functions involving direct binding to chromatin.

6. BPTF is necessary for the reprogramming of murine fibroblasts into induced pluripotent stem cells.

7. BPTF is expressed at high levels in human tumors of diverse origin. Its expression positively correlates with the activation of c-MYC, but not N-MYC or L-MYC, driven gene signatures.

8. BPTF has tissue-specific roles in cell differentiation: while dispensable for the formation of the mouse pancreas, it is crucial for the generation of mature B cells in bone marrow and spleen.

9. Preliminary data indicate that, in mice, BPTF plays a critical function in the formation and/or maintenance of c-MYC-driven tumors.

Conclusiones

CONCLUSIONES

1. BPTF es un componente del complejo NURF con un papel crítico en la proliferación de células normales y cancerosas. Su *knock-down* en fibroblastos humanos resulta en un bloqueo en la entrada en fase S.

2. Los niveles de BPTF son modulados durante la progresión del ciclo celular: en fibroblastos humanos, BPTF es inducido al entrar las células en G_1 y se *down*-regula en fase S.

3. Por medio de una combinación de ensayos bioquímicos hemos demostrado que BPTF y c-MYC se encuentran en el mismo complejo proteico y que interaccionan directamente.

4. En fibroblastos humanos transducidos con la proteína de fusión MYC-ER, BPTF es requerido para la activación completa del programa transcripcional de c-MYC a través de la remodelación de la cromatina en sus promotores diana.

5. En fibroblastos embrionarios de ratón transducidos con MYC-ER, BPTF es necesario para la proliferación inducida por c-MYC, pero no para la apoptosis dirigida por este oncogén, sugiriendo que BPTF solo es necesario para aquellas funciones de c-MYC que implican la unión directa a la cromatina.

6. BPTF es necesario para la reprogramación de fibroblastos de ratón a células madre de pluripotencia inducida.

7. BPTF se expresa a niveles altos en diversos tipos de tumores humanos. Su expresión correlaciona positivamente con la activación de programas de expresión génica instruidos por c-MYC, pero no por N-MYC o L-MYC.

8. BPTF tiene funciones tejido-específicas en diferenciación celular: mientras que es dispensable para la formación del páncreas de ratón, es crucial para la generación de células B maduras en la médula ósea y bazo.

9. Datos preliminares sugieren que, en ratones, BPTF juega un papel crítico en la formación y/o mantenimiento de tumores dirigidos por c-MYC.

References

REFERENCES

1. Acosta, J.C., Ferrándiz, N., Bretones, G., Torrano, V., Blanco, R., et al. (2008). Myc inhibits p27-induced erythroid differentiation of leukemia cells by repressing erythroid master genes without reversing p27-mediated cell cycle arrest. *Mol Cell Biol.*, 28, 7286-95.
2. Adams, J.M., Harris, A.W., Pinkert, C.A., Corcoran, L.M., Alexander, W.S. *et al*. (1985). The c-myc oncogene driven by immunoglobulin enhancers induces lymphoid malignancy in transgenic mice. *Nature*, 318, 533-8.
3. Adhikary, S. and Eilers, M. (2005). Transcriptional regulation and transformation by Myc proteins. *Nat Rev Mol Cell Biol.*, 6, 635-45.
4. Agrawal, P., Yu, K., Salomon, A.R. and Sedivy, J.M. (2010). Proteomic profiling of Myc associated proteins. *Cell Cycle*, 9, 4908-21.
5. Alarcon, R.M., Rupnow, B.A., Graeber, T.G., Knox, S.J., Giaccia, A.J. (1996) Modulation of c-Myc activity and apoptosis in vivo. *Cancer Res.*, 56, 4315-19.
6. Alberts, B., Johnson, A., Lewis, J., Raff, M., Roberts, K. et al. (2002). Molecular Biology of the Cell, 4th edition. New York, NY: Garland Science.
7. Alkhatib, S.G. and Landry, J.W. (2011). The nucleosome remodeling factor. *FEBS lett.*, 585, 3197-207.
8. Alland, L., Muhle, R., Hou, H. Jr., Potes, J., Chin, L. *et al.* (1997). Role for N-CoR and histone deacetylase in Sin3-mediated transcriptional repression. *Nature*, 387, 49-55.
9. Andersen, E.C., Lu, X., Horvitz, H.R. (2006). C. elegans ISWI and NURF301 antagonize an Rb-like pathway in the determination of multiple cell fates. Development, 133, 2695-704.
10. Arabi, A., Wu, S., Ridderstråle, K., Bierhoff, H., Shiue, C. *et al.* (2005). c-Myc associates with ribosomal DNA and activates RNA polymerase I transcription. *Nat. Cell. Biol.*, 7, 303-10.
11. Armstrong, J.A., Papoulas, O., Daubresse, G., Sperling, A.S., Lis, J.T. *et al*. (2002). The *Drosophila* BRM complex facilitates global transcription by RNA polymerase II. *EMBO J.*, 21, 5245-54.
12. Arvanitis, C. and Felsher, D.W. (2006). Conditional transgenic models define how MYC initiates and maintains tumorigenesis. *Semin. Cancer Biol.,* 16, 313-7.
13. Badenhorst, P., Voas, M., Rebay, I., Wu, C. (2002) Biological functions of the ISWI chromatin remodeling complex NURF. *Genes Dev.*, 16, 3186-98.
14. Badenhorst, P., Xiao, H., Cherbas, L., Kwon, S.Y., Voas, M. *et al.* (2005). The *Drosophila* nucleosome remodeling factor NURF is required for Ecdysteroid signaling and metamorphosis. *Genes Dev.*, 19, 2540-45.

15. Bailey, T.L., Boden, M., Buske, F.A., Frith, M., Grant, C.E. *et al.* (2009). MEME SUITE: tools for motif discovery and searching. *Nucleic Acids Res.*, 37 (Web Server issue), W202-W208.
16. Balbás-Martínez, C., Sagrera, A., Carrillo-de-Santa-Pau, E., Earl, J., Márquez, M. *et al.* (2013). Recurrent inactivation of STAG2 in bladder cancer is not associated with aneuploidy. *Nat Genet.*, 45, 1464-9.
17. Bannister, A.J., and Kouzarides, T. (2011). Regulation of chromatin by histone modifications. *Cell Res.*, 21, 381-95.
18. Barak, O., Lazzaro, M.A., Lane, W.S., Speicher, D.W., Picketts, D.J. *et al*. (2003) Isolation of human NURF: a regulator of Engrailed gene expression. *EMBO J.*, 22, 6089-100.
19. Barbie, D.A., Tamayo, P., Boehm, J.S., Kim, S.Y., Moody, S.E. *et al.* (2009). Systematic RNA interference reveals that oncogenic KRAS-driven cancers require TBK1. *Nature*, 462, 108-12.
20. Bedford, D.C., Kasper, L.H., Fukuyama, T. and Brindle, P.K. (2010). Target gene context influences the transcriptional requirement for the KAT3 family of CBP and p300 histone acetyltransferases. *Epigenetics*, 5, 9-15.
21. Blackwell, T.K., Huang, J., Ma, A., Kretzner, L., Alt, F.W. *et al*. (1993). Binding of Myc proteins to canonical and noncanonical DNA sequences. *Mol Cell Biol.*, 13, 5216-24.
22. Blackwood, E.M. and Eisenman, R.N. (1991). Max: a helix-loop-helix zipper protein that forms a sequence-specific DNA-binding complex with Myc. *Science*, 251, 1211-7.
23. Bonal, C., Thorel, F., Ait-Lounis, A., Reith, W., Trumpp, A. *et al.* (2009). Pancreatic inactivation of c-Myc decreases acinar mass and transdifferentiates acinar cells into adipocytes in mice. *Gastroenterology*, 136, 309-19.
24. Bouchard, C., Lee, S., Laulus-Hock, V., Loddenkemper, C., Eilers, M. *et al*. (2007). FoxO transcription factors suppress Myc-driven lymphomagenesis via direct activation of Arf. *Gene Dev.*, 21, 2775-87.
25. Bown, N., Cotterill, S., Lastowska, M., O'Neill, S., Pearson, A.D., *et al.* (1999) Gain of chromosome arm 17q and adverse outcome in patients with neuroblastoma. *N Engl J Med.*, 340, 1954-61.
26. Brenner, C., Deplus, R., Didelot, C., Loriot, A., Viré, E. *et al.* (2005) Myc represses transcription through recruitment of DNA methyltransferase corepressor. *EMBO J.*, 24, 336-46.
27. Buganim, Y., Goldstein, I., Lipson, D., Milyavsky, M., Polak-Charcon, S. *et al.* (2010). A novel translocation breakpoint within the BPTF gene is associated with a pre-malignant phenotype. *PloS One*, 5, e9657.

28. Burgio, G., La Rocca, G., Sala, A., Arancio, W., Di Gesu, D., *et al.* (2008). Genetic identification of a network of factors that functionally interact with the nucleosome remodeling ATPase ISWI. *PLoS Genet.*, 4, e1000089.
29. Calado, D.P., Sasaki, Y., Godinho, S.A., Pellerin, A., Köchert, K., *et al*. (2012). The cell-cycle regulator c-Myc is essential for the formation and maintenance of germinal centers. *Nat Immunol.*, 13, 1092-100.
30. Carré, C., Ciurciu, A., Komonyi, O., Jacquier, C., Fagegaltier, D. *et al*. (2008). The Drosophila NURF remodelling and the ATAC histone acetylase complexes functionally interact and are required for global chromosome organization. *EMBO Rep.*, 9, 187-92.
31. Cartwright, P., McLean, C., Sheppard, A., Rivett, D., Jones, K. *et al.* (2005). LIF/STAT3 controls ES cell self-renewal and pluripotency by a Myc-dependent mechanism. *Development*, 132, 885-96.
32. Chai, B., Huang, J., Cairns, B.R., Laurent, B.C. (2005). Distinct roles for the RSC and Swi/Snf ATP-dependent chromatin remodelers in DNA double-strand break repair. *Genes Dev.*, 19, 1656-61.
33. Chandriani, S., Frengen, E., Cowling, V.H., Pendergrass, S.A., Perou, C.M. *et al*. (2009). A core MYC gene expression signature is prominent in basal-like breast cancer but only partially overlaps the core serum response. *PLoS One*, 4, e6693.
34. Cheng, S.W., Davies, K.P., Yung, E., Beltran, R.J., Yu, J. *et al.* (1999). c-MYC interacts with INI1/hSNF5 and requires the SWI/SNF complex for transactivation function. *Nat Genet.*, 22, 102-5.
35. Cheng, A.S., Jin, V.X., Fan, M., Smith, L.T., Liyanarachchi, S., *et al.* (2006). Combinatorial analysis of transcription factor partners reveals recruitment of c-MYC to estrogen receptor-alpha responsive promoters. *Mol Cell*, 21, 393-404.
36. Cherry, C.M. and Matunis, E.L. (2010). Epigenetic regulation of stem cell maintenance in the Drosophila testis via the nucleosome-remodeling factor NURF. *Cell Stem cell*, 6, 557-67.
37. Choi, J., Ko, M., Jeon, S., Jeon, Y., Park, K. *et al*. (2012). The SWI/SNF-like BAF complex is essential for early B cell development. *J Immunol.*, 188, 3791-803.
38. Choudhary, C., Kumar, C., Gnad, F., Nielsen, M.L., Rehman, M. *et al*. (2009). Lysine acetylation targets protein complexes and co-regulates major cellular functions. *Science*, 325, 834-40.
39. Clapier, C.R. and Cairns, B.R. (2009). The biology of chromatin remodeling complexes. *Annu Rev Biochem.*, 78, 273-304.
40. Cohen, S.M., Chastain, P.D., Rosson, G.B., Groh, B.S., Weissman, B.E. *et al*. (2010). BRG1 co-localizes with DNA replication factors and is required for efficient replication fork progression. *Nucleic Acids Res.*, 38, 6906-19.

41. Collins, N., Poot, R.A., Kukimoto, I., Garcia-Jimenez, C., Dellaire, G., *et al.* (2002). An ACF1-ISWI chromatin-remodeling complex is required for DNA replication through hetero- chromatin. *Nat Genet.*, 32, 627-32.
42. Cowling, V.H., Chandriani S., Whitfield M.L., Cole M.D. (2006). A conserved Myc protein domain, MBIV, regulates DNA binding, apoptosis, transformation and G2 arrest. *Mol Cell Biol.*, 26, 4226-39.
43. Cowling, V.H. and Cole, M.D. (2006). Mechanism of transcriptional activation by the Myc oncoproteins. *Semin Cancer Biol.*, 16, 242-52.
44. Cowling, V.H. and Cole, M.D. (2007). The Myc transactivation domain promotes global phosphorylation of the RNA polymerase II carboxy-terminal domain independently of direct DNA binding. *Mol Cell Biol.*, 27, 2059-73.
45. Cowling, V.H. and Cole, M.D. (2010). Myc Regulation of mRNA Cap Methylation. *Genes Cancer*, 1, 576-9.
46. Dang, C.V. (2012). MYC on the path to cancer. *Cell*, 149, 22-35.
47. Dang, C.V. (2014). Gene regulation: fine-tuned amplification in cells. *Nature*, 511, 417-8.
48. Danielian, P.S., White, R., Hoare, S.A., Fawell, S.E., Parker, M.G. (1993). Identification of residues in the estrogen receptor that confer differential sensitivity to estrogen and hydroxytamoxifen. *Mol Endocrinol.*, 7, 232-40.
49. Dar, A.A., Nosrati, M., Bezrookove, V., de Semir, D., Majid, S. *et al*. (2015). The Role of BPTF in Melanoma Progression and in Response to BRAF-Targeted Therapy. *J Natl Cancer Inst.*, 107, pii: djv034.
50. Dawson, M., Bannister, A.J., Göttgens, B., Foster, S.D., Bartke, T. *et al*. (2009). JAK2 phosphorylates histone H3Y41 and excludes HP1alpha from chromatin. *Nature*, 461, 819-22.
51. Dawson, M., Prinjha, R., Dittmann, A., Giotopoulos, G., Bantscheff, M. *et al*. (2011). Inhibition of BET recruitment to chromatin as an effective treatment for MLL-fusion leukaemia. *Nature*, 478, 529-33.
52. Dawson, M., and Kouzarides, T. (2012). Cancer epigenetics: from mechanism to therapy. *Cell*, 150, 12-27.
53. de la Serna, I.L., Ohkawa, Y., Berkes, C.A., Bergstrom, D.A., Dacwag, C.S., *et al*. (2005). MyoD targets chromatin remodeling complexes to the myogenin locus prior to forming a stable DNA-bound complex. *Mol Cell Biol.*, 25, 3997-4009.
54. Delmore, J.E., Issa, G.C., Lemieux, M.E., Rahl, P.B., Shi, J. *et al*. (2011). BET bromodomain inhibition as a therapeutic strategy to target c-Myc. *Cell*, 146, 904-17.
55. Dephoure, N., Zhou, C., Villen, J., Beausoleil, S.A., Bakalarski, C.E. *et al*. (2008). A quantitative atlas of mitotic phosphorylation. *Proc Natl Acad Sci USA.*, 105, 10762-7.

56. Deuring, R., Fanti, L., Armstrong, J.A., Sarte, M., Papoulas, O. *et al.* (2000) The ISWI chromatin-remodeling protein is required for gene expression and the maintenance of higher order chromatin structure in vivo. *Mol Cell*, 5, 355-65.
57. Dey, A., Nishiyama, A., Karpova, T., McNally, J. and Ozato, K. (2009) Brd4 marks select genes on mitotic chromatin and directs postmitotic transcription. *Mol Cell Biol.*, 20, 4899-909.
58. Di Stefano, B., Sardina, J.L., van Oevelen, C., Collombet, S., Kallin, E.M. *et al.* (2014). C/EBPα poises B cells for rapid reprogramming into induced pluripotent stem cells. *Nature*, 506, 235-9.
59. Dixon, J.R., Selvaraj, S., Yue, F., Kim, A., Li, Y. *et al.* (2012). Topological domains in mammalian genomes identified by analysis of chromatin interactions. *Nature*, 485, 376-80.
60. Doerks, T., Copley, R., and Bork, P. (2001). DDT -- a novel domain in different transcription and chromosome remodeling factors. *Trends Biochem Sci.*, 26, 145-6.
61. Dominguez-Sola, D., Ying, C.Y., Grandori, C., Ruggiero, L., Chen, B. *et al.* (2007). Non- transcriptional control of DNA replication by c-Myc. *Nature*, 448, 445-51.
62. Dubois, N.C., Adolphe, C., Ehninger, A., Wang, R.A., Robertson, E.J. *et al*. (2008). Placental rescue reveals a sole requirement for c-Myc in embryonic erythroblast survival and hematopoietic stem cell function. *Development*, 135, 2455-65.
63. Durinck, S., Ho, C., Wang, N.J., Liao, W., Jakkula, L.R. *et al*. (2011). Temporal dissection of tumorigenesis in primary cancers. *Cancer Discov.*, 1, 137-43.
64. Eberhardy, S. and Farnham, P. (2001). c-Myc mediates activation of the cad promoter via a post-RNA polymerase II recruitment mechanism. *J. Biol. Chem.*, 276, 48562-71.
65. Egle, A., Harris, A.W., Bouillet, P., Cory S. (2004). Bim is a suppressor of Myc-induced mouse B cell leukemia. *Proc Natl Acad Sci USA*, 101, 6164-9.
66. Eilers, M. and Eisenman, R.N. (2008). Myc's broad reach. *Genes Dev.*, 22, 2755-66.
67. Eischen, C.M., Woo, D., Roussel, M.F., Cleveland, J.L. (2001). Apoptosis triggered by Myc-induced suppression of Bcl-XL or Bcl-2 is bypassed during lymphomagenesis. *Mol Cell Biol.*, 21, 5063-70.
68. Erdel, F. and Rippe, K. (2011). Chromatin remodelling in mammalian cells by ISWI-type complexes--where, when and why? *FEBS J.*, 278, 3608-18.
69. Erokhin, M., Davydova, A., Kyrchanova, O., Parshikov, A., Georgiev, P. (2011). Insulators form gene loops by interacting with promoters in Drosophila. *Development*, 138, 4097-106.
70. Espada, J. and Esteller, M. (2010). DNA methylation and the functional organization of the nuclear compartment. *Semin Cell Dev Biol.*, 21, 238-46.

71. Evan, G.I., Wyllie, A.H., Gilbert, C.S., Littlewood, T.D., Land, H. *et al.* (1992). Induction of apoptosis in fibroblasts by c-Myc protein. *Cell*, 69, 119-28.
72. Faiola, F., Liu, X., Lo, S., Pan, S., Zhang, K. *et al*. (2005). Dual regulation of c-Myc by p300 via acetylation-dependent control of Myc protein turnover and coactivation of Myc-induced transcription. *Mol Cell Biol.*, 25, 10220-34.
73. Falbo, K. B. and Shen, X. (2006). Chromatin remodelling in DNA replication. *J Cell Biochem.*, 97, 684-–9.
74. Fernandez, P.C., Frank, S.R., Wang, L., Schroeder, M., Liu, S., *et al*. (2003). Genomic targets of the human c-Myc protein. *Genes Dev.*, 17, 1115-29.
75. Fernandez, D., Sanchez-Arevalo, V.J. and de Alboran, I.M. (2012). The role of the proto-oncogene c-myc in B lymphocyte differentiation. *Crit Rev Immunol.*, 32, 321-34.
76. Ferreira, R., Eberharter, A., Bonaldi, T., Chioda, M., Imhof, A. *et al*. (2007). Site-specific acetylation of ISWI by GCN5. *BMC Mol Biol.*, 8, 73.
77. Fladvad, M., Zhou, K., Moshref, A., Pursglove, S., Säfsten, P. *et al.* (2005). N and C-terminal sub-regions in the c-Myc transactivation region and their joint role in creating versatility in folding and binding. *J Mol Biol.*, 346, 175-89.
78. Frank, S.R., Parisi, T., Taubert, S., Fernandez, P., Fuchs, M. *et al*. (2003). MYC recruits the TIP60 histone acetyltransferase complex to chromatin. *EMBO rep.*, 4, 575-80.
79. Fry, C.J. and Peterson, C.L. (2001). Chromatin remodeling enzymes: who's on first? *Curr. Biol.*, 11, R185-97.
80. Fujimoto, A., Totoki, Y., Abe, T., Boroevich, K.A., Hosoda, F. *et al.* (2012). Whole-genome sequencing of liver cancers identifies etiological influences on mutation patterns and recurrent mutations in chromatin regulators. *Nat Genet.*, 44, 760-4.
81. Gabay, M., Li, Y. and Felsher, D.W. (2014). MYC activation is a hallmark of cancer initiation and maintenance. *Cold Spring Harb. Perspect. Med.*, 4, pii: a014241.
82. Garson, J.A., Pemberton, L.F., Sheppard, P.W., Varndell, I.M., Coakham, H.B. *et al.* (1989). N-myc gene expression and oncoprotein characterization in medulloblastoma. *Br J Cancer*, 59, 889-94.
83. Gartel, A.L., Ye, X., Goufman, E., Shianov, P., Hay, N. *et al*. (2001) Myc represses the p21 (WAF1/CIP1) promoter and interacts with Sp1/Sp3. *Proc Natl Acad Sci USA.*, 98, 4510-5.
84. Gebhardt, A., Frye, M., Herold, S., Benitah, S.A., Braun, K. (2006). Myc regulates keratinocyte adhesion and differentiation via complex formation with Miz1. *J Cell Biol.*, 172, 139-49.
85. Goldman, J.A., Garlick, J.D. and Kingston, R.E. (2010). Chromatin remodeling by imitation switch (ISWI) class ATP-dependent remodelers is stimulated by histone variant H2A.Z. *J. Biol. Chem*., 285, 4645-51.

86. Goldmark, J.P., Fazzio, T.G., Estep, P.W., Church, G.M., Tsukiyama, T. (2000). The Isw2 chromatin remodeling complex represses early meiotic genes upon recruitment by Ume6p. *Cell*, 103, 423-33.
87. Goller, T., Vauti, F., Ramasamy, S., Arnold, H.H. (2008) Transcriptional regulator BPTF/FAC1 is essential for trophoblast differentiation during early mouse development. *Mol Cell Biol*., 28, 6819-27.
88. Gomez-Roman, N., Grandori, C., Eisenman, R.N., White, R.J. (2003). Direct activation of RNA polymerase III transcription by c-Myc. *Nature*, 421, 290-4.
89. González-Pérez, A., Jene-Sanz, A. and López-Bigas, N. (2013). The mutational landscape of chromatin regulatory factors across 4,623 tumor samples. *Genome Biol.*, 14, r106.
90. Goren, A., Tabib, A., Hecht, M., Cedar, H. (2008). DNA replication timing of the human beta-globin domain is controlled by histone modification at the origin. *Genes Dev.*, 22, 1319-24.
91. Gregory, M.A., Qi, Y. and Hann, S.R. (2003) Phosphorylation by glycogen synthase kinase-3 controls c-myc proteolysis and subnuclear localization. *J. Biol. Chem.*, 278, 51606-12.
92. Guccione, E., Martinato, F., Finocchiaro, G., Luzi, L., Tizzoni, L. *et al*. (2006). Myc-binding-site recognition in the human genome is determined by chromatin context. *Nat Cell Biol.*, 8, 764-70.
93. Gundem, G., Perez-Llamas, C., Jene-Sanz, A., Kedzierska, A., Islam, A. *et al*. (2010). IntOGen: Integration and data-mining of multidimensional oncogenomic data. *Nat Methods*, 7, 92-3.
94. Habib, T., Park, H., Tsang, M., De Alborán, I. M., Nicks, A. *et al.* (2007). Myc stimulates B lymphocyte differentiation and amplifies calcium signalling. *J Cell Biol.*, 179, 717-31.
95. Hamiche, A., Sandaltzopoulos, R., Gdula, D.A. and Wu, C. (1999). ATP-dependent histone octamer sliding mediated by the chromatin remodeling complex NURF. *Cell*, 97, 833-42.
96. Hanahan, D and Weinberg, R.A. (2011). Hallmarks of cancer: the next generation. *Cell*, 144, 646-74.
97. Hann, S.R. and Eisenman, R.N. (1984). Proteins encoded by the human c-myc oncogene: differential expression in neoplastic cells. *Mol Cell Biol.*, 4, 2486-97.
98. Hanna, J., Markoulaki, S., Schorderet, P., Carey, B.W., Beard, C. *et al*. (2008). Direct reprogramming of terminally differentiated mature B lymphocytes to pluripotency. *Cell*, 133, 250-64.
99. Hansson, J., Rafiee, M.R., Reiland, S., Polo, J.M., Gehring, J. *et al.* (2012). Highly Coordinated Proteome Dynamics during Reprogramming of Somatic Cells to Pluripotency. *Cell Rep.*, 2, 1579-92.

100. Harris, A.W., Pinkert, C.A., Crawford, M., Langdon, W.Y., Brinster, R.L. *et al.* (1988). The E mu-myc transgenic mouse. A model for high-incidence spontaneous lymphoma and leukemia of early B cells. *J Exp Med.*, 167, 353-71.
101. Hayes, J.J. and Hansen, J.C. (2001). Nucleosomes and the chromatin fiber. *Curr Opin Genet Dev.*, 11, 124-9.
102. Hebbar, P.B. and Archer, T.K. (2003) Chromatin remodeling by nuclear receptors. *Chromosoma*, 111, 495-504.
103. Heintzman, N.D., Stuart, R.K., Hon, G., Fu, Y., Ching, C.W. *et al*. (2007). Distinct and predictive chromatin signatures of transcriptional promoters and enhancers in the human genome. *Nat Genet.*, 39, 311-8.
104. Helming, K., Wang, X., Roberts, C. (2014). Vulnerabilities of mutant SWI/SNF complexes in cancer. *Cancer Cell*, 4, 309-17.
105. Herkert, B. and Eilers, M. (2010). Transcriptional repression: the dark side of myc. *Genes Cancer*, 1, 580-6.
106. Hill, D.A. and Imbalzano, A.N. (2000). Human SWI/SNF nucleosome remodeling activity is partially inhibited by linker histone H1. *Biochemistry*, 39, 11649-56.
107. Hobeika, E.S., Thiemann, B., Storch, H. Jumaa, P.J., Nielsen, R. *et al.* (2006). Testing gene function early in the B cell lineage in mb1-cre mice. *Proc Natl Acad Sci USA.*, 103, 13789-94.
108. Hoffman, B. and Liebermann, D.A. (2008). Apoptotic signaling by c-MYC. *Oncogene*, 27, 6462-72.
109. Holley, D.W., Groh, B.S., Wozniak, G., Donohoe, D.R., Sun, W. *et al*. (2014). The BRG1 chromatin remodeler regulates widespread changes in gene expression and cell proliferation during B cell activation. *J Cell Physiol.*, 229, 44-52.
110. Holmes, J.K. and Solomon, M.J. (1996). A predictive scale for evaluating cyclin-dependent kinase substrates. A comparison of p34cdc2 and p33cdk2. *J Biol Chem.*, 271, 25240-6.
111. Hopewell, R. and Ziff, E.B. (1995). The nerve growth factor-responsive PC12 cell line does not express the Myc dimerization partner Max. *Mol Cell Biol.*, 15, 3470-8.
112. Hou, C., Li, L., Qin, Z.S., Corces, V.G. (2012). Gene density, transcription, and insulators contribute to the partition of the Drosophila genome into physical domains. *Mol Cell*, 48, 471-84.
113. Inui, M., Miyado, M., Igarashi, M., Tamano, M., Kubo, A. *et al.* (2014). Rapid generation of mouse models with defined point mutations by the CRISPR/Cas9 system. *Sci Rep.*, 4, 5396.
114. Iritani, B.M., Forbush, K.A., Farrar, M.A., Perlmutter, R.M. (1997). Control of B cell development by Ras-mediated activation of Raf. *EMBO J.*, 16, 7019-31.
115. Jacobsen, K.A., Prasad, V.S., Sidman, C.L., Osmond, D.G. (1994). Apoptosis and macrophage-mediated deletion of precursor B cells in the bone marrow of E mu-myc transgenic mice. *Blood*, 84, 2784-94.

116. Jani, A., Wan, M., Zhang, J., Cui, K., Wu, J. *et al*. (2008). A novel genetic strategy reveals unexpected roles of the Swi-Snf-like chromatin-remodeling BAF complex in thymocyte development. *J Exp Med.*, 205, 2813-25.
117. Ji, H., Wu, G., Zhan, X., Nolan, A., Koh, C. *et al*. (2011). Cell-type independent MYC target genes reveal a primordial signature involved in biomass accumulation. *PLoS One*, 6, e26057.
118. Jin, C. and Felsenfeld, G. (2007) Nucleosome stability mediated by histone variants H3.3 and H2A.Z. *Genes Dev.*, 21, 1519-29.
119. Jones, M.H., Hamana, N. and Shimane, M. (2000). Identification and characterization of BPTF, a novel bromodomain transcription factor. *Genomics*, 63, 35-9.
120. Jordan-Sciutto, K.L., Dragich, J.M., Rhodes, J.L., Bowser, R. (1999a). Fetal Alz-50 clone 1, a novel zinc finger protein, binds a specific DNA sequence and acts as a transcriptional regulator. *J. Biol. Chem.*, 274, 35262-8.
121. Jordan-Sciutto, K.L., Dragich, J.M., Bowser, R. (1999b). DNA binding activity of the fetal Alz-50 clone 1 (FAC1) protein is enhanced by phosphorylation. *Biochem Biophys Res Commun*., 260, 785-9.
122. Kagey, M.H., Newman, J.J., Bilodeau, S., Zhan, Y., Orlando, D.A. *et al*. (2010). Mediator and cohesin connect gene expression and chromatin architecture. *Nature*, 467, 430-5.
123. Kamakaka, R.T. and Biggins, S. (2005). Histone variants: deviants? *Genes Dev.*, 19, 295-310.
124. Kanazawa, S., Soucek, L., Evan, G., Okamoto, T. and Peterlin, B.M. (2003). c-Myc recruits P-TEFb for transcription, cellular proliferation and apoptosis. *Oncogene*, 22, 5707-11.
125. Karlsson, A., Deb-Basu, D., Cherry, A., Turner, S., Ford, J. (2003). Defective double-strand DNA break repair and chromosomal translocations by MYC overexpression. *Proc Natl Acad Sci USA.*, 100, 9974-9.
126. Kawaguchi, Y., Cooper, B., Gannon, M., Ray, M., MacDonald, R.J. *et al.* (2002). The role of the transcriptional regulator Ptf1a in converting intestinal to pancreatic progenitors. *Nat Genet.*, 32, 128-34.
127. Kim, S.Y., Herbst, A., Tworkowski, K.A., Salghetti, S.E. and Tansey, W.P. (2003). Skp2 regulates Myc protein stability and activity. *Mol. Cell.*, 11, 1177-88.
128. Kim, Y.H., Girard, L., Giacomini, C.P., Wang, P., Hernandez-Boussard, T. *et al.* (2006). Combined microarray analysis of small cell lung cancer reveals altered apoptotic balance and distinct expression signatures of MYC family gene amplification. *Oncogene*, 25, 130-8.
129. Kim, J., Woo, A.J., Chu, J., Snow, J.W., Fujiwara, Y. *et al.* (2010). A Myc network accounts for similarities between embryonic stem and cancer cell transcription programs. *Cell*, 143, 313-24.

130. Kingston, R.E. and Narlikar, G.J. (1999). ATP-dependent remodeling and acetylation as regulators of chromatin fluidity. *Genes Dev.*, 13, 2339-52.
131. Kopinke, D., Brailsford, M., Pan, F.C., Magnuson, M.A., Wright, C.V. *et al.* (2011). Ongoing Notch signaling maintains phenotypic fidelity in the adult exocrine pancreas. *Dev Biol.*, 362, 57-64.
132. Kouzarides, T. (2007). Chromatin modifications and their function. *Cell*, 128, 693-705.
133. Krebs, A.R., Karmodiya, K., Lindahl-Allen, M., Struhl, K., Tora, L. (2011). SAGA and ATAC histone acetyl transferase complexes regulate distinct sets of genes and ATAC defines a class of p300-independent enhancers. *Mol Cell*, 44, 410-23.
134. Krivega, I. and Dean, A. (2012). Enhancer and promoter interactions-long distance calls. *Curr Opin Genet Dev.*, 22, 79-85.
135. Kurland, J.F. and Tansey, W.P. (2008) Myc-mediated transcriptional repression by recruitment of histone deacetylase. *Cancer Res.*, 68, 3624-9.
136. Kwon, S.Y., Xiao, H., Glover, B.P., Tjian, R., Wu, C. *et al*. (2008). The nucleosome remodeling factor (NURF) regulates genes involved in Drosophila innate immunity. *Dev Biol.*, 316, 538-47.
137. Kwon, S.Y., Xiao, H., Wu, C., Badenhorst, P. (2009). Alternative splicing of NURF301 generates distinct NURF chromatin remodeling complexes with altered modified histone binding specificities. PLoS Genet., 5, e1000574.
138. Landry, J., Sharov, A.A., Piao, Y., Sharova, L.V., Xiao, H. *et al*. (2008). Essential role of chromatin remodeling protein Bptf in early mouse embryos and embryonic stem cells. *PLoS Genet.*, 4, e1000241.
139. Landry, J., Banerjee, S., Taylor, B., Aplan, P.D., Singer, A. *et al*. (2011). Chromatin remodeling complex NURF regulates thymocyte maturation. *Genes Dev.*, 25, 275-86.
140. Langdon, W.Y., Harris, A.W., Cory, S. and Adams, J.M. (1986). The c-myc oncogene perturbs B lymphocyte development in Eμ-myc transgenic mice. *Cell*, 47, 11-8.
141. Laurenti, E., Wilson, A., Trumpp, A. (2009). Myc's other life: stem cells and beyond. *Curr. Opin. Cell. Biol.*, 21, 844-54.
142. Laybourn, P.J., Kadonaga, J.T. (1991). Role of nucleosomal cores and histone H1 in regulation of transcription by RNA polymerase II. *Science*, 254, 238-45.
143. Lessard, J., Wu, J.I., Ranish, J.A., Wan, M., Winslow, M.M., *et al.* (2007). An essential switch in subunit composition of a chromatin remodelling complex during neural development. *Neuron*, 55, 201-15.
144. Li, F., Wang, Y., Zeller, K.I., Potter, J.J., Wonsey, D.R. *et al*. (2005). Myc stimulates nuclearly encoded mitochondrial genes and mitochondrial biogenesis. *Mol Cell Biol.*, 25, 6225-34.

145. Li, H., Ilin, S., Wang, W., Duncan, E.M., Wysocka, J. *et al.* (2006) Molecular basis for site-specific read-out of histone H3K4me3 by the BPTF PHD finger of NURF. *Nature*, 442, 91-5.
146. Li, B., Carey, M., Workman, J.L. (2007). The role of chromatin during transcription. *Cell*, 128, 707-19.
147. Li, H., Collado, M., Villasante, A., Strati, K., Sagrario, O. *et al*. (2009). The Ink4/Arf locus is a barrier for iPS cell reprogramming. *Nature*, 460, 1136-9.
148. Li, M., Belozerov, V.E., Cai, H.N. (2010). Modulation of chromatin boundary activities by nucleosome-remodeling activities in Drosophila melanogaster. *Mol Cell Biol.*, 30, 1067-76.
149. Li, X., Wang, S., Li, Y., Deng, C., Steiner, L.A. *et al.* (2011). Chromatin boundaries require functional collaboration between the hSET1 and NURF complexes. *Blood*, 118, 1386-94.
150. Lin, C.Y., Lovén, J., Rahl, P.B., Paranal, R.M., Burge, C.B. *et al.* (2012). Transcriptional amplification in tumor cells with elevated c-Myc. *Cell*, 151, 56-67.
151. Littlewood, T.D., Hancock, D.C., Danielian, P.S., Parker, M.G., Evan, G.I. (1995). A modified oestrogen receptor ligand-binding domain as an improved switch for the regulation of heterologous proteins. *Nucleic Acids Res.*, 23, 1686-90.
152. Liu, X., Vorontchikhina, M., Wang, Y.L., Faiola, F. and Martinez, E. (2008a). STAGA recruits mediator to the MYC oncoprotein to stimulate transcription and cell proliferation. *Mol Cell Biol.,* 28, 108-21.
153. Liu, Y.C., Li, F., Handler, J., Huang, C.R., Xiang, Y. *et al.* (2008b). Global regulation of nucleotide biosynthetic genes by c-Myc. *PLoS One*, 3, e2722 (2008).
154. Liu, Z., Scannell, D.R., Eisen, M.B., Tjian, R. (2011). Control of embryonic stem cell lineage commitment by core promoter factor, TAF3. *Cell*, 146, 720-31.
155. Livak, K.J. and Schmittgen, T.D. (2001). Analysis of relative gene expression data using real-time quantitative PCR and the 2(-Delta Delta C(T)) Method. *Methods*, 25, 402.
156. Lovén, J., Orlando, D.A., Sigova, A.A., Lin, C.Y., Rahl, P.B. *et al*. (2012). Revisiting global gene expression analysis. *Cell*, 151, 476-82.
157. Luger, K., Mader, A.W., Richmond, R.K., Sargent, D.F. and Richmond, T.J. (1997). Crystal structure of the nucleosome core particle at 2.8 Å resolution. *Nature*, 389, 251-60.
158. Lüscher, B. and Vervoorts, J. (2012). Regulation of gene transcription by the oncoprotein MYC. *Gene*, 494, 145-60.
159. Maksimenko, O. and Georgiev, P. (2014). Mechanisms and proteins involved in long-distance interactions. *Front Genet.*, 5, 28.
160. Malumbres, M. (2011). Physiological relevance of cell cycle kinases. *Physiol Rev.*, 91, 973-1007.

161. Markenscoff-Papadimitriou, E., Allen, W.E., Colquitt, B.M., Goh, T., Murphy, K.K. *et al*. (2014). Enhancer interaction networks as a means for singular olfactory receptor expression. *Cell*, 159, 543-57.
162. Marqués, M., Kumar, A., Cortés, I., Gonzalez-García, A., Hernández, C. *et al*. (2008). Phosphoinositide 3-kinases p110alpha and p110beta regulate cell cycle entry, exhibiting distinct activation kinetics in G1 phase. *Mol Cell Biol*., 28, 2803-14.
163. Marques, M., Laflamme, L., Gervais, A.L. and Gaudreau, L. (2010). Reconciling the positive and negative roles of histone H2A.Z in gene transcription. *Epigenetics*, 5, 267-72.
164. Marshall, N.F., Peng, J., Xie, Z. and Price, D.H. (1996). Control of RNA polymerase II elongation potential by a novel carboxyl-terminal domain kinase. *J Biol Chem.*, 271, 27176-83.
165. Martinato, F., Cesaroni, M., Amati, B. and Guccione, E. (2008). Analysis of Myc-induced histone modifications on target chromatin. *PloS One*, 3, e3650.
166. Martinelli, P., Cañamero, M., Del Pozo, N., Madriles, F., Zapata, A. *et al.* (2013). Gata6 is required for complete acinar differentiation and maintenance of the exocrine pancreas in adult mice. *Gut*, 62, 1481-8.
167. Martinelli, P., Madriles, F., Cañamero, M., Pau, E.C., Pozo, N.D. *et al*. (2015). The acinar regulator Gata6 suppresses KrasG12V-driven pancreatic tumorigenesis in mice. *Gut*, pii: gutjnl-2014-308042. [Epub ahead of print]
168. Matsuoka, S., Ballif, B.A., Smogorzewska, A., McDonald, E.R. III, Hurov, K.E. *et al*. (2007). ATM and ATR substrate analysis reveals extensive protein networks responsive to DNA damage. *Science*, 316, 1160-6.
169. Mayya, V., Lundgren, D.H., Hwang, S.-I., Rezaul, K., Wu, L. *et al.* (2009) Quantitative phosphoproteomic analysis of T cell receptor signaling reveals system-wide modulation of protein-protein interactions. *Sci. Signal.*, 2, RA46.
170. McMahon, S.B., Wood, M.A. and Cole, M.D. (2000). The essential cofactor TRRAP recruits the histone acetyltransferase hGCN5 to c-Myc. *Mol. Cell. Biol.*, 20, 556-62.
171. McNairn, A.J., Gilbert, D.M. (2003). Epigenomic replication: Linking epigenetics to DNA replication. *Bioessays*, 25, 647-56.
172. Merkenschlager, M. and Odom, D.T. (2013). CTCF and cohesin: linking gene regulatory elements with their targets. *Cell*, 152, 1285-97.
173. Mertz, J.A., Conery, A.R., Bryant, B.M., Sandy, P., Balasubramanian, S. *et al.* (2011). Targeting MYC dependence in cancer by inhibiting BET bromodomains. *Proc Natl Acad Sci USA.*, 108, 16669-74.
174. Meyer, N. and Penn, L. (2008). Reflecting on 25 years with MYC. *Nat Rev Cancer*, 8, 976-90.

175. Mitchell, K.O., Ricci, M.S., Miyashita, T., Dicker, D.T., Jin, Z. *et al.* (2000). Bax is a transcriptional target and mediator of c-Myc-induced apoptosis. *Cancer Res.*, 60, 6318-25.
176. Mizuguchi, G., Tsukiyama, T., Wisniewski, J., Wu, C. (1997). Role of nucleosome remodeling factor NURF in transcriptional activation of chromatin. *Mol Cell*, 1, 141-50.
177. Mizuguchi, G., Shen, X., Landry, J., Wu, W.H., Sen, S. *et al*. (2004). ATP-driven exchange of histone H2AZ variant catalyzed by SWR1 chromatin remodeling complex. *Science*, 303, 343-8.
178. Moreau, J.L., Lee, M., Mahachi, N., Vary, J., Mellor, J. *et al*. (2003). Regulated displacement of TBP from the PHO8 promoter in vivo requires Cbf1 and the Isw1 chromatin remodeling complex. *Mol Cell*, 11, 1609-20.
179. Morillon, A., Karabetsou, N., O'Sullivan, J., Kent, N., Proudfoot, N. *et al*. (2003). Isw1 chromatin remodeling ATPase coordinates transcription elongation and termination by RNA polymerase II. *Cell*, 115, 425-35.
180. Morrison, A.J., Kim, J.A., Person, M.D., Highland, J., Xiao, J. *et al.* (2007). Mec1/Tel1 phosphorylation of the INO80 chromatin remodeling complex influences DNA damage checkpoint responses. *Cell*, 130, 499-511.
181. Mulder, K.W., Wang, X., Escriu, C., Ito, Y., Schwarz, R.F., Gillis, J. *et al*. (2012). Diverse epigenetic strategies interact to control epidermal differentiation. *Nat Cell Biol.*, 14, 753-63.
182. Murakami, H., Sanderson, N.D., Nagy, P., Marino, P.A., Merlino, G. (1993) Transgenic mouse model for synergistic effects of nuclear oncogenes and growth factors in tumorigenesis: interaction of c-myc and transforming growth factor alpha in hepatic oncogenesis. *Cancer Res.*, 53, 1719-23.
183. Murga, M., Campaner, S., Lopez-Contreras, A.J., Toledo, L.I., Soria, R. *et al.* (2011) Exploiting oncogene-induced replicative stress for the selective killing of Myc-driven tumors. *Nat Struct Biol.*, 18, 1331-5.
184. Murphy, D.J., Junttila, M.R., Pouyet, L., Karnezis, A., Shchors, K. *et al.* (2008) Distinct Thresholds Govern Myc's Biological Output In Vivo. *Cancer Cell*, 14, 447-57.
185. Nagy, Z. and Tora, L. (2007). Distinct GCN5/PCAF-containing complexes function as co-activators and are involved in transcription factor and global histone acetylation. *Oncogene*, 26, 5341-57.
186. Nakagawa, M., Koyanagi, M., Tanabe, K., Takahashi, K., Ichisaka, T. *et al*. (2008) Generation of induced pluripotent stem cells without Myc from mouse and human fibroblasts. *Nat Biotechnol.*, 26, 101-6.
187. Nasmyth, K. and Haering, C.H. (2009). Cohesin: its roles and mechanisms. *Annu Rev Genet.*, 43, 525-58.

188. Neri, F., Zippo, A., Krepelova, A., Cherubini, A., Rocchigiani, M. *et al.* (2012). Myc regulates the transcription of the PRC2 gene to control the expression of developmental genes in embryonic stem cells. *Mol Cell Biol.*, 32, 840-51.
189. Nie, Z., Hu, G., Wei, G., Cui, K., Yamane, A. *et al*. (2012). c-Myc is a universal amplifier of expressed genes in lymphocytes and embryonic stem cells. *Cell*, 151, 68-79.
190. O'Connell, B.C., Cheung, A.F., Simkevich, C.P., Tam, W., Ren, X. *et al*. (2003). A large scale genetic analysis of c-Myc-regulated gene expression patterns. *J Biol Chem.*, 278, 12563-73.
191. O'Donnell, K.A., Yu, D., Zeller, K.I., Kim, J.W., Racke, F. et al. (2006). Activation of transferrin receptor 1 by c-Myc enhances cellular proliferation and tumorigenesis. *Mol Cell Biol.*, 26, 2373-86.
192. Olsen, J.V., Blagoev, B., Gnad, F., Macek, B., Kumar, C. *et al*. (2006). Global, in vivo, and site-specific phosphorylation dynamics in signaling networks. *Cell*, 127, 635-48.
193. Olsen, J.V., Vermeulen, M., Santamaria, A., Kumar, C., Miller, M.L. *et al*. (2010). Quantitative phosphoproteomics reveals widespread full phosphorylation site occupancy during mitosis. *Sci Signal.*, 3, RA3.
194. Ong, C.T. and Corces, V.G. (2014). CTCF: an architectural protein bridging genome topology and function. *Nat Rev Genet.*, 15, 234-46.
195. Park, J., Wood, M.A. and Cole, M.D. (2002). BAF53 forms distinct nuclear complexes and functions as a critical c-Myc-interacting nuclear cofactor for oncogenic transformation. *Mol Cell Biol.*, 22, 1307-16.
196. Perna, D., Fagà, G., Verrecchia, A., Gorski, M.M., Barozzi, I. *et al.* (2012). Genome-wide mapping of Myc binding and gene regulation in serum-stimulated fibroblast. *Oncogene*, 31, 1695-1709.
197. Peukert, K., Staller, P., Schneider, A., Carmichael, G., Hanel, F. *et al.* (1997) An alternative pathway for gene regulation by Myc. *EMBO J.*, 16, 5672-86.
198. Phatnani, H.P. and Greenleaf, A.L. (2006). Phosphorylation and functions of the RNA polymerase II CTD. *Genes Dev.*, 20, 2922-36.
199. Poot, R.A., Bozhenok, L., van den Berg, D.L., Steffensen, S., Ferreira, F. *et al.* (2004). The Williams syndrome transcription factor interacts with PCNA to target chromatin remodelling by ISWI to replication foci. *Nat Cell Biol.*, 6, 1236-44.
200. Qiu, Z., Song, C., Malakouti, N., Murray, D., Hariz, A. *et al.* (2015). Functional Interactions between NURF and Ctcf Regulate Gene Expression. *Mol Cell Biol.*, 35, 224-37.
201. Rada-Iglesias, A., Bajpai, R., Swigut, T., Brugmann, S.A., Flynn, R.A. *et al*. (2011). A unique chromatin signature uncovers early developmental enhancers in humans. *Nature*, 470, 279-83.

202. Rahl, P.B., Lin, C.Y., Seila, A.C., Flynn, R.A., Mccuine, S. *et al*. (2010). c-Myc Regulates Transcriptional Pause Release. *Cell*, 141, 432-45.
203. Ramachandran A., Omar M., Cheslock P. and Schnitzler G.R. (2003). Linker histone H1 modulates nucleosome remodeling by human SWI/SNF. *J Biol Chem.*, 278, 48590-601.
204. Rigbolt, K.T., Prokhorova, T.A., Akimov, V., Henningsen, J., Johansen, P.T. *et al.* (2011). System-wide temporal characterization of the proteome and phosphoproteome of human embryonic stem cell differentiation. *Sci Signal.*, 4, RS3.
205. Ruthenburg, A.J., Li, H., Milne, T.A., Dewell, S., McGinty, R.K. *et al*. (2011). Recognition of a mononucleosomal histone modification pattern by BPTF via multivalent interactions. *Cell*, 145, 692-706.
206. Ruzankina, Y., Pinzon-Guzman, C., Asare, A., Ong, T., Pontano, L. *et al*. (2007). Deletion of the developmentally essential gene ATR in adult mice leads to age-related phenotypes and stem cell loss. *Cell Stem Cell*, 1, 113-26.
207. Sabò, A., Kress, T.R., Pelizzola, M., de Pretis, S., Gorski, M.M. *et al*. (2014). Selective transcriptional regulation by Myc in cellular growth control and lymphomagenesis. *Nature*, 511, 488-92.
208. Saborowski, M., Saborowski, A., Morris, J.P. 4th, Bosbach, B., Dow, L.E. *et al.* (2014). A modular and flexible ESC-based mouse model of pancreatic cancer. *Genes Dev.*, 28, 85-97.
209. Saha, A., Wittmeyer, J. and Cairns, B. R. (2006). Chromatin remodelling: the industrial revolution of DNA around histones. *Nat Rev Mol Cell Biol.*, 7, 437-47.
210. Sandgren, E.P., Quaife, C.J., Paulovich, A.G., Palmiter, R.D., Brinster, R.L. (1991). Pancreatic tumor pathogenesis reflects the causative genetic lesion. *Proc Natl Acad Sci USA.*, 88, 93-7.
211. Sansom, O.J., Meniel, V.S., Muncan, V., Phesse, T.J., Wilkins, J.A. *et al.* (2007). Myc deletion rescues Apc deficiency in the small intestine. *Nature*, 446, 676-9.
212. Sanyal, A., Lajoie, B.R., Jain, G., Dekker, J. (2012). The long-range interaction landscape of gene promoters. *Nature*, 489, 109-13.
213. Sarid, J., Halazonetis, T.D., Murphy, W. and Leder, P. (1987). Evolutionarily conserved regions of the human c-myc protein can be uncoupled from transforming activity. *Proc Natl Acad Sci USA.*, 84, 170-3.
214. Savkur, R.S. and Burris, T.P. (2004). The coactivator LXXLL nuclear receptor recognition motif. *J. Peptide Res.*, 63, 207-12.
215. Schlosser, I., Hölzel, M., Hoffmann, R., Burtscher, H., Kohlhuber, F. *et al.* (2005). Dissection of transcriptional programmes in response to serum and c-Myc in a human B-cell line. *Oncogene*, 24, 520-4.
216. Schmidt, D., Schwalie, P.C., Ross-Innes, C.S., Hurtado, A., Brown, G.D. *et al.* (2010). A CTCF-independent role for cohesion in tissue-specific transcription. *Genome Res.*, 20, 578-88.

217. Schnetz, M.P., Handoko, L., Akhtar-Zaidi, B., Bartels, C.F., Pereira, C.F., *et al.* (2010). CHD7 targets active gene enhancer elements to modulate ES cell-specific gene expression. *PLoS Genet.*, 6, pe1001023.
218. Schoenenberger, C.A., Andres, A.C., Groner, B., van der Valk, M., LeMeur, M. *et al.* (1988) Targeted c-myc gene expression in mammary glands of transgenic mice induces mammary tumours with constitutive milk protein gene transcription. *EMBO J.*, 7, 169-75.
219. Schuhmacher, M., Kohlhuber, F., Hölzel, M., Kaiser, C., Burtscher, H. *et al*. (2001). The transcriptional program of a human B cell line in response to Myc. *Nucleic Acids Res.*, 29, 397-406.
220. Sears, R., Nuckolls, F., Haura, E., Taya, Y., Tamai, K. *et al.* (2000). Multiple Ras-dependent phosphorylation pathways regulate Myc protein stability. *Genes Dev.* 14, 2501-14.
221. Seitz, V., Butzhammer, P., Hirsch, B., Hecht, J., Gütgemann, I., *et al.* (2011). Deep sequencing of MYC DNA-binding sites in Burkitt lymphoma. *PLoS One*, 6, e26837.
222. Seoane, J., Pouponnot, C., Staller, P., Schader, M., Eilers, M. *et al.* (2001). TGFbeta influences Myc, Miz-1 and Smad to control the CDK inhibitor p15INK4b. *Nat Cell Biol.*, 3, 400-8.
223. Shen, Y., Yue, F., McCleary, D. F., Ye, Z., Edsall, L. *et al.* (2012). A map of the cis-regulatory sequences in the mouse genome. *Nature*, 488, 116-20.
224. Shim, H., Dolde, C., Lewis, B.C., Wu, C.S., Dang, G. *et al*. (1997). c-Myc transactivation of LDH-A: implications for tumor metabolism and growth. *Proc Natl Acad Sci USA.*, 94, 6658-63.
225. Shim, E.Y., Hong, S.J., Oum, J.H., Yanez, Y., Zhang, Y., Lee, S.E. (2007). RSC mobilizes nucleosomes to improve accessibility of repair machinery to the damaged chromatin. *Mol Cell Biol.*, 27, 1602-13.
226. Sif, S., Stukenberg, P.T., Kirschner, M.W., Kingston, R.E. (1998). Mitotic inactivation of a human SWI/SNF chromatin remodeling complex. *Genes Dev.*, 12, 2842-51.
227. Smallwood, A. and Ren, B. (2013). Genome organization and long-range regulation of gene expression by enhancers. *Curr Opin Cell Biol.*, 25, 387-94.
228. Songyang, Z., Lu, K.P., Kwon, Y.T., Tsai, L.H., Filhol, O. *et al.* (1996). A structural basis for substrate specificities of protein Ser/Thr kinases: primary sequence preference of casein kinases I and II, NIMA, phosphorylase kinase, calmodulin-dependent kinase II, CDK5, and Erk1. *Mol Cell Biol.*, 16, 6486-93.
229. Soucek, L., Jucker, R., Panacchia, L., Ricordy, R., Tato, F. *et al*. (2002). Omomyc, a potential Myc dominant negative, enhances Myc-induced apoptosis. *Cancer Res*, 62, 3507-10.

230. Soucek, L., Whitfield, J., Martins, C.P., Finch, A.J., Murphy, D.J. *et al*. (2008). Modelling Myc inhibition as a cancer therapy. *Nature*, 455, 679-83.
231. Soufi, A., Donahue, G. and Zaret, K. S. (2012). Facilitators and Impediments of the Pluripotency Reprogramming Factors' Initial Engagement with the Genome. *Cell*, 151, 994-1004.
232. Spotts, G.D., Patel, S.V., Xiao, Q. and Hann, S.R. (1997). Identification of downstream-initiated c-Myc proteins which are dominant-negative inhibitors of transactivation by full-length c-Myc proteins. *Mol. Cell. Biol.*, 17, 1459-68.
233. Sridharan, R., Tchieu, J., Mason, M. J., Yachechko, R., Kuoy, E. *et al.* (2009). Role of the murine reprogramming factors in the induction of pluripotency. *Cell*, 136, 364-77.
234. Staller, P., Peukert, K., Kiermaier, A., Seoane, J., Lukas, J. *et al*. (2001) Repression of p15INK4b expression by Myc through association with Miz-1. *Nat. Cell. Biol.*, 3, 392-9.
235. Steiger, D., Furrer, M., Schwinkendorf, D. and Gallant, P. (2008). Max-independent functions of Myc in Drosophila melanogaster. *Nat. Genet.*, 40, 1084-91.
236. Stewart, T.A., Pattengale, P.K. and Leder P. (1984). Spontaneous mammary adenocarcinomas in transgenic mice that carry and express MTV/myc fusion genes. *Cell*, 38, 627-37.
237. Strahl, B.D. and Allis, C.D. (2000). The language of covalent histone modifications. *Nature*, 403, 41-5.
238. Strasser, A., Harris, A.W., Bath, M.L. and Cory, S. (1990) Novel primitive lymphoid tumours induced in transgenic mice by cooperation between myc and bcl-2. *Nature*, 348, 331-3.
239. Sugiyama, A. and Kume, A. (1989). Isolation and characterization of s-myc, a member of the rat myc gene family. *Proc Natl Acad Sci USA.*, 86, 9144-8.
240. Takahashi, K., Tanabe, K., Ohnuki, M., Narita, M., Ichisaka, T. *et al*. (2007). Induction of pluripotent stem cells from adult human fibroblasts by defined factors. *Cell*, 131, 861-72.
241. Talbert, P.B. and Henikoff, S. (2010). Histone variants--ancient wrap artists of the epigenome. *Nat Rev Mol Cell Biol.*, 11, 264-75.
242. Tan, M., Luo, H., Lee, S., Jin, F., Yang, J.S., *et al.* (2011). Identification of 67 histone marks and histone lysine crotonylation as a new type of histone modification. *Cell*, 146, 1016-28.
243. Tarutani, M., Itami, S., Okabe, M., Ikawa, M., Tezuka, T. *et al.* (1997). Tissue-specific knockout of the mouse Pig-a gene reveals important roles for GPI-anchored proteins in skin development. *Proc Natl Acad Sci USA.*, 94, 7400-5.

244. Taub, R., Kirsch, I., Morton, C., Lenoir, G., Swan, D. *et al.* (1982). Translocation of the c-myc gene into the immunoglobulin heavy chain locus in human Burkitt lymphoma and murine plasmacytoma cells. *Proc Natl Acad Sci USA. ,* 79, 7837-41.
245. Taylor, B.S., Schultz, N., Hieronymus, H., Gopalan, A., Xiao, Y. *et al.* (2010). Integrative genomic profiling of human prostate cancer. *Cancer Cell*, 18, 11-22.
246. Thurman, R.E., Rynes, E., Humbert, R., Vierstra, J., Maurano, M.T. *et al.* (2012). The accessible chromatin landscape of the human genome. *Nature*, 489, 75-82.
247. Vafa, O., Wade, M., Kern, S., Beeche, M., Pandita, T.K. *et al*. (2002) c-Myc can induce DNA damage, increase reactive oxygen species, and mitigate p53 function: A mechanism for oncogene-induced genetic instability. *Mol Cell*, 9, 1031-44.
248. Vallespinós, M., Fernández, D., Rodríguez, L., Alvaro-Blanco, J., Baena, E. *et al.* (2011). B Lymphocyte commitment program is driven by the proto-oncogene c-Myc. *J Immunol.*, 186, 6726-36.
249. Vennstrom, B., Sheiness, D., Zabielski, J. and Bishop, J.M. (1982). Isolation and characterization of c-myc, a cellular homolog of the oncogene (v-myc) of avian myelocytomatosis virus strain 29. *J Virol.*, 42, 773-9.
250. Versteege, I., Sevenet, N., Lange, J., Rousseau-Merck, M.F., Ambros, P. *et al.* (1998). Truncating mutations of hSNF5/INI1 in aggressive paediatric cancer. *Nature*, 394, 203-6.
251. Vervoorts, J., Luscher-Firzlaff, J.M., Rottmann, S., Lilischkis, R., Walsemann, G. *et al.* (2003). Stimulation of c-MYC transcriptional activity and acetylation by recruitment of the cofactor CBP. *EMBO Rep.*, 4, 484-90.
252. Vicent, G.P., Nacht, A.S., Font-Mateu, J., Castellano, G., Gaveglia, L. *et al.* (2011). Four enzymes cooperate to displace histone H1 during the first minute of hormonal gene activation. *Genes Dev.*, 25, 845-62.
253. Vilá, M.R., Lloreta, J., Schüssler, M.H., Berrozpe, G., Welt, S., Real, F.X. (1995). New pancreas cancers cell lines that represent distinct stages of ductal differentiation. *Lab Invest.*, 72, 395-404.
254. Vogelauer, M., Rubbi, L., Lucas, I., Brewer, B.J., Grunstein, M. (2002). Histone acetylation regulates the time of replication origin firing. *Mol Cell*, 10, 1223-33.
255. Waikel, R.L., Kawachi, Y., Waikel, P.A., Wang, X.J. and Roop, D.R. (2001). Deregulated expression of c-Myc depletes epidermal stem cells. *Nat. Genet.*, 28, 165-8.
256. Walz, S., Lorenzin, F., Morton, J., Wiese, K.E., von Eyss, B., *et al*. (2014). Activation and repression by oncogenic MYC shape tumour-specific gene expression profiles. *Nature*, 511, 483-7.
257. Wang, G.G., Allis, C.D., Chi, P. (2007). Chromatin remodeling and cancer, Part II: ATP-dependent chromatin remodeling. *Trends Mol Med.*, 13, 373-80.

258. Wanzel, M., Russ, A.C., Kleine-Kohlbrecher, D., Colombo, E., Pelicci, P.G. *et al.* (2008). A ribosomal protein L23-nucleophosmin circuit coordinates Miz1 function with cell growth. *Nat. Cell. Biol.*, 10, 1051-61.

259. Wolf, E., Lin, C.Y., Eilers, M., Levens, D.L. (2014). Taming of the beast: shaping Myc-dependent amplification. *Trends Cell Biol.*, pii: S0962-8924(14)00193-7.

260. Wu, R., Lin, L., Beer, D.G., Ellenson, L.H., Lamb, B.J. *et al.* (2003). Amplification and overexpression of the L-MYC proto-oncogene in ovarian carcinomas. *Am. J. Pathol.*, 162, 1603-10.

261. Wysocka, J., Swigut, T., Xiao, H., Milne, T.A., Kwon, S.Y. *et al.* (2006). A PHD finger of NURF couples histone H3 lysine 4 trimethylation with chromatin remodelling. *Nature*, 442, 86-90.

262. Xiao, H., Sandaltzopoulos, R., Wang, H.M., Hamiche, A., Ranallo, R. *et al.* (2001). Dual functions of largest NURF subunit NURF301 in nucleosome sliding and transcription factor interactions. *Mol Cell*, 8, 531-43.

263. Xiao, F., Kim, Y.C., Snyder, C., Wen, H., Chen, P.X. *et al*. (2014a). Genome instability in blood cells of a BRCA1+ breast cancer family. *BMC Cancer*, 14, 342.

264. Xiao, S., Liu, L., Fang, M., Zhou, X., Peng, X. *et al*. (2014b). BPTF Associated with EMT Indicates Negative Prognosis in Patients with Hepatocellular Carcinoma. *Dig Dis Sci.* [Epub ahead of print]

265. Xiao, S., Liu, L., Lu, X., Long, J., Zhou, X. *et al.* (2015). The prognostic significance of bromodomain PHD-finger transcription factor in colorectal carcinoma and association with vimentin and E-cadherin. *J Cancer Res Clin Oncol.* [Epub ahead of print]

266. Yada, M., Hatakeyama, S., Kamura, T., Nishiyama, M., Tsunematsu, R. *et al* (2004). Phosphorylation-dependent degradation of c-Myc is mediated by the F-box protein Fbw7. *EMBO J.*, 23, 2116-25.

267. Yan, J., Enge, M., Whitington, T., Dave, K., Liu, J., Sur, I., et al. (2013). Transcription factor binding in human cells occurs in dense clusters formed around cohesin anchor cites. *Cell*, 154, 801-13.

268. Yang, Z., Yik, J.H., Chen, R., He, N., Jang, M.K. *et al.* (2005). Recruitment of P-TEFb for stimulation of transcriptional elongation by the bromodomain protein Brd4. *Mol Cell.*, 19, 535-45.

269. Ye, T., Krebs, A.R., Choukrallah, M.A., Keime, C., Plewniak, F. *et al.* (2010). SeqMINER: an integrated ChIP-seq data interpretation platform. *Nucleic Acids Res.,* 39, e35.

270. Zeller, K.I., Zhao, X., Lee, C.W., Chiu, K.P., Yao, F. *et al.* (2006). Global mapping of c-Myc binding sites and target gene networks in human B cells. *Proc Natl Acad Sci USA.*, 103, 17834-9.

271. Zentner, G.E., Tsukiyama, T., Henikoff, S. (2013). ISWI and CHD chromatin remodelers bind promoters but act in gene bodies. *PLoS Genet.*, 9, e1003317.

272. Zhang, Y. and Reinberg, D. (2001). Transcription regulation by histone methylation: interplay between different covalent modifications of the core histone tails. *Genes Dev.*, 15, 2343-60.
273. Zhang, H., Roberts, D.N., Cairns, B.R. (2005). Genome-wide dynamics of Htz1, a histone H2A variant that poises repressed/basal promoters for activation through histone loss. *Cell*, 123, 219-31.
274. Zindy, F., Eischen, C.M., Randle, D.H., Kamijo, T., Cleveland, J.L. *et al*. (1998) Myc signaling via the ARF tumor suppressor regulates p53-dependent apoptosis and immortalization. *Genes Dev.*, 12, 2424-33.